Journal of Energy Storage 53 (2022) 105187

Contents lists available at ScienceDirect

Journal of Energy Storage

journal homepage: www.elsevier.com/locate/est

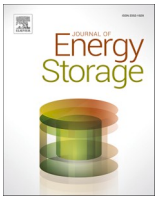

Review article

Fundamentals and recent progress of Sn-based electrode materials for supercapacitors: A comprehensive review

Mohd Zahid Ansari [a], Sajid Ali Ansari [b,*], Soo-Hyun Kim [a,c,**]

[a] School of Materials Science and Engineering, Yeungnam University, 280 Daehak-Ro, Gyeongsan, Gyeongbuk 38541, Republic of Korea
[b] Department of Physics, College of Science, King Faisal University, P.O. Box 400, Hofuf, Al-Ahsa 31982, Saudi Arabia
[c] Institute of Materials Technology, Yeungnam University, 280 Daehak-Ro, Gyeongsan, Gyeongbuk 38541, Republic of Korea

ARTICLE INFO

Keywords:
Sn-based
$SnO_{x=1\&2}$
$SnS_{x=1\&2}$
Supercapacitors
Electrodes materials
Composites

ABSTRACT

Supercapacitors are extremely capable electrochemical energy storage devices owing to their high power density, long cyclability, rapid charge-discharge rates, and environmentally benign nature. They are equipped with absolutely demanding commercial features, thus employed in a wide range of applications including convenient electronics to electric automobiles. Electrode materials are considered an important feature in the electrochemical performance of supercapacitors, among which tin-based electrode materials (Sn oxides and sulfides) are quite attractive electrode materials. Their unique features involve numerous valence states, good redox chemistry, high thermal and mechanical stability, enriching conductivity, and long cyclability. This review tries to summarize the importance and contribution of Sn-based electrode materials for supercapacitors to date via organizing them into various sections based on chemical composition. Also, the role of different nanoarchitectures in deciding the electrochemical performance is discussed. A brief history of the supercapacitor background, involving the charge storage mechanism is presented. The summary of the results intricates the association between the synthesis and the properties as well as the performance of the supercapacitor that would be helpful to set a guide for future research relying on the suitable preparation route for the variety of applications which is aimed. Although Sn-based electrode materials for supercapacitors are not so much explored, highlighting the potential aspects of these materials with future perspectives and challenges is the main purpose of this review.

1. Introduction

The rapid development of the global economy has raised several major issues like depletion of fossil fuels, energy crises, and environmental pollution. Such development is not sustainable and therefore needs serious attention. Efforts should be made to utilize and develop such energy sources that are clean, abundant, efficient, and economic. The generation of energy from renewable energy sources and its storage is a sustainable way to bring both energies as well as environmental security. Such an approach undoubtedly can establish a balance between energy production and its utilization [1]. Among various energy storage technologies, electrochemical energy storage (EES) is the most effective and practical technology well known for a long time. This class comprises batteries, fuel cells, and electrochemical supercapacitors (ES) [1]. Batteries and supercapacitors are the most widely explored ones [1,2].In recent time, supercapacitors or ultracapacitors has gained great attention for commercial and research purposes. High energy/power density, fast charge/discharge, long cycle life, wide functioning temperature range compared to conventional capacitors, good efficiency up to 95 %, less maintenance and leakage current, long service, and reliability are the unique features of this device [3]. They are utilized in numerous uses including minuscule handy electronics to mixture electrical automobiles [4]. The whole device performance relies on several components including current collectors, separators, electrolytes, and electrode materials. Although the device possesses huge potential applications, it suffers from a low energy density and high manufacturing cost. Active electrode materials are played a crucial part in deciding the electrochemical performance of SCs and can surpass the limitations of this

* Corresponding author.
** Correspondence to: S.H. Kim, School of Materials Science and Engineering, Yeungnam University, 280 Daehak-Ro, Gyeongsan, Gyeongbuk 38541, Republic of Korea.
E-mail addresses: sansari@kfu.edu.sa (S.A. Ansari), soohyun@ynu.ac.kr (S.-H. Kim).

https://doi.org/10.1016/j.est.2022.105187
Received 15 April 2022; Received in revised form 3 June 2022; Accepted 19 June 2022
Available online 29 June 2022

device.

Carbonaceous materials, conducting polymers, metal oxides and hydroxides are the major classes of electrode materials for SCs [5,6]. Due to high energy density and excellent conductivity than carbon materials and conducting polymers, metal oxides are the most anticipated electrode materials for SCs [6–9]. Ruthenium is the most favourable electrode material for SCs due to its large potential window, presence of multiple oxidation states, excellent conductivity, long cycle life, high reversibility, and large specific capacitance [10]. But its commercial utilization is hindered by the less abundance and hence high cost. Then, engineering and constructing suitable active materials with high charge density, long-term cyclic stability, and appropriate working potential is a major shortcoming presently facing SCs. Among various materials, metallic tin (Sn) and Sn-based materials such as its oxides, sulfides, nitrides and their composites have gained remarkable devotion recently and demonstrate abundant prospective as electrode materials due to their exceptional physicochemical properties [11–19]. Tin is among one of the most significant silvery-white metals from history and was discovered much earlier, with two popular forms of allotropes, which look and behave differently due to their various crystalline structure and nature. The most familiar variant of Sn is called white tin or beta tin, which mostly forms easily at ambient temperatures, and is silvery-white with a body-centred tetragonal structure. Alternatively, the second form is called grey tin or alpha tin, with a less dense powdery form (about two thirds as dense) and appears more suited in lower temperatures. This variant is not so useful because of its weaker and more brittleness and has face-centred cubic crystal systems. The process where white tin sudden deteriorates to its grey form is known as a tin pest. Sn has two oxidation states: divalent Sn (Sn^{+2}) and tetravalent Sn (Sn^{+4}). Depending upon its valency, tin forms two types of compounds: tin with divalent compounds known as stannous and tin with tetravalent Sn is known as stannic. Significant Sn compounds contain Sn + 2 chloride which is popularly applied in galvanizing, dyeing, and perfume manufacturing; Sn + 2 fluoride is mostly used for fluoride in toothpaste, and tin IV oxide is a popular catalyst for industries. Besides, Sn is an earth-abundant and cheap element (~20$/Kg), moderately harmless to work with [10,20,21]. The major problems of most Sn-based electrode materials are mechanical issues (poor structural stability and flexibility) like large volume expansion and formation of the cluster. To overcome this drawback, a variety of Sn-based materials with various morphologies and structures have been engineered. Recent research has emphasized that tin-based nanomaterials are quite promising for SCs due to their high conductivity, thermal and chemical stability, nontoxic nature, and huge natural abundance [20–22]. The electrochemical performance of tin can be enhanced by incorporating it with carbon-based materials in the form of nanocomposites such as Sn@C, SnO_2@C.

Table 1 provides the review literature that covered the studies about Sn-based materials for various applications so far. Although the electrochemical tests of Sn-based electrodes have been reported since 1998, there are numerous literatures since then. An organized review involving the preparation process, specific properties, and applications based on different reports are yet to be done.

There are quite a few excellent review articles on the tin-based electrode materials, which mainly focused on specific rechargeable batteries as can be seen in Table 1, but based on our literature survey, no review has summarized the latest outcomes of this material for SCs. Therefore, an up-to-date summarization is necessary to review the rapid advancement of novel Sn-based nanostructures in the SCs field. Herein, we took an effort to summarize and focused on the development to most recent progress on the Sn-based electrode materials for SCs along with the storage mechanisms, different synthetic techniques, and the electrochemical performance. Foremost, we have given some introductory background of SCs that would help the understanding of the current review, including the types and charge storage mechanism.

Table 1
Existing review literature on Sn-based materials.

Sr. No	Title of paper	Reviewed area or topic	Year up to literature covered	Topic covered for super -capacitors	Ref.
1	Green energy storage materials: Nanostructured TiO_2 and Sn-based anodes for lithium-ion batteries	Developments of nanostructured including rutile, anatase, TiO_2 (B), and coated TiO_2, and pristine SnO_2, and its composites.	2009	Not available	[11]
2	SnO_2-based nanomaterials: Synthesis and application in lithium-ion batteries and supercapacitors	Different morphologies as well as their modifications by doping and compositing with other materials.	2014	Not available	[12]
3	Promises and challenges of tin-based compounds as anode materials for lithium-ion batteries	Design and synthesis of nano- and microstructures with different morphologies, and their relationships with Li-ion storage properties	2015	Not available	[13]
4	Tin-based anode materials with well-designed architectures for next generation lithium-ion batteries	Structural design, fabrication methods, and battery performance with focus on material structures	2016	Not available	[14]
5	Tin-based nanomaterials for electrochemical energy storage	Nanostructured Sn-based compound for Li-ion batteries, Na-ion batteries, supercapacitors	2016	Partly discussed	[15]
6	Metallic Sn-based anode materials: application in high-performance lithium-ion and sodium-ion batteries	Modification strategies including size control, alloying, and structure design to improve the electrochemical properties.	2017	Not available	[16]
7	Tin-based materials as versatile anodes for alkali (earth)-ion batteries	Effects of morphologies, and the integration with carbon for Li-ion batteries, Na-ion batteries, Mg-ion batteries	2018	Not available	[17]
8	Advances in synthesis, properties and emerging applications of tin sulfides and its heterostructures	Preparation strategies and applications in water splitting, rechargeable batteries, supercapacitor, photocatalyst etc.	2020	Partly discussed	[18]
9	Advances in Sn-based catalysts	Synthesis, catalytic	2019	Not available	[19]

(continued on next page)

Table 1 (*continued*)

Sr. No	Title of paper	Reviewed area or topic	Year up to literature covered	Topic covered for super -capacitors	Ref.
	for electrochemical CO_2 reduction	performance, and reaction mechanisms for CO_2 electroreduction			
10	Research progress on tin-based anode materials for sodium ion batteries	Synthesis of tin metal, tin alloy, and its composites with different nanostructures	2020	Not available	[78]
11	Tin and tin compound materials as anodes in lithium-ion and sodium-ion batteries: A review	Sn, SnO_2,SnS_2-based composites for rechargeable batteries	2020	Not available	[79]
12	Tin oxide for optoelectronic, photovoltaic and energy storage devices: a review	Experimental approaches to doping of SnO_2 with foreign elements for TCO and ETL application.	2021	Not available	[80]
13	Sn-Based electrocatalyst stability: A crucial piece to the puzzle for the electrochemical CO_2 reduction towards formic acid	Highlighting the importance of correctly selected process conditions and an optimized reactor design	2021	Not available	[81]
14	A review of tin disulfide (SnS_2) composite electrode materials for supercapacitors	Survey and summarize the findings of the studies on tin (IV) sulfide in supercapacitors.	2021	Only SnS_2-based discussed	[82]
15	Challenges and development of tin-based Anode with high volumetric capacity for li-ion batteries	Discussion on the series of Sn–Fe–C, Sn_yFe, Sn—C composites with capacity retention and rate capability	2020	Not available	[83]

1.1. Charge storage mechanism of supercapacitors

The energy storage process depends on basically two mechanisms that take part in the overall capacitance of electrochemical capacitors (ECs) [4,5]:

(1) Electric double-layer capacitance (EDLC) - this charge storage principle relies on electrostatic storage of charges at the conducting interface of the electrode and electrolyte. It results in the formation of the Helmholtz double layer. The electrical energy is stored through reversible and physical adsorption of electrolyte ions at the electrode interface, with no actual transfer of charges between the two mediums. The extremely small separation distance of static charges in a double-layer results in the enhanced capacitance of the electrode [6].
(2) Pseudocapacitance – this principle of electrical energy storage depends on faradaic charge storage, where electrons generated with the help of reversible redox reactions are moved across the joint interface of electrode and electrolyte. The formation of no new chemical species occurs because of the highly reversible intercalation of electrolyte ions in the lattice of the electrode materials [7–9,23].

1.2. Supercapacitor types

Based on the above-mentioned charge storage mechanism and design of the electrodes, SCs have been broadly classified into electric double-layer capacitors (EDLCs), pseudocapacitors (PCs), and hybrid capacitors.

1.2.1. Electric double-layer capacitors (EDLCs)

The development of SC technology is still going on since its invention by General Electric in 1957. The Japanese company "Nippon Electric (NE)" was the first commercial-scale producer of double-layer capacitors in the year 1975 with the name supercapacitors. EDLCs share a similar charge storage mechanism as conventional capacitors. However, in place of a solid dielectric medium, they exhibit an ionically conducting solution between the electrodes. Thus, make use of the interfaces present between the electrode material and the conducting electrolyte solution for energy storage [22]. Fig. 1a [24] shows the underlying charge storage mechanism of EDLCs. An externally applied voltage across the EDLC induces the electrodes with different polarities, resulting in the movement of the oppositely charged electrolyte ions to the pores of the electrodes. The resulted molecular layer of adsorbed ions at the electrode surface, surrounded by solvent molecules, makes the actual 'dielectric' of the double-layer capacitors [8,9]. The formation of such double layers takes place at the two adjacent positions in the device. The width of the double layer formed at the interface of electrode and electrolyte determines the EDLCs capacitance, which is much smaller than the thickness of the ion-permeable separator. This versatile change makes EDLCs possess much-enhanced capacitance compared to conventional capacitors according to Eq. (1) [25,26].

$$C = (\mathcal{E}_0 \mathcal{E}r A)/d \quad (1)$$

where C, $\mathcal{E}_0$, $\mathcal{E}r$, A, and d denote the specific capacitance of EDLC, vacuum permittivity, the relative permittivity of the electrolyte, specific surface area of the electrode accessible to the electrolyte ions, and EDL effective thickness respectively. Owing to merely physical charge transfer, slight volumetric fluctuations happen in the electrode of EDLCs. Therefore, they possess enormous cyclic constancies. In this, carbon-based materials consider the favourable constituents for EDLC electrodes because of their high specific surface area, great mechanical and chemical strength, admirable electronic conductivity, and economical [8]. Endo et al. in-depth have summarized facts based on electric double-layer capacitors [27]. Currently, numerous carbonaceous constituents like activated carbons (ACs), carbon nanotubes, graphene etc., obtained from many sources, were applied as electrode EDLCs [5,6]. Nowadays, EDLCs research is highly focused on improving energy density, without losing the remarkable power density and cycle life.

1.2.2. Pseudocapacitors (PCs)

The charge storage process of pseudocapacitors (PCs) occurs from the fast and highly reversible redox reactions taking place on the surface of electrode materials. Here, the genuine transmission of ions involves across the generated double layer, which is quite alike the storage mechanism of batteries. Except for the fact that instead of reactions taking place in the bulk, faradaic reactions majorly occur at the surface of synthesized electrodes. Depending upon the types of electrode materials and electrolytes, the faradaic process occurs in three different manners: reversible adsorption, redox reactions of transition metal oxides, and reversible electrochemical doping–dedoping in conductive polymers [5,6]. However, all the transition metal oxides are not suitable for pseudocapacitance in SCs. Only reactions going on at the surface and

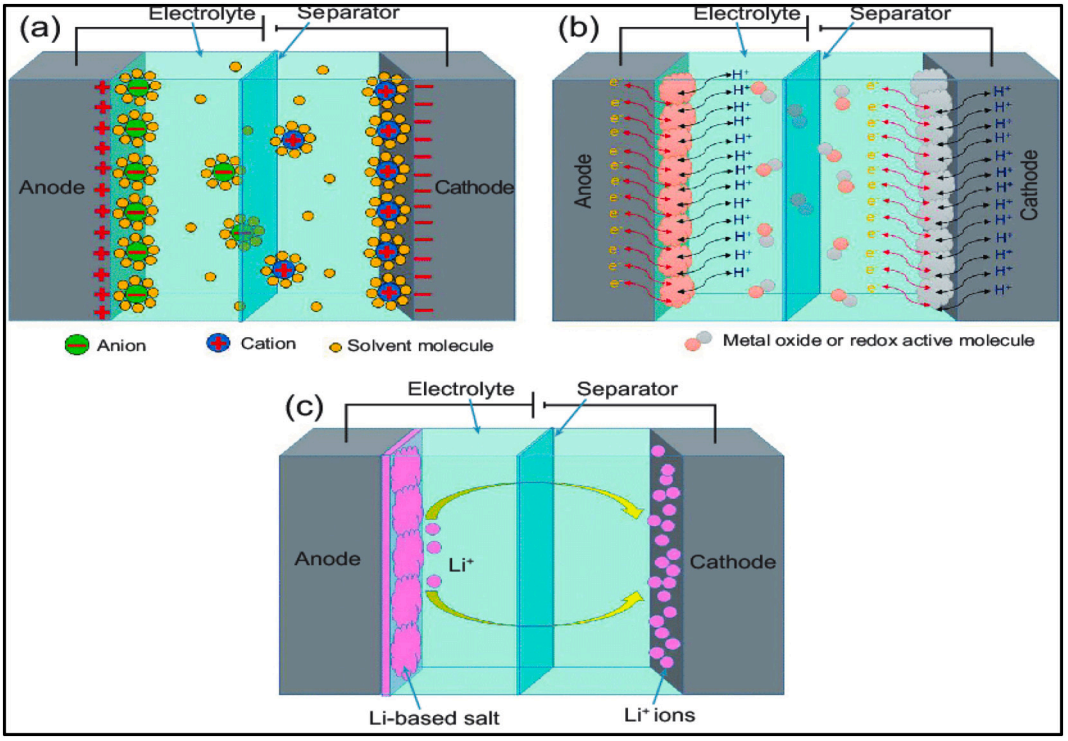

Fig. 1. Schematic representation of charge storage mechanism of (a) electric double-layer capacitors (EDLCs), (b) pseudocapacitors (PCs), and (c) hybrid capacitors (HCs). Reproduced with permission. [28] Copyright 2017, Oxford Academy.

are limited by the solid-state diffusion show high-rate capability, e.g., RuO_2. While the materials that use the bulk of the solid-state to store charges result in higher energy densities and are utilized in rechargeable batteries [9]. The fast and reversible faradaic redox reactions make PCs more capacitive than EDLCs, about 10–100 times larger. The enhanced capacitance is due to the occurrence of electrochemical reactions both on the electrode surface and near the surface [24]. A comparison of the charge storage mechanism of EDLCs and PCs is shown in Fig. 1 [25]. The frequently used electrodes for PCs are metal oxides and conducting polymers due to high specific capacitance, conductivity, high surface area, and high energy/power densities [25]. However, the power performance and cyclic stability of PCs are hindered by the slow faradaic mechanism, swelling, and phase transformations of electrode materials during charge-discharge processes [26]. Increasing the surface area through nanostructuring can improve the working efficiency of PC materials due to a decrease in diffusion distances and in some cases, control over phase transformations.

1.2.3. Hybrid capacitors

This category of supercapacitors takes advantage of both electrostatic and faradaic storage of charges within the same system. The incorporation of both the capacitor type and the pseudocapacitive type electrodes results in high energy and power densities. Also, this class of SC provides better cyclic stability and low production cost. Based on designs and materials of various electrode configurations, the hybrid capacitors are classified as, asymmetric, composite, and battery-type as shown in Fig. 2 [26,27,29].

a) Asymmetric hybrid supercapacitors (ASCs)

The ASCs are well known for their superior energy and power delivery, due to the presence of two different electrodes within the same system. These systems are devised to work together to address the high energy as well as power density requirement. Carbonaceous materials due to their high conductivity and large surface area work as an anode

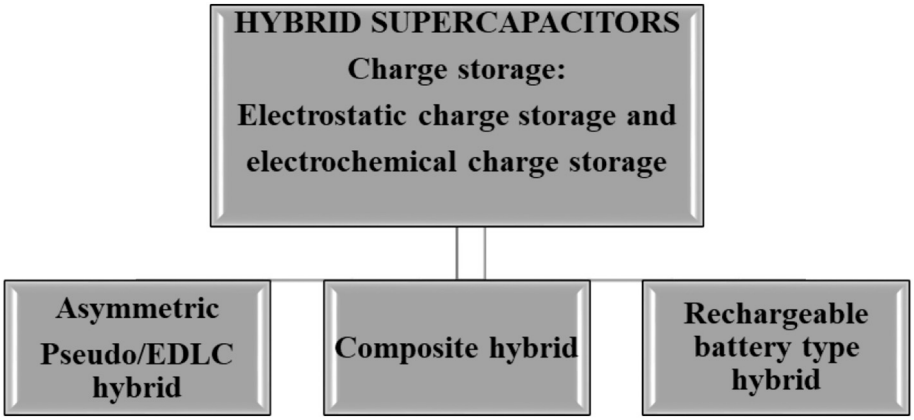

Fig. 2. Classification of hybrid supercapacitors based on electrode configurations [30].

and act as a power source while metal electrodes due to high intrinsic volumetric capacity behave as a cathode and act as an energy source [31]. Self-discharge and low working voltage are the major limitations of aqueous SCs. The incorporation of the asymmetric electrode configuration helps in increasing the operating voltage window. Gao et al. [32], fabricated an asymmetric SC using 3D porous graphene hydrogel as anode and MnO_2 nanoplates on Nickel foam as a cathode. The device exhibited a high energy density of 23.2 Wh kg^{-1} at a power density of 1 kW/kg with 83.4 % capacitance retention after 5000 charge-discharge cycles. The asymmetric configuration in aqueous electrolytes broadens the operating voltage window up to 2 V. However, organic electrolytes can provide large operational voltage, but their high ionic resistance increases the overall equivalent series resistance (ESR) of the device. ASCs can potentially deliver higher power densities as compared to fuel cells, batteries, and symmetric supercapacitors.

b) Composite hybrid supercapacitors (CHSs)

The CHSs are based on the combined properties of both carbon and metal oxides through merging the two types of materials within the same electrode [33,34]. The synergistic characteristics of both materials contribute positively to conductivity, specific capacitance, and cyclic stability. The enhanced performance is attributed to the high conducting and porous nature of carbon materials, which provide a short ionic diffusion path for electrolyte ions. Also, the extreme redox nature of metal oxides promotes high specific capacitance and high energy density [32]. The composite hybrids undergo several challenges of imbalance between the redox activity and conductivity of the composite. Also, dendrites' growth on the surface of porous carbonaceous materials during charge-discharge processes declines the successive ionic diffusion into electrode materials [33]. A composite based on graphene/MnO_2 was successfully synthesized through microwave irradiation by the group of Yan et al. [34]. The composite material displayed a maximum specific capacitance of 310 F/g at 2 mV/s, which is nearly three times larger than pure graphene. The overall performance is attributed to the effective interfacial area and conductivity of the electrode materials.

c) Rechargeable battery-type hybrid supercapacitors

So far, Lithium-ion batteries possess the highest energy density but have shortcomings of small cycle life, low power density, and high cost. These limitations hamper their widespread application in Hybrid Electric Vehicles [35]. On the other hand, EDLCs store energy through the accumulation of charges at the electrode-electrolyte interface via electrostatic forces of attraction. Hence, can deliver very high-power density but suffer from low energy density. To fuel hybrid electric vehicles, both high energy as well as high power densities are required. In an approach to realizing such energy and power requirements within a single device, the concept of battery-type hybrid materials for SCs has emerged. Till now, many studies based on the hybridization of EDLC's, and Lithium-ion batteries materials have been explored [35,36]. In such configurations, the total stored charge is the sum of the charge stored by each component. It has been revealed that electrode configurations, surface modifications, and optimized composition of nanomaterials contribute significantly to the energy and power delivery performances [36]. A suitable example is a work performed by the group Zhang et al. [37]. In an urge to obtain high energy density with no sacrifice in power density, the hybrid SC based on Fe_3O_4/G//3D graphene delivered ultrahigh-energy of 147 W h kg^{-1}, at a power density of 150 W/kg. Interestingly, this energy density was comparable to that of Lithium-ion batteries. However, the major drawback of this approach is the decoupling of energy and power performances of individual counterparts in the hybridized systems. Such limitations can be overcome by optimizing such hybrid electrodes, that take the synergetic use of both battery and capacitor type materials equally rather than dominating.

1.3. Supercapacitor performance parameters and components

Before going through the detailed study and exploration of Sn-based electrode materials for SCs, a brief knowledge of the fundamentals of SCs is discussed here. The whole device comprises several components like electrode materials, electrolytes, separators, and current collectors, which work simultaneously to deliver desirable output. The operation of such physical components results in several key parameters such as voltage, capacitance, energy, and power density that need to consider in improving the overall device performance. These are quite important for determining the deliverable performances of SCs in numerous real-life applications.

1.3.1. Supercapacitor capacitance, voltage, energy, and power density

In a supercapacitor cell, the formation of double layers at the positive and negative electrodes acts as two capacitors connected in series. The overall capacitance (C) of the whole cell is given as Eq. (2) [33–36]:

$$1/C = 1/C_1 + 1/C_2 \quad (2)$$

If the anode and cathode are of the same nature then $C_1 = C_2$ therefore, total capacitance C would be equal to half of the capacitance of either electrode. Such configurations are called symmetric SCs. In another case, if $C_1 \neq C_2$, that is when both electrodes are made from different materials such that their capacitances are different, then net capacitance would be dominated by the electrode with smaller capacitance. This configuration is present in asymmetric type SCs. During the charged state of SC, a potential difference V is developed across the electrode. The theoretical value of energy (E) and power densities (P) is expressed as Eqs. (3) and (4) respectively [33,34],

$$E = 1/2\, CV^2 = 1/2\, (QV) \quad (3)$$

$$P = V^2/4R \quad (4)$$

where Q is the total charge stored in the supercapacitor, and R is the equivalent series resistance of the cell. It is clear from Eqs. (3) and (4) that C, V, and R are the key variables in determining the overall device performance. To increase the energy and power densities, one must focus to improve both V and C values along with reducing the value of R. Such values can be increased by the optimization of electrode materials and electrolytes. Aqueous electrolytes provide a voltage window of up to 1 V, while organic electrolytes provide a wide operating voltage window more than 3 V. The cell voltage window depends on the electrolyte stability within the cell [38]. It is clear from Eqs. (3) and (4) that energy and power densities are directly proportional to the square of voltages. Hence the role of V is more dominant in the energy and power density performance. Also, inner resistance R should be small to enhance the SC performance in terms of power density. Eq. (3) expresses that energy density is directly proportional to the capacitance. The correct choice of electrode materials including their structures such as the utilization of layered electrode structure helps in capacitance enhancement.

1.3.2. Electrode materials

As discussed above, electrode materials are considered an important parameter in enhancing the capacitance and energy density of SCs. Further improvement in the existing electrode materials is essential for the execution of SCs for progressive applications [39–41]. The term specific surface area of electrode materials gives a general idea for the capacitance improvement, but in actuality, it is the electrochemically accessible surface area, which is within reach of the electrolyte ions [39]. Since all the available surface areas do not contribute to the specific capacitance. Only the area with appropriate porous morphology and optimized pore size distribution comparable to the ionic size contributes significantly to the diffusion of electrolyte ions into the electrode materials. Electrode materials for SCs are generally classified into three categories: (1) carbonaceous materials [38], (2) conducting

polymers [25], and (3) metal oxides and hydroxides [32–34].

1.3.3. Carbon materials

Carbon materials are the most employed electrode materials for EDLCs, more profoundly the carbon nanoarchitectures. Their advantages include huge abundance, low cost, smooth processing, high electronic conductivity, mechanical stability, large specific surface area, and nontoxic nature. Based on the morphology, pore size distribution, surface area, and carbon content, the carbonaceous materials are classified as:

1. Carbon foams (microporous), carbon nanofibers, carbon aerogels, and carbide-derived carbons [5,38]
2. Graphene and carbon nanotubes (CNTs) [37,42,43]
3. Activated carbons (ACs) [44]

Several reviews have appreciably described these materials along with performance evaluations [5,6,26,41,42,44]. To match the theoretically predicted high specific capacitance values of real SCs with the experimentally determined values, several approaches are going on. One such effective approach is the doping of heteroatoms such as nitrogen, oxygen, sulfur, or boron into the carbon nanoarchitecture [45], as shown in Fig. 3(a) [46]. It is reasoned that heteroatom doping in carbonaceous structures increases the hydrophilicity, leading to improved wettability of the electrode surface. Also, these heteroatoms boost the redox reactions through the generation of more electroactive sites on the surface of porous carbon structures. For example, Li et al. [47] prepared nitrogen/sulfur co-doped porous graphene hydrogels through the self-assembly technique. The device delivered a specific capacitance of 251 F/g, the energy density of 4.7 Wh kg^{-1}, at a power delivery of 25.47 kW/kg with 96.8 % of maintenance of capacitance after 2000 cycles (Fig. 3b). Another method to increase the capacitance of carbonaceous materials is the introduction of conducting polymers or transition metal oxides [32–34]. In summary, future research directions must focus on the development of carbon materials possessing large electrochemically active surface area, appropriate pore size distribution, and surface optimization to improve the overall performance without sacrificing stability.

1.3.4. Conducting polymers (CPs)

Conducting polymers due to their excellent redox behaviour are considered high-performance electrode materials for SCs. Their potential advantages include low cost, rich conductivity in the doped state, low toxic nature, wide voltage window, excellent reversibility, and adjustable redox behaviour during chemical reactions [47,48]. The different conducting polymers are polythiophene (PTh), polyaniline (PANI), poly(3,4-ethylene dioxythiophene) (PEDOT), and polypyrrole (PPy) [49]. They exist in various morphologies, such as nanotubes, nanowires, nanofibers, nanorods, nanoarrays, and nanorings. Their working mechanism includes, during oxidation motion of ions occur towards polymer chain and during reduction, the same ions are ejected from the chain into the electrolyte medium. Here, the entire polymer body contributes to the redox reactions with high reversibility. Recently Zhou et al. [49] synthesized hydrogel of pure PANI nanofibers with the help of $V_2O_5.nH_2O$ using in-situ polymerization. The 3D assembled hydrogel consists of a cross-linked nanostructure and possesses high conductivity of 0.12 S/cm. The electrode achieved a specific capacitance of 636 F/g at a current density of 2 A g^{-1} with 83.3 % capacitance retention after 10,000 cycles. The study reveals the high conducting behaviour of CPs in the field of energy storage. In another study, Yang et al. [48] successfully fabricated a flexible supercapacitor based on PEDOT/PANI hydrogel. The device showed good performance with deliverable outcomes of a high volumetric energy density of 0.25 mW h cm^{-3} at a power density of 107.14 mW cm^{-3}.

1.3.5. Metal oxides (MOs)

MOs and their complexes have been used for conveying high energy density and excellent conductivity than carbon materials in energy storage [50–52]. One of the biggest limitations of SCs is their low energy density. Therefore, to improve this parameter, metal oxides are the most anticipated electrode materials for SCs. They are highly valued as they provide both electrostatic as well as faradaic storage of charges with

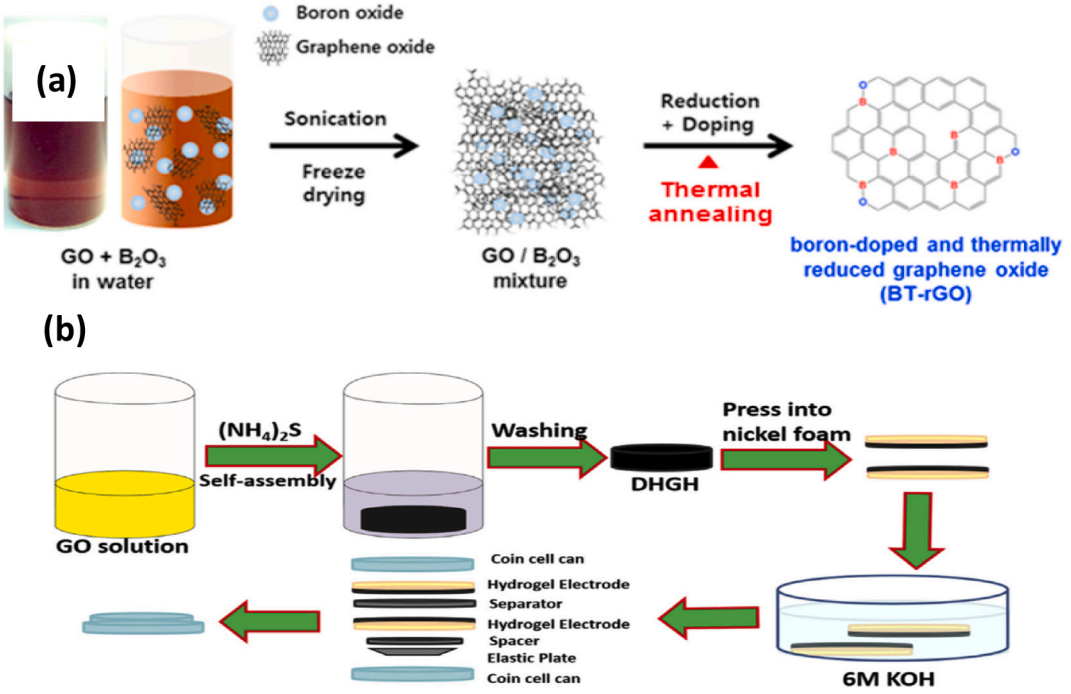

Fig. 3. An effective approach to improve the surface chemistry is the doping of heteroatom: (a) graphene oxide doped with boron was synthesized by thermal annealing of GO/B_2O_3. Reproduced with permission. [46] Copyright 2015, Nature Publisher; (b) The representation for the synthesis, assembling process, and internal structure of the coin cell shaped SC. Reproduced with permission. [47] Copyright 2017, Elsevier.

large operating potential windows [37]. The major energy storage relevant properties of metal oxides are: (1) high electronically conducting nature, (2) presence of a large no of oxidation states, (3) huge natural abundance, and (4) easy tunability with various dimensional architectures. The most researched metal oxides include RuO_2, MnO_x, V_2O_5 etc. [50,51]. Many reviews have significantly described the latest advances made in metal oxides and their composites as electrode materials for SCs [33,34]. For example, compared to the mono metal oxides NiO and Co_3O_4, the composite material spinel $NiCo_2O_4$ has two to three times higher electrical conductivity [53]. Also, compared to the bulk counterpart, the composites of metal oxides with porous nanostructures are highly desirable to obtain a large specific surface area. The optimized design of nanoarchitecture with unique pore size distribution and appropriate SSA helps in improving the capacitance of metal oxides-based electrodes. For instance, hierarchical mesoporous SnO_2@Ni-Co_2O_4/N-MWCNT acquired a specific capacitance of ~728 F g^{-1} (at 4 A g^{-1}) in 6 M KOH electrolyte with 92 % capacitance retention after 5000 cycles [54]. Apart from the above-mentioned strategies, the hybridization of metal oxides with other high electronic conducting materials is quite popular to increase the electroconductivity of metal oxides.

1.3.6. Electrolytes

In addition to the electrodes, an electrolyte that exists between the two electrodes and the separator is a key component of SCs. A suitable electrolyte for SC must have a wide voltage window, rich ionic concentration, low resistivity, large electrochemical stability, small toxicity, lost cost, and high purity [41]. Depending upon the constituents, they are classified into three categories: (a) aqueous electrolytes, (b) organic electrolytes, and (c) ionic liquids (ILs) [55,56]. Aqueous electrolytes provide a huge concentration of ions as well as high conductance than organic electrolytes. They include H_2SO_4 (aq.), KOH (aq.), Na_2SO_4 (aq.), NH_4Cl (aq.) [57]. For high capacitance and power delivery, these are far better than organic and ionic liquid electrolytes. Their synthesis route is also cheap, simple, and does not require strict processes to control ionic size. However, a small voltage window of about 1.2 V is the major disadvantage of aqueous electrolytes and restricts SCs to deliver high energy density. It is suitable to use organic electrolytes to obtain a large voltage window [58]. These are propylene carbonate, acetonitrile, ethylene carbonate–diethyl carbonate, and so on [59]. The major benefits of organic electrolytes include a large electrochemical operating window, wide operating temperature range, environmental friendliness, and good conductivity. Organic electrolytes mainly suffer from high resistance and less chemical stability. Among various electrolytes, ionic liquids (molten state of salts at room temperature) are gaining huge research attention [60]. Their wide operating voltage window ranges from 2 to 6 V and their high conductivity of up to 10 mS cm^{-1} makes them unique among all electrolytes [61]. Since these are solvent-free, so provide well-identified ionic size. Also, the low vapour pressure, and large thermal, and chemical stability make them extremely suitable for high-performance SC devices.

1.3.7. Separators

The good dielectrics that provide maximum conductance of electrolyte ions through them are called separators. Like other components of SCs, these are also of huge importance, as they help sustain cell functions [62]. A good separator must be: a) non-conducting, b) provide high permeability to electrolyte ions, c) must hold low intrinsic resistance to the flow of ions, d) must have high mechanical strength, e) possess high wetting nature, f) should possess electrochemical stability in the electrolyte. The available separators are made up of glass, ceramics, papers, conducting polymers, cellulose-based electrodes, etc. [63]. Polymer-based separators are in huge demand due to their low cost, flexibility, and porous nature. The various polymeric separators are polyamide, polypropylene, polyvinylidene difluoride, polypropylene-carbonate, and polyethylene [64]. Cellulose-based electrodes in SCs have been considered as a favourable separator because of many unique properties such as natural biopolymer, an excess of hydroxyl reactive surfaces, admirable wettability, low production cost, biocompatibility, great mechanical properties [65]. Although huge research is going on SCs, very little research has been focused on exploring separators. But it should be noticed that separators also affect negatively the performance of SCs if not utilized properly. As they can either short the circuit or can induce additional resistance in the cell. The group of Szubzda et al. [66] has studied the effect of plasma modification on the separators made of polyamide and polypropylene polymer. They conclude that the modification improves the overall wettability of the separator by electrolyte and results in increased power performance. In an interesting study, Shulga et al. [67] have employed oxidized graphene oxide as separator materials for SCs.

1.3.8. Current collectors

The role of current collectors (CCs) in SCs is quite appreciated, as they take the responsibility to efficiently transfer the charges during charge-discharge processes. They usually do the collection and conduction of electric charges from electrodes to the load as well as from supply to the electrodes [68]. An ideal CC must possess low contact resistance with the electrodes, high electrical conductivity, high chemical stability, and a large conductive surface area [69]. The commonly used CC are aluminium, iron, nickel foam, steel, etc. [70]. Since CC enhances the electrochemical performance of SCs, therefore recent research is focusing to modify them. For example, surface modification of CC by using laser ablation, nanostructured morphology, and chemical activation [70]. Recently, Liu et al. [71] have summarized the recent advancements made in the nanostructured current collectors for pseudocapacitive electrode materials. They emphasized that the utilization of both nanosized current collectors and electrode materials improves the charge transfer efficiency by providing a large conductive surface area to the electrodes. Furthermore, recently a group by Huang et al. [72] employed laser treatment on aluminium CC to obtain hierarchical nanoarchitectures on the surface. Such modifications contribute positively to the overall device performance.

1.4. Applications of supercapacitors

If we explore the past and present of SCs, we will realize huge development in all the aspects of this technology [1–7]. Such advances include improvements in both the energy and power densities of SCs. Simultaneously, SCs possess a wide range of applications [73]. Due to rapid power delivery with ultralong cycle life, the SC demand is progressively increasing in consumer electronics. Since such devices require instantaneous power to operate their various features. The various SC-driven consumer electronics are LED flashlights, internet, wireless remote control, screwdriver, signal transmission in mobile phones, etc. [74]. Another broad area is the automotive industry where SCs are currently utilized in electric vehicles (EVs) and hybrid electric vehicles (HEVs) [74]. They are used under applications such as regenerative braking, powering of onboard electronic features, and start and stop systems. Since batteries with low power density are not able to provide peak loads during acceleration hence, SCs are utilized to fulfil such demands. Also, combining SCs with batteries in HEVs result in highly improved performances such as easily starting in extremely cold weather, enhanced battery life, and powerful acceleration. Railways are also part of SC applications as they provide safety, efficiency, power quality, energy conservation, and power recuperation [75]. In the renewable energy sectors such as wind energy and solar energy, SCs are quite potential devices for energy storage. Presently, SCs are extremely applied in wind turbines. Their usage involves pitch control and powers them to adjust their blades in the wind direction for smooth power output [76]. According to Maxwell technologies [77], nearly 20–30 % of the global wind turbines are equipped with SC pitch control systems. With the progress in the deployment of renewable energy sectors, SCs will be in huge demand for energy storage in the future. According to the

new studies, SCs can effectively be applied in the grid integration of renewable energy sectors [78].

2. Sn-based electrode materials for supercapacitors

Tin-based electrode materials are quite promising and well known for electrochemical energy storage. Its unique properties like low cost, high chemical stability, large theoretical capacity (~992 mAh g^{-1}), and environmentally benign nature make it a superb energy storage material [15,17].

Although tin possesses outstanding properties, its low electrical conductivity and poor electrochemical stability are the major limitations that need to be overcome. Introducing conducting phases like the incorporation of carbon-based materials, other metal, or metal oxides, and conducting polymers are a few approaches proven to improve the cyclic stability and rate capability. The tin-based materials are enormously explored in gas sensors, solar cells, photocatalysts, lithium-ion batteries, and supercapacitors [15,17,18,79–84]. Herein, we provide an in-depth review of Tin-based oxides, sulfides, and the hybrid form reported in the literature (Fig. 4).

2.1. Tin based oxides ($SnO_{x=1\&2}$)

The hydrous RuO_2 electrode material is found to be the most suitable material for supercapacitor electrodes due to its extraordinary capacitance properties. However, due to the inadequate abundance and therefore high cost, the wide usage of RuO_2 in supercapacitors is limited. Hence, efforts have been derived to explore inexpensive metal oxides, such as MnO_2, Fe_2O_3, SnO_2, NiO, and Co_3O_4 for supercapacitor applications [50]. Among various metal oxides, SnO_x is a suitable semiconductor and gained huge attention as an SC electrode material due to its significant advantages. Firstly, they possess a large theoretical capacity (≈780–1378 mAh g^{-1}), better electronic conductivity (21 Ωcm), high electron mobility (100–200 cm^2/Vs) and thus show high power density [85,86]. Secondly, these possess a low potential window and charge-discharge plateau, excellent corrosion-resistant electrode against acidic/alkaline electrolyte with wide stable potential window. Third, these are high temperature and chemically stable compared to other metal oxides and thus hold a long lifetime. Forth, these are cheap and environmentally friendly and allow for a long range of morphology and structures [87]. These unique features make them high-performance electrode materials for SCs. Generally, Sn possesses two valences which make two different oxides, one is Sn with divalent leads to the formation of tin monoxide (SnO), and the other one is Sn with tetravalent which leads to the formation of tin dioxide (SnO_2). The phase of

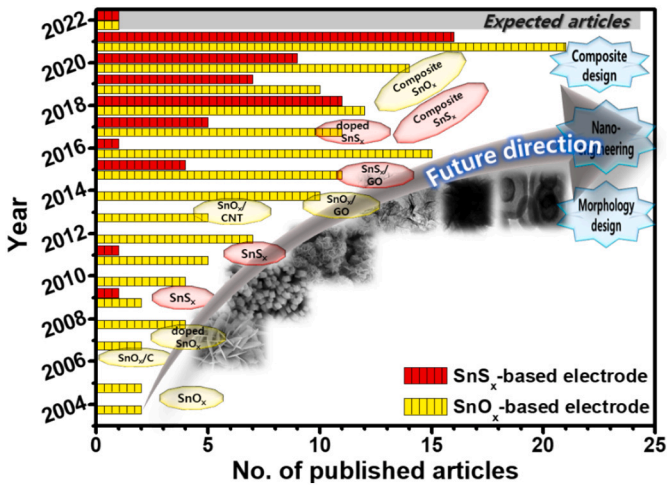

Fig. 4. Timeline of key strategies and results for Sn-based material for SCs.

SnO_2 is more thermodynamically strong than that of the SnO under usual environments and therefore it has been extensively explored for various applications. On the other hand, the synthesis of pure SnO is comparatively challenging compared to SnO_2 due to its valence state of SnO to SnO_2 might be impulsive under a basic room environment based on the formation of standard Gibbs free energy [87]. Many research studies conducted on Sn oxides have shown the different methods for the synthesis of electrode materials like sol-gel synthesis [72], arc plasma [88], hydrothermal synthesis [89], chemical precipitation [90], pulse microwave deposition [91], and electrochemical deposition [92]. These studies have specified the use of tin-based oxides in SCs. Supercapacitor performance is extremely dependent on the morphology of electrodes, and therefore improved performance is quite observed with porous morphology of various dimensions [93–95]. Thus, facilitates the better penetration of electrolyte ions within the pores of electrode material.

2.1.1. Pure $SnO_{x=1\&2}$

Sn-based materials with porous architectures have been widely explored. Zhao et al. [15] have summarized Sn-based nanomaterials for electrochemical energy storage, specifying the direct relation between nanostructures and electrochemical performance. For example, Liu et al. have synthesized hierarchical SnO_2 nanostructures by a facile hydrothermal method. This technique is simple, cost-effective, and provides a green synthesis route for the industrial production of SnO_2 nanostructures. The 3D hierarchical SnO_2 morphology allows short ionic diffusion pathways for the electrolyte ions to penetrate as well as can alleviate the volume changes occurring during the charge/discharge process [23]. In 2004 for the first time, Prasad et al. introduced nanostructured SnO_2 for redox SCs application. The active materials were directly deposited on the stainless steel electrode and used for evaluating SCs performance. A high capacitance value with 285 F/g at 10 mV/s and 101 F/g at 200 mV/s were achieved which were higher than some of the other reported composites SnO_2 values [96]. Next year, Rao et al. prepared SnO nanoparticles by hydrothermal process from urea hydrolysis and applied them for the first time as electrode material for the SC. A maximum specific capacitance of 17.3 F/g at a scan rate of 100 μA was obtained with 1000 charge/discharge stability [97]. The obtained values and exploration are very low and limited and therefore further electrochemical performance for SC materials needs to be explored. In this regard, Wang et al. [87] established a simplistic, straight ultrasonic synthesis of gram-scale and shape-controlled SnO using anhydrous $SnCl_2$ and the organic solvent of ethanolamine (ETA). The ETA alkalinity and ultrasound play a vital role in the formation of SnO as the prepared SnO in nanocluster form and changes to microplates after the hydrothermal process. The prepared SnO with the morphology of nanoclusters and microplates shows a high specific capacitance of 208.9 F/g at a scan rate of 0.1 A/g and an admirable rate capability of 65.8 F/g at the scan rate of 40 A/g with better cyclic performance (10,000 cycles with 119 % retention). The innovative synthetic method for SnO is an appropriate and prospective means for other energy materials which are believed that will be open a new way for the synthesis of large-scale other metal oxide nanoparticles with higher SCs performance [87].

In general, the preparation of innovative nanostructured electrode materials by tailoring the shape, size and morphology play an important role in their properties and nanotechnology applications. The layered SnO micro-plates were prepared using ammonia as a reducing agent via a low-temperature hydrothermal method. By altering the ammonia concentration, the surface morphology, crystal structure and thickness of SnO (Fig. 5(a)) can be easily altered which has notable effects on their supercapacitor performance. It exhibited a great specific capacity of 1080 Fg^{-1} at the scan rate of 1 A g^{-1}, which achieves ~75 % of its theoretical faradaic capacitance. Also, the specific capacity preserves about 849 F/g after the 1000 charge-discharge process, displaying great cyclic stability that is presented in Fig. 5(b) [99]. Controlling shapes and structures of SnO_2 nanostructure to be considered an important factor in their chemical, physical, and optoelectrical properties, which influences

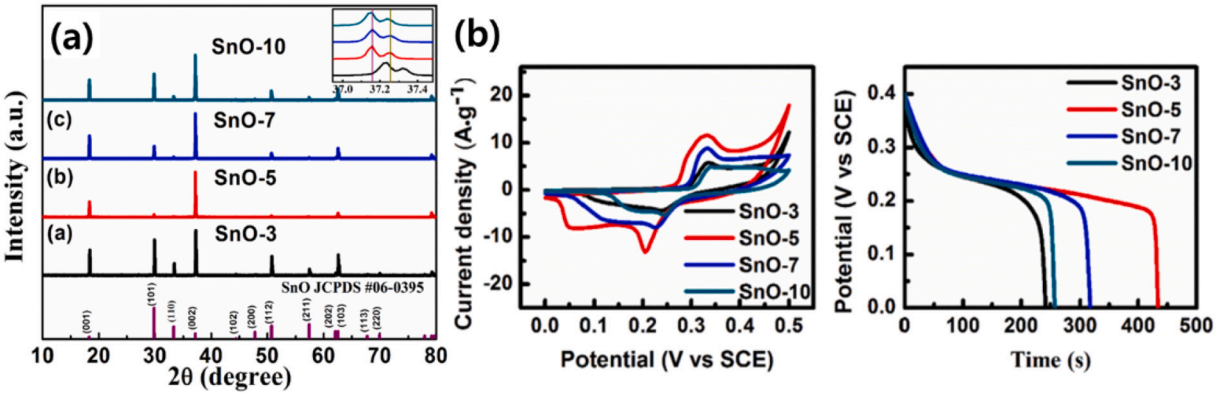

Fig. 5. (a) XRD pattern of all prepared samples, and (b) CV and CD profiles of all SnO electrodes measured at the same scan/current rate. Reproduced with permission. [98] Copyright 2017, Elsevier.

electrochemical performance. There is various kind of morphology of SnO_2 like nanoparticles, nanowires, nanosheets, nanorods, nanotubes, nanobelts etc. have been reported. The 3D assembled construction has been hardly found because of very slow progression which restrictive the structures in few nanometres with poorly organized aggregation as Zhuang et al. found out the aggregation-induced growth from nano-SnO_2 to bulk SnO_2 for a longer treatment time [98]. In this case, Wei et al. prepared SnO_2 nanostructured materials with uniform pores distribution by a gas-liquid interfacial reaction in an autoclave and allows to adjust the aggregated particle sizes through the amount of ethylene glycol and water. The prepared electrode exhibited outstanding charge-discharge cyclic performance over 1000 cycles with ~97 % capacity retention. The improved electrochemical performance could be ascribed to the presence of the nanopores SnO_2 aggregation nanostructure, which enhances the surface area between the as-prepared electrode and electrolyte, prominent to an improved supercapacitor performance [100].

One of the key disadvantages of SnO_2 as electrode material is the low specific capacitance, which hinders its practical use. Nanocrystalline porous SnO_2 thin films as electrode materials were successfully synthesized by Pusawale and co-workers by applying a chemical route onto a directly stainless-steel substrate. The prepared electrode showed high pseudocapacitance activity of 66 F/g in 0.5 M Na_2SO_4 electrolyte with a scan rate of 10 mV/s [20]. Similarly, Yadav et al. [101] deposited SnO_2 films by spraying pyrolysis technique with the effect of $SnCl_4$ which affects the film properties such as crystallinity, shape and size, optical, and SC properties. The films displayed a better SC activity with a maximum capacitance value of 119 F/g at a scan rate of 10 mV/s. Thus, based on the above results, it could be said that the SnO_2 thin films based electrode could be one of the capable electrodes for use in SCs.

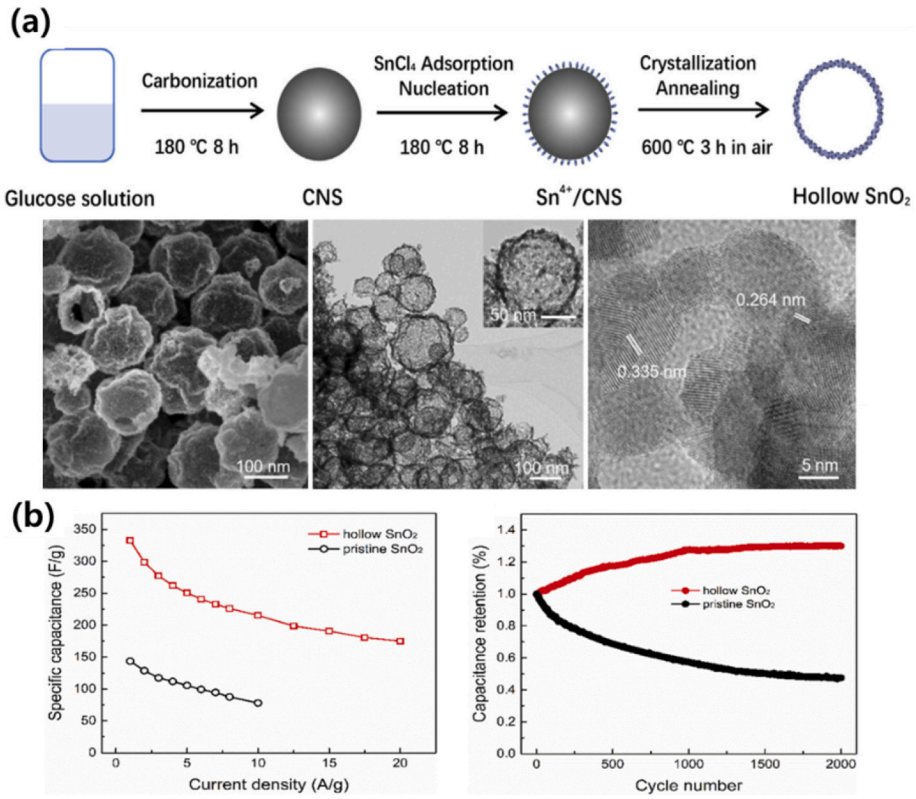

Fig. 6. (a) Schematic diagram of the preparation of SnO_2 nanospheres, and (b) specific capacitance and cyclic performance of the samples. Reproduced with permission. [105] Copyright 2017, Elsevier.

Furthermore, the electrochemical activity of SnO_2 can be upgraded by dropping the particle size and morphology of the prepared nanoparticles and current collector, which was experimentally confirmed by several studies. With the advantage of hollow geometry, several hollow structures such as hollow spheres, and hollow fibers with promising energy storage properties have been reported [102,103]. The unique hollow geometry not only provides a higher surface to volume ratio area that contributes to higher capacitance but also facilitates shorter ion diffusion pathways and accommodation for large volume variation, hence improving the rate capability and providing good cycling stability [104]. For example, Kang et al. [105] prepared the hollow SnO_2 nanospheres from carbon spheres as the template in the autoclave, which has a uniform and single shelled structure (Fig. 6). The prepared SnO_2 materials showed a significant capacitance value of 332.7 F/g at 1 A/g and better cycling performance over 2000 charge-discharge times, which is considerably higher than the pristine SnO_2 particles (143.5 F/g).

The higher capacitive behaviour could be credited to its single shell and nanoscale size hollow SnO_2 structure, providing high surface area and hierarchical porosity, which ultimately enhance the performance. Dodoo-Arhin et al. [106] prepared well crystalline SnO_2 particles with various morphology and structure in the range of 2–10 nm by hydrothermal synthesis under mild conditions using different surfactants and reducing agents and checked its effect on the electrochemical analysis. CV results in Fig. 6 [106] showed two main peaks, a broad cathodic peak and anodic peaks related to the redox peak of Sn^{+4} and Sn^{+3}. The electron addition phenomena for the SnO_2 electrode is shown in the following reaction scheme [106]:

$$Sn^{IV}O_2 + e^- \text{ (external)} + H^+ \text{ (solution)} \rightarrow Sn^{III}O\,(OH^-)$$

A capacitance value over 1.6 F/g at a 5 mV/s scan rate with pseudocapacitor behaviour was achieved. This low capacitance values noted possibly be ascribed to the poor conductivity of the synthesized SnO_2 nanoparticles, which is apparent from the high internal resistance [106]. Studying the unique characteristics of smaller size nanocrystals like quantum dots (QDs) can provide the increased interface for the interaction between SnO_2 and other phenomena on facts behind the improved performance and it also helps in applying QDs or reduced size nanoparticles vast in diverse applications. Bonu et al. prepared pure SnO_2 quantum dots and bigger size nanoparticles with different compositions by a simple soft chemical method and studied them as electrode materials for SCs and compared them with bigger size nanoparticles [107]. The specific capacitance of the SnO_2 QDs was obtained at 10 F/g at a 20 mV/s scan rate which is about 9 % decay in the capacitance upon increasing the scan rate to 500 mV/s. A set of broad peaks showed up at 0.12 (cathodic) and 0.135 (anodic) for SnO_2 QDs whereas one set of distinctive redox peaks showed up at 0.25 (cathodic) and also at 0.32 (anodic). Redox transformation of SnO_2 related to those peaks could be written as [107]:

$$SnO_2 + K^+{}_a + e^- \leftrightarrow SnOOK_a$$

Change in the peak position towards the higher possible potential side in the instance of 25 nm NPs of SnO_2 is because of the prevented redox/electronic shift in the SnO_2. In the instance of QDs, there is a presence of a simplistic diffusion layer of ions as a result of its hydrous

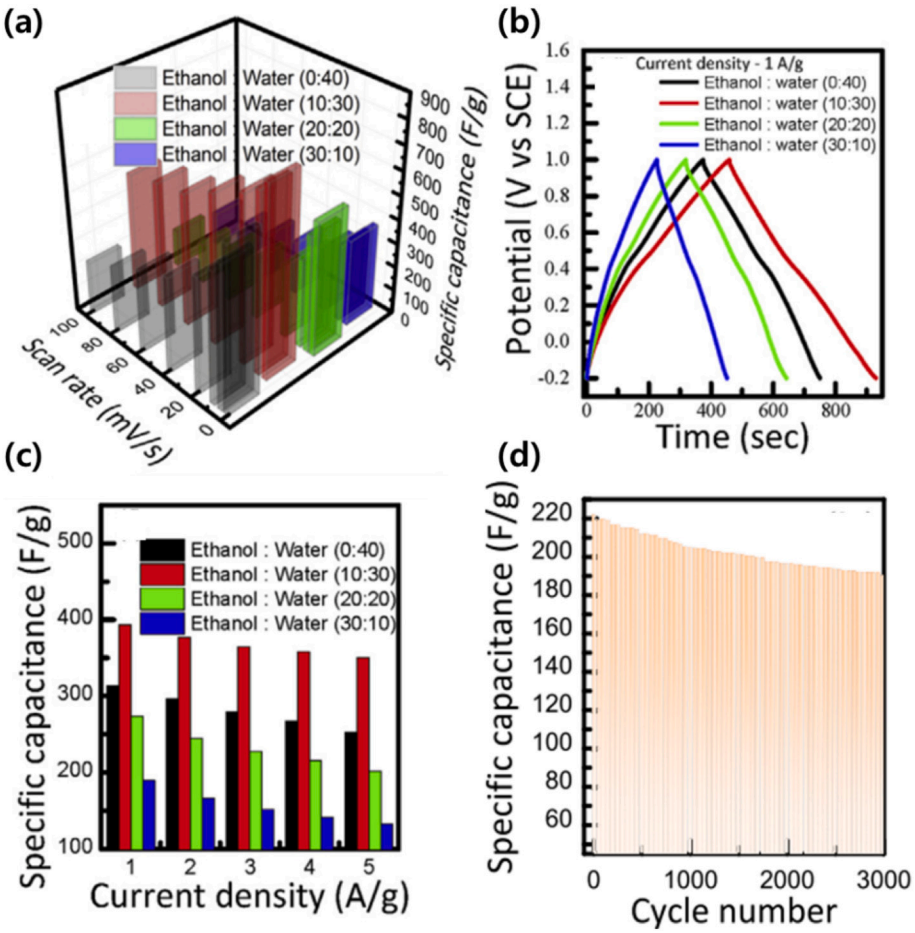

Fig. 7. (a) specific capacitance as a function of scan rate, (b) charge-discharge profile with different ethanol to water content, (c) specific capacitance with the variation of current density, (d) Cyclic stability from specific capacitance as a function of cycle number at 1 A/g. Reproduced with permission. [94] Copyright 2017, Elsevier.

structure which hampers the ionic flux in the direction of the electrode.

Capacitance decay for the SnO_2 QDs is less than 2 % after 1000 cycles of stability, while 8 % remained for the bigger particle size [107]. Similarly, Geng et al. [94] took an effort to prepare a simple, greener and fast synthesis of SnO_2 QDs with 4–6 nm particle size using only precursor without any surfactant/reagent as an active material for solid-state asymmetric supercapacitor (ASC) for the first time. The capacitance values decrease with scan rate for all the samples that are ascribed to the diffusion result as represented in Fig. 7(a). The prepared electrode displays a pseudocapacitive nature with the capacitance over 315 Fg^{-1} at 1 A g^{-1} current density in a 3-electrode testing scheme. Further, the ASC system, exhibited higher capacitance, energy density, and long cycle performance (Fig. 7(b–d)). The reason behind the improved performance is the high surface area which allows more interaction or active sites between SnO_2 and the other species [94]. The novel studies about the SnO_2 quantum dots can benefit in applying it capably in a wide range of application from electronic and optoelectronic.

It is well understood that the reasons influencing the performance depend on particle sizes and testing conditions such as electrolyte, and its concentration scan rate. Few other characteristics such as surface electrode activation, oxygen content, surface oxides and lattice defects influence the performance which is resulting from the preparation process. Mevada et al. [86] successfully synthesized SnO_2 nanoparticles using gallic acid monohydrate with the help of the precipitation method as shown in Fig. 8. The nanocomposite consists of spherical morphology with a size under the range of 6–55 nm as mentioned in Fig. 8(b). The S-SnO_2NPs@ETCC electrode exhibited a high specific capacitance of 523 F/g at a scan rate of 5 mV/s. As a device, the symmetrical supercapacitor displayed good specific capacitance (156 F/g at a scan rate of 5 mV/s), and capacitance retention of up to 94.7 % after 5000 charge-discharge cycles at 20 A/g current density [86]. In order to store charges, two steps are involved, as shown in the following process [86]:

$$SnO_2 + \alpha H^+ + \alpha e^- \leftrightarrow SnO_{2-\alpha}(OH)_\alpha$$

While proton transfer from the electrolyte to the electrode surface is observed during discharging (S-SnO_2NPs@ETCC), the phenomenon is reversed upon charging when the proton departs from the electrode surface and moves back into the electrolyte. The general low capacitance recorded for the SnO_2 nanoparticles from the various treatments can be attributed to the low conductivity of SnO_2. Although SnO_2 has the characteristics to be used as an SC electrode, this material further needs attention to improve both the capacitance and conductivity.

Many researchers tried to synthesize tin oxide-based composite materials, as a strategy to improve both the capacitance and electronic conductivity. Hence, these are incorporated with other materials like carbonaceous materials [26], metal oxides [50] and conducting polymers [108].

2.1.2. *SnO_x on carbonaceous materials*

Tin oxide is considered one of the widely explored metal oxides for

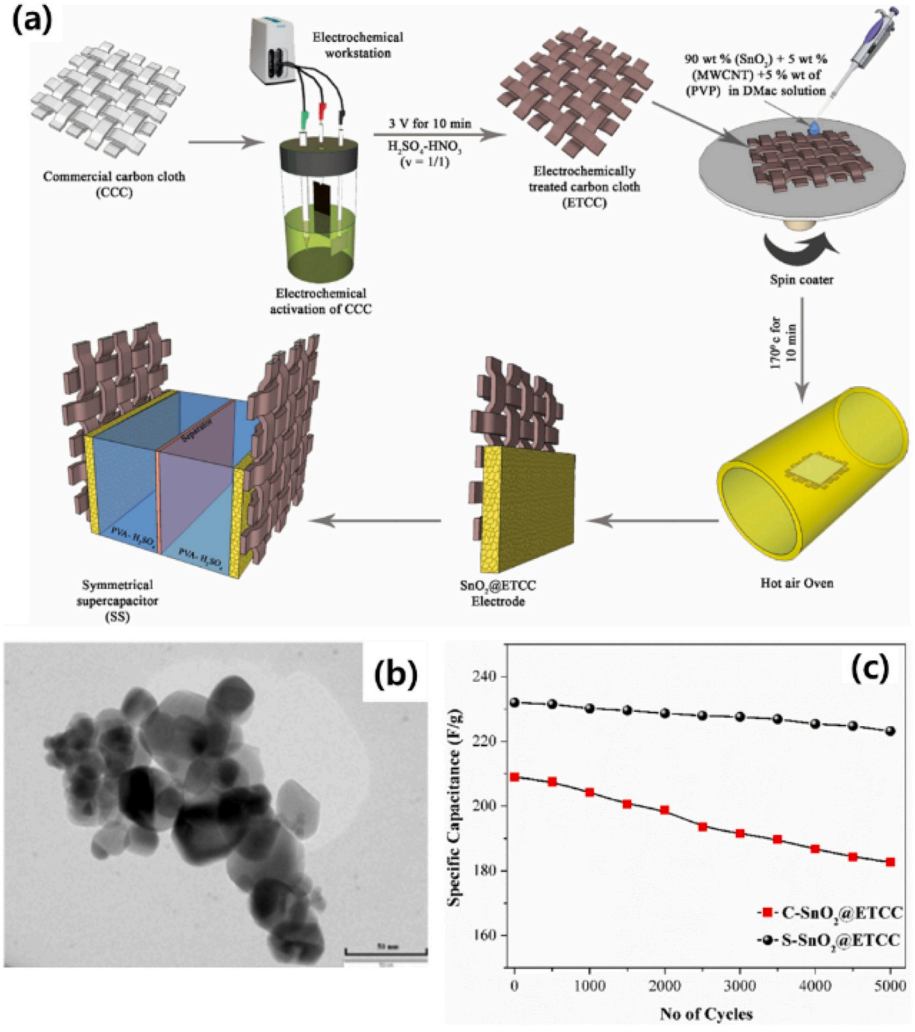

Fig. 8. (a) Schematic diagram of preparation of S-SnO_2NPs@ETCC, (b) TEM images of S-SnO_2NPs, and (c) cyclic performance of the samples for 5000 charge-discharge process. Reproduced with permission. [86] Copyright 2017, Elsevier.

supercapacitor electrodes, due to its capability for fast redox reactions at the electrode surface. However, this oxide faces the drawback of low electrical conductivity [109–111]. Substantial efforts like the incorporation of highly conducting carbon-based materials such as graphene, carbon nanotubes, and activated carbon have been done to enhance the supercapacitive performance of tin oxides. Carbon-based electrode materials are of particular interest due to their low cost and ability to possess both high specific capacitance and power density delivered by their high surface areas. Their incorporation with the active electrode material improves the electrical and electrochemical properties.

2.1.2.1. Graphene. Graphene is a monoatomic-thick two-dimensional single layer of C atoms, that has been applied as a unique class of electrode materials because of its excellent electrical conductivity, better capacitive performance, large surface area, suitable porosity, and explosive interest from the past. It is well understood from the studies that carbonaceous and metal oxide materials are taking immense attention as electrode materials for various energy storage applications. If coupling the SnO_2 and graphene materials into the active electrodes of SCs, their capacitive activity would be significantly improved as most of the metal oxide contributes pseudo-capacitance behaviour to the overall capacitance values apart from the EDLC from carbonaceous electrodes. Therefore, coupled SnO_2 with graphene for the SCs can boost electrochemical capacitance. In dealing with graphene, one of the essential points is to emphasize the well-organized interaction between the graphene and the other dimensions materials. Associated with the other phases such as SnO_2 nanoparticles and nanowires, the desired phase would be two-dimensional SnO_2 materials because of the 2D phase of graphene. Therefore, suitable surface-to-surface interaction between SnO_2 nanomaterials and graphene pieces could be designed. Li and coworkers prepared for the first time 2D SnO_2 nanoplatelets/graphene nanocomposite by facile hydrothermal process. The proposed composite electrode delivered an improved capacitance value of 294 F/g and better cycling performance compared to pristine SnO_2. The synthesized SnO_2 nanoplatelets attached very well on every edge of graphene sides which barred the graphene sheets from aggregation [112]. In another study, Hsieh et al. fabricated SnO_2/graphene oxide 3D framework for SC electrodes [113]. A high specific capacitance value of 384 F/g at 50 mA/g current density was achieved at almost 98 % compared to the only graphene electrode due to high surface area which enhances the fraction of hydrophilic area, allowing more accessible sites in the electrochemical test. Further, Chang and coworkers introduced a new fabrication process of an atmospheric pressure plasma jet for rapid synthesis of SnO_2-rGO nanocomposites on carbon cloth for SC electrode materials [91]. In this work, they directly used SnCl2 liquid precursor instead of SnO_2 particles blended into the rGO paste which is directly converted into SnO_2 by NAPPJ (Fig. 9(a)) [91].

The areal capacitance of the prepared flexible rGO-SnO_2

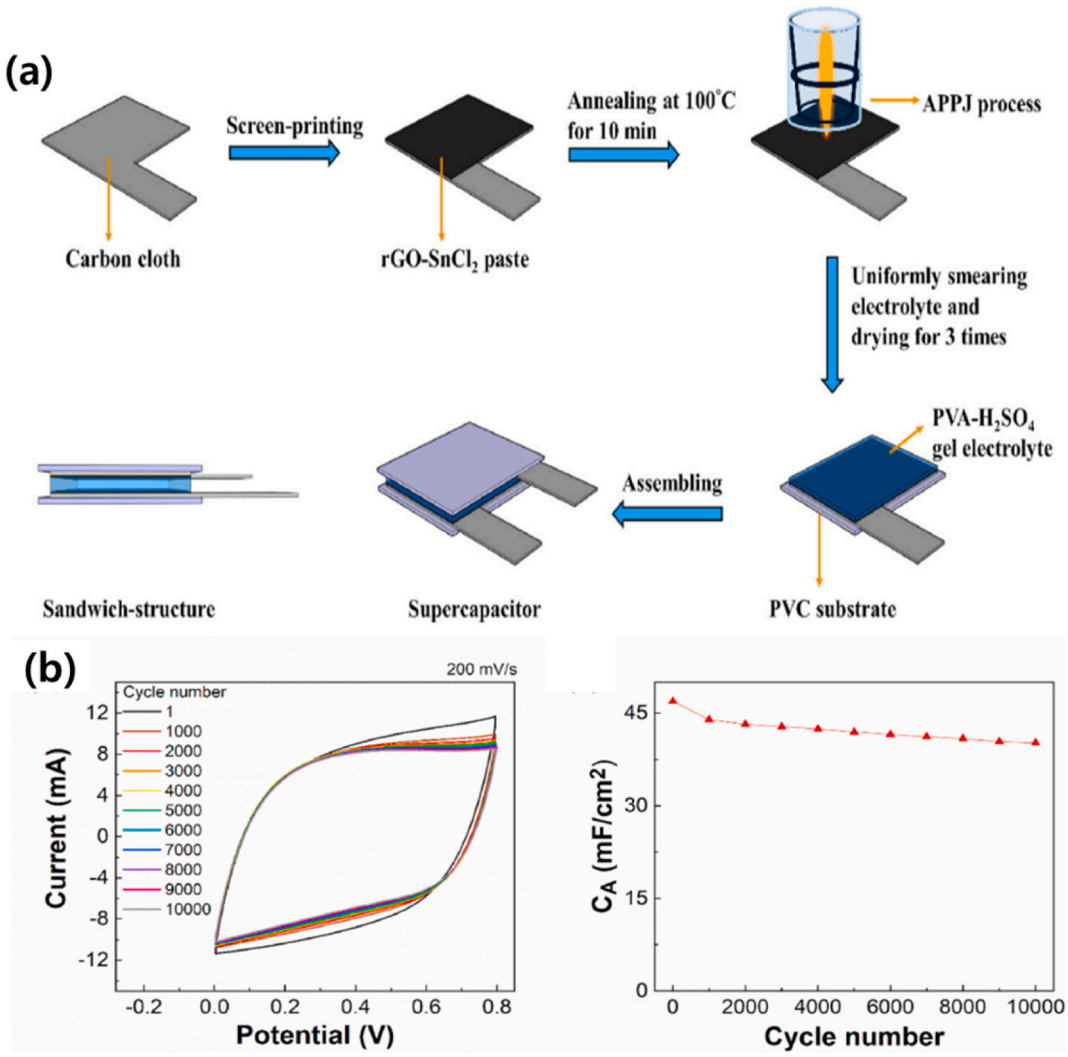

Fig. 9. (a) Schematic representation of rGO-SnO_2 SC fabrication process, and (b) cyclic stability of 10,000 cycles at a scan rate of 200 mV/s. Reproduced with permission. [91] Copyright 2017, Elsevier.

nanocomposites increases with the APPJ treating time and achieves the highest value of 97.5 mF/cm^2 for a treating time of 300 s. It is also showed a capacitance retention rate of ~85 % after a 10,000 long-term cycling test (Fig. 9(b)) and further capacity enhanced by 11 % after a 1000 cycle number under a flexible limit of 7.5 mm with no degradation, markedly due to strong electrode/electrolyte interaction and reduction in the ions transference resistance after the mechanical test.

The basic flexibility of textiles is considered appropriate substrates for smart wearable materials. In the view of SCs, textile flexible substrates are taken as wearable substrates due to their superior flexibility. Kim and co-workers [114] presented a scalable facile, and speedy fabrication procedure supersonic spraying, to coat rGO and SnO_2 on a wearable fabric for flexible SCs applications as shown in Fig. 10.

As can be seen in Fig. 10(a), the rGO/SnO_2 solution was fed on the carbon cloth using a syringe with an atomizer. The atomizer created droplets comprising rGO/SnO_2 and after that fell into hot steam air and vapourised and hence coated directly on the fabric. They studied the consequence of the SnO_2 concentration on the SCs performance of the flexible supercapacitor.

In this system, rGO contributes to the electrical conductivity of fabrics, whereas SnO_2 contributes to active energy storage capabilities. The synergetic behaviour of the mixture of rGO and SnO_2 on the complete electrochemical performance through changing the SnO_2 concentration. Mechanical durability in terms of stretched and relaxing tests for1100 cycles over a time interval of the 2000s, validated the mechanical strength of the wearable and flexible SC (11 (a)). The optimal electrode showed the highest specific capacitance of 1008 mF/cm^2 at 1.5 mA/cm^2, with capacitance retention of 93 % over the 10,000 charge-discharge processes as mentioned in Fig. 11(b). These favourable outcomes endorse that the supersonic spraying method could be appropriate for making large scale wearable SC based on fabrics.

Haldorai et al. [92] reported a facile, and easy route to prepare flower-like SnO_2 nanoparticles decorated graphene electrodes by thermal reduction process composites and used them for SCs application. The nanocomposite displayed a high capacitance value of 396 F/g at 4.5 A/g current density and 1000 cyclic stability (92.6 % capacitance retention) due to the synergetic effect from both SnO_2 and rGO. Similarly, SnO_2 nanoparticles decorated on a flexible cellulose/rGO hybrid framework by a simple hydrothermal process followed by a freeze-drying process. The 3D porous cellulose-based framework was believed to be higher accessibility of electrode-electrolyte through higher surface contact and a short diffusion path for ions/e^- transportation. The prepared electrode showed a high capacitance value of 4.3 F/cm^2 with great cyclic stability and capacitance retention. Thus, the CNFs/RGO/SnO_2 electrodes adequate intersected macrostructured networks that allowed them to realize better capacitive activity which could be applied for flexible supercapacitors [115]. As cellulose-based electrodes have been taken promising for flexible SCs for their flexibility, porous nature, lightweight, and cost-effective, Liu and co-workers have prepared the flexible SC electrode composed of SnO_2 nanoparticles

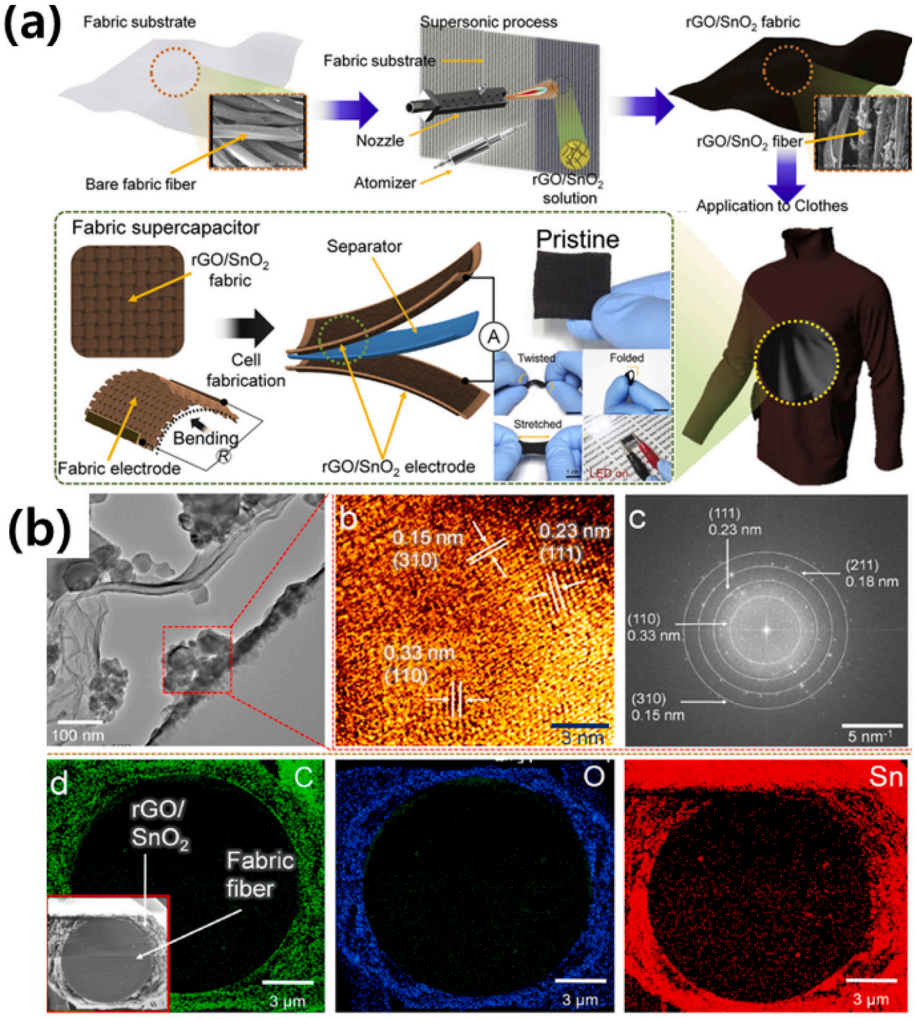

Fig. 10. (a) Schematic diagram of the preparation of flexible rGO-SnO_2 electrode, and (b) TEM images, SAED pattern, and elemental mapping of the electrode. Reproduced with permission. [114] Copyright 2017, Elsevier.

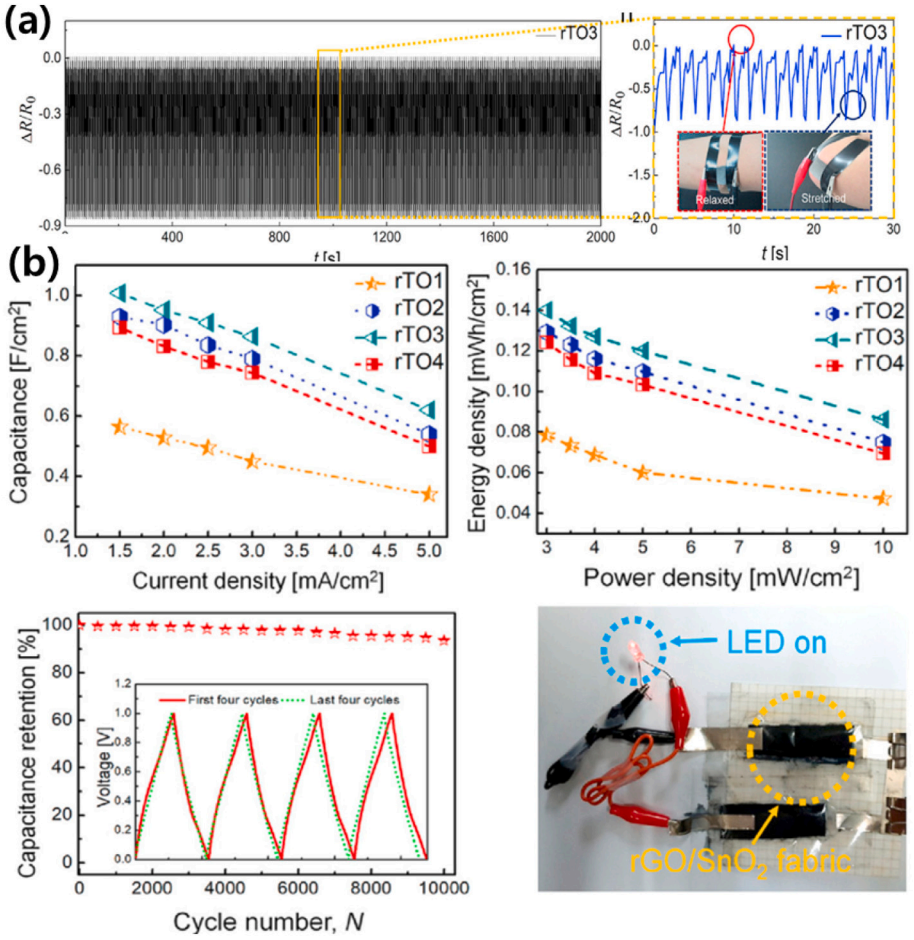

Fig. 11. (a) Resistance change and zoomed view of the optimal sample subjected to cyclic stretching, and (b) SC performances with LED lighting test performed on the electrodes. Reproduced with permission. [114] Copyright 2017, Elsevier.

incorporated GO flakes into cellulose matrix followed by conducting polymer coating. The SCs electrode showed a noteworthy enhancement with the integration of SnO_2 nanoparticles into the framework, e.g. specific capacitance of 445 F/g with almost 84 % capacity retention after the 2500 charge-discharge process. These recent reports further signify the advantages of cellulose with the rGO for applications in energy storage. However, compared to hybrid supercapacitors, EDLCs exhibit relative low specific capacitance.

Recently, the N-doped GO-metal oxide is widely used as electrode material for various applications due to its synergistic effect. The porous SnO_2@NGO nanocomposite for the SC electrode was prepared using urea as a catalyst through a thermal reduction process in the NH_3 environment (Fig. 12). The TEM images show that the nanocrystalline SnO_2 nanoparticles with 10-20 nm size successfully incorporated in NGO presented in Fig. 13(a–c) for low internal resistance and high electrical conductivity [116].

The electrochemical activity of the composite electrode in Fig. 13 (d–e) showed a specific capacitance of ~378 F/g at 4A/g and higher cycle stability with better capacitance retention (89 % after 5000 cycles). The improvement of SCs performance is primarily due to the greater surface area and suitable porosity ascends in the SnO_2@NGO nanocomposite.

Based on the literature studies, reducing the particle size to the nanoscale is one of the possible ways to attain better electrochemical performance due to its unique characteristics. Jayachandiran and coworkers [117] prepared ultra-small SnO_2 nanoparticles by hydrothermal process and blend them with rGO through an ultrasonic-assisted route for SC electrode and compared them with bare SnO_2. The particle size was measured to be with an average size below 10 nm. This is significant for the present synthesis method as the polyvinyl alcohol work as a template, which can hinder the nanoparticle overgrowth and cluster. Additionally, the diethylamine capping agent efficiently

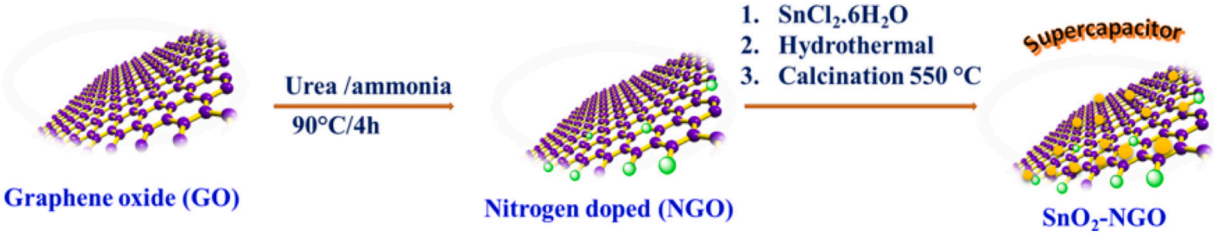

Fig. 12. Schematic diagram of the preparation of SnO_2@NGO by the thermal reduction process. Reproduced with permission. [116] Copyright 2019, Nature Publisher.

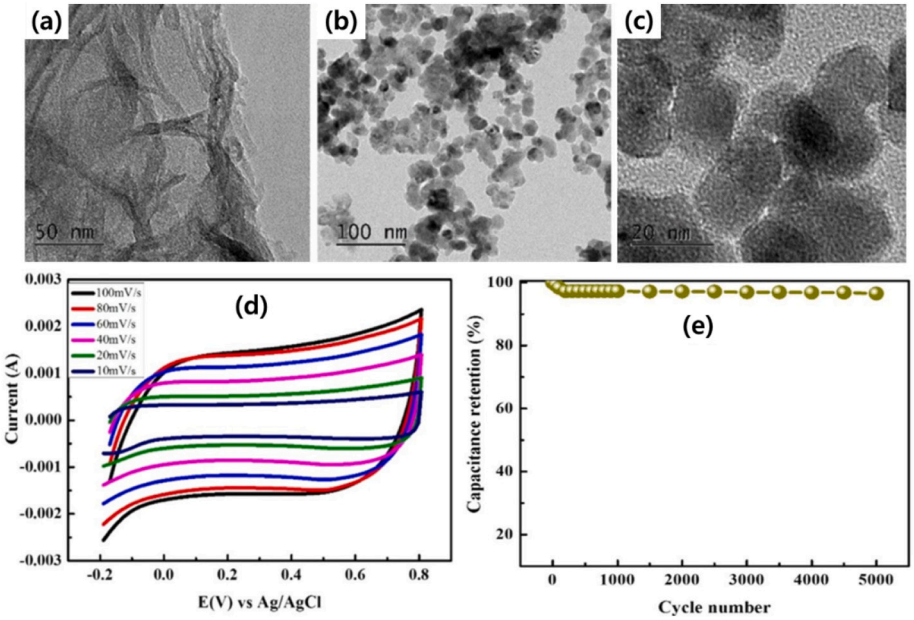

Fig. 13. TEM images of (a) only N doped GO, (b–c) HR-images of SnO_2@NGO composite, (d) CV at the different current rate of SnO_2@NGO nanocomposite, and (d) Cyclic stability of SnO_2 and rGO/SnO_2 nanocomposite as an electrode for SCs. Reproduced with permission. [116] Copyright 2015, Nature Publisher.

passivates the surface and so, precise the particle size, resulting in the development of ultra-small nanoparticles that were uniformly distributed and decorated over and above the surface and the interior of rGO nanosheets. The electrochemical performance of SnO_2 and rGO/SnO_2 nanocomposites exhibited a higher specific capacitance value (545 F g1) at 1 A/g and long cyclic stability and better capacity retention (96 % after 5000 charge-discharge cycles) compared to bare SnO_2 electrode. The values are even higher than the earlier reported values, and the reasons are the uniform distribution of ultra-small SnO_2 nanoparticles on GO sheets which works as a synergistic effect [117]. Lim and co-workers reported a facile solvent-based synthesis of SnO_2/graphene nanocomposite, resulting in an excellent specific capacitance of 363.3 F/g, which is five times more than the graphene-based electrode (68.4 F/g) [118]. The group of Zhang et al. synthesized SnO_2 nanoparticles uniformly distributed on the reduced graphene oxide (rGO) sheets through a colloid electrostatic self-assembly method. The dimension of SnO_2 nanoparticles was found around 5 nm. The output-specific capacitance of the nanocomposite was reported as 347.3 F/g at 5 mV/s in 1 M Na_2SO_4 electrolyte solution [119]. This set of investigations suggests that the construction of nanomaterials with a suitable amount of SnOx on graphene oxide has been explored as a useful approach for the construction of numerous functional nanomaterials for charge storage applications [120–130].

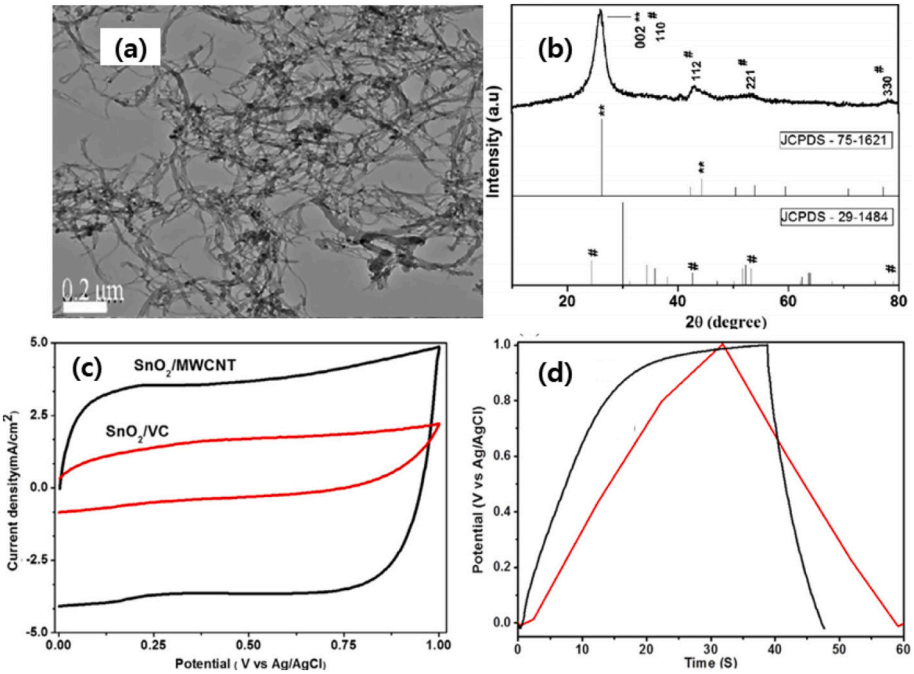

Fig. 14. (a) TEM images and (b) XRD patterns of the SnO_2/MWCNT composite, and CV and CD profiles of (c) SnO_2/VC and (d) SnO_2/MWCNT in 1 M Na2SO4 electrolyte. Reproduced with permission. [131] Copyright 2017, Elsevier.

2.1.2.2. Carbon nanotubes (CNTs). The EDLC storage mechanism is mainly detected for carbon black, GO, mesoporous carbon, carbon nanofibers (CNF) and CNTs with high surface area. Carbonaceous materials tend to show a comparatively high electrical conductivity. Whereas, the pseudocapacitive behaviour with Faradaic reactions is mostly detected in the transition-metal oxides. For instance, the conductivity of MWCNT (1.85×10^3 S/cm) is higher than that of graphene (3.51×10^2 S/cm). CNTs are being considered a promising material for their feasibly suitable structural, optical, mechanical, and electrical properties. CNTs also possess a unique 1D cylindrical nanostructure with a vastly available surface size, low resistivity, and great stability. A comparison in the specific capacitances of SnO_2/MWCNTs and SnO_2/VC nanocomposites (Fig. 14) is reported by Vinoth et al. [131]. A facile sonochemical method is adopted for the synthesis and accordingly, the specific capacitance of SnO_2/MWCNTs electrode is found to be 133.33 F/g, at a charge-discharge current density of 0.5 mA cm^{-2}, while for SnO_2/VC electrode, it is 112.14 F/g. They used the sonochemical method to decorate SnO_2 nanoparticles with highly dispersed carbon materials.

This method permits to activation of carbon nanoparticles via avoiding the development of aggregates and inducing more uniformity coverage permitting the coating of a high SnO_2 nanoparticle loading without aggregation which is not so easy to control by other conventional methods.

Xu and co-workers [132] group used an atmospheric pressure plasma jet sintering process at several APPJ scan rates to fabricate the electrode for SCs. Changing the APPJ scan rate and duration influences the properties of SnO_2/CNT nanocomposite including the wettability that improved better contact between the electrolyte and the active electrode material, and then, improved electrochemical performance and specific capacitance are achieved. Generally, graphene nanosheets fold to form MWCNTs while unfolded MWCNTs form unzipped MWCNTs by well-ordered graphene nanosheets that possess high surface area and conductivity, promising for electrode materials. Krishnaveni and co-workers [133] synthesized unzipped MWCNTs by an ultrasound-assisted method in the presence of tin chlorides as Lewis catalyst and reducing agent in a short range of time and used them for SC electrode. Here, Sn^{2+} cleaved the C—C bond in the nanotubes ensuing in the creation of a nanosheet shape through ring-opening to form nanosheets to reduce their surface energy. At the same time, Sn2+ self-oxidized to Sn4+ to form SnO_2 with the corresponding insertion into the nanosheets to avoid the agglomeration of sheets. After the electrochemical test, they obtained higher specific capacitance of 351 F/g and 148 F/g in 1 M Na2SO4 and 6 M KOH respectively. Further, this composite showed enhanced charge storage capability and strong cyclic stability with better retention of 64 % in 1 M Na2SO4 and 52 % in 6 M KOH after the 3000 charge-discharge processes. Further, the group of Rakhi et al. [134] successfully synthesized SnO_2–MWCNTs uniformly dispersed onto graphene nanosheets (GNs/SnO_2–MWCNTs) by a chemical method followed by calcination. The resulting SnO_2–MWCNTs nanoparticles were homogeneously anchored on graphene nanosheets (GNs). Compared with GNs, the synthesized material can be charged-discharged very fast and had higher capacitance. The specific capacitance of GNs/SnO_2–MWCNTs nanocomposite electrode is 224 F g^1, with 81 % capacitance retention after 6000 cycles. The improved electrochemical performance is attributed to a positive synergistic effect from all the individual components of the nanocomposite. Nitrogen-doped MWCNTs reveal notable electrical, mechanical, and electrochemical properties because the nitrogen valence electrons are combined into the graphitic plane, and thus p-electrons are formed, resulting high surface energy and polarization effect. A study based on N-MWCNTs with SnO_2 electrode exhibited a high specific capacitance of ~728 F/g at 4 A/g in 6 M KOH solution [135]. The hybrid nanocomposite showed admirable capacitance maintenance with~92 % after the 5000 charge-discharge processes. Therefore, these studies show that the development of SnOx with CNT allows available active sites for electric charge and offered potential use of SnO_2-CNT for SCs application [113,114].

2.1.2.3. Carbon nanofibers (CNFs). In addition to CNTs, CNFs have been fascinated more and more consideration as a class of chemically stable backings designing and constructing SnO_2-based nanocomposites as the effective electrode materials because of their 1D properties such as large specific surface area and better electrical conductivity [138]. Mu et al. [139] SnO_2/CNFs nanocomposites with uniform distribution of SnO_2 particles synthesized by a simple merging of the electrospinning and support-free solvent–thermal method. The characterization outcomes show that the coverage of SnO_2 nanoparticles on the electrospun nanofibers can be easily managed by adjusting the mass ratio. The electrochemical performance was measured through CV and GCD measurement in a 1 M H_2SO_4 electrolyte. As suggested by the following equation [129], a reaction occurs in the H_2SO_4 electrolyte [139]:

$$SnO_2 + H^+ + e^- \leftrightarrow SnO\ OH$$

The optimal electrode prepared with a 1:7 mass ratio delivered a specific capacitance of 187 F/g at 20 mV/s and after the 1000 charge-discharge process, the capacitance retention was over 95 %. As a result of the presence of the one-dimensional CNFs, the electric conductivity of the SnO2 particles can be increased, the thermodynamic/kinetic stability preserved, and the charge-transfer resistance lowered. By using the same technique, Liu et al. [140] have used the thermal reduction process (TRP) of fibers comprising Sn precursor to prepare cage-like mesoporous CNFs. In this process, the TRP allowed the SnO_2 to metallic tin simultaneously with the depletion of carbon that allows Sn to roam out from the carbon fibers and thus mesoporous formed in the CNFs. A specific capacitance of 105 F/g with high energy density and long cyclic strength (4200 cycles) was achieved.

The core-shell structure enables decreasing ions/e^- diffusion path using the carbon shell, resulting high rate capability performance. Also, the redox process improves by moving e^- through a continuous 1D morphology. Samuel and co-workers [141] set an example for the fabrication of SnOx (core)/CNFs (shell) heterostructure using a single nozzle tip and used them as flexible electrodes for SCs. In that system shown in Fig. 15(c–i), PMMA was used as sacrificial material which generates pores and replaced by SnOx and forms a core after the heating process.

The prepared composite attained the excellent specific capacitance of 289 F/g at 10 mV/s. Also, it maintained high capacitive retention with 86 % after a long 5000 charge/discharge process due to the large expanse of Sn and appropriate hollow space (Fig. 15(g)). Also, Luan et al. [142] introduced novel architectures of SnO_2/CNFs where SnO_2 dots are homogenously confined in the activated CNFs using support templates of Cu and its oxides for creating porous. The prepared flexible electrode used in the quasi solid-state asymmetric SC achieved better energy density (10.3 Wh kg^{-1}) and power density (325 W/kg) with stable cyclic performance over 2500 times, suggesting the strong potential for practical uses. Most of the studies discussed above-used carbon sources containing PAN and other complex polymers that are unsustainable and complex. Because of this, a sustainable lignin precursor of multichannel CNFs obtained from poplar sawdust by Cao and co-workers [143] was used as an electrode shown in Fig. 16(a–e). The optimized CNFs with a 5:5 lignin to PMMA ratio, a satisfactory capacitance value of 406 F/g and long term cyclic stability with 95 % capacity retention after 10,000 cycles. Further, the optimal composite delivered the highest power density of 18,514 W/kg.

These admirable performances are ascribed owing to the hierarchical channels of multichannel CNFs, high surface area, faradaic pseudocapacitance of SnO_2, and hole-creating effect of Sn precursors (Fig. 16 (b–c)). As shown in Fig. 16(e), both positive and negative electrode layers of the supercapacitors were made from MCNFs@SnO2-5 nanocomposites, which were directly contacted with the electrolyte and separated by cellulose membranes. The symmetric supercapacitor would

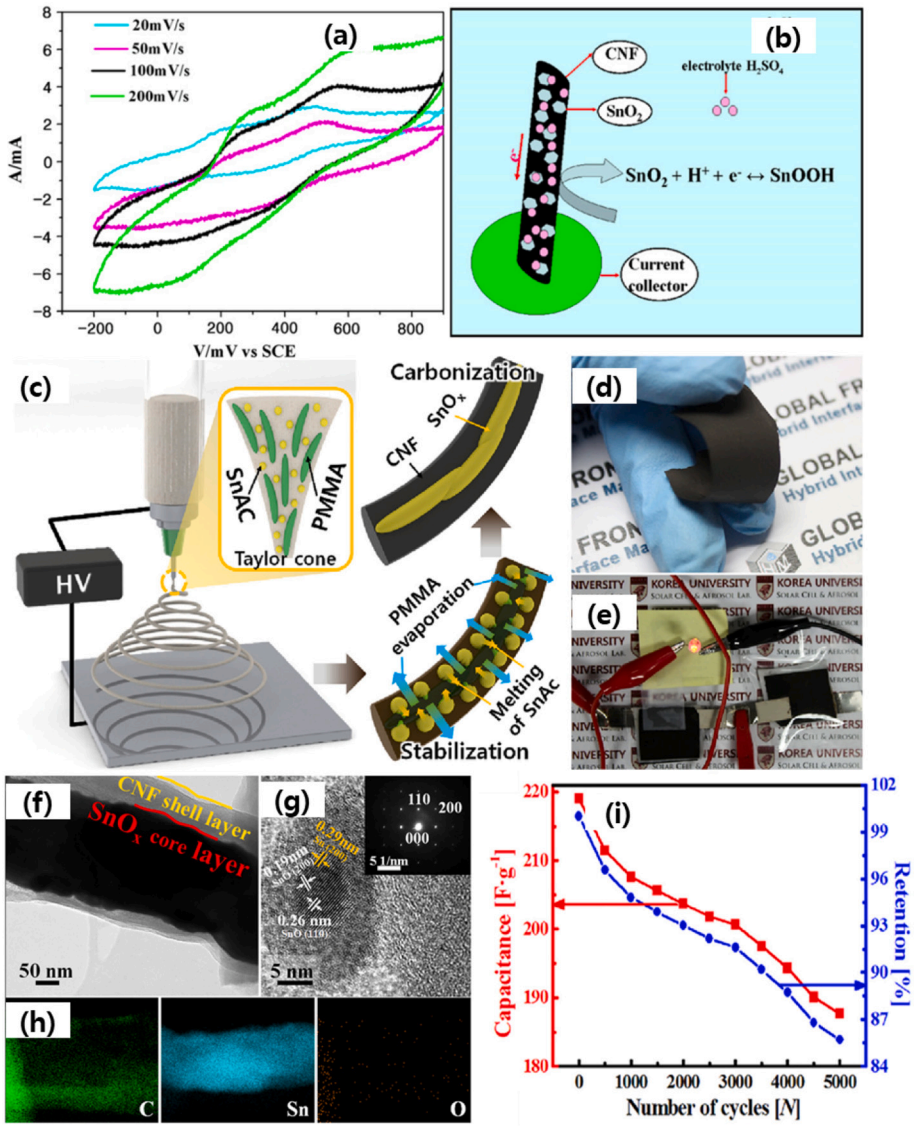

Fig. 15. (a) CV graph of the as-prepared CS3 electrode, (b) the graphical representation of the charge storage mechanism of SnO_2/CNFs electrode in SCs. Reproduced with permission. [129] Copyright 2017, Elsevier. (c) Schematic diagram of the preparation of SnO_x/CNF via electrospinning, (d) digital picture of flexible SnO_x/CNF, (e) LED test executed by two symmetric SCs, (f) TEM image, (g) HRTEM image of SnO-3, (h) EDS mapping for C, Sn, O, and (i) electrochemical stability measurements of SnO_x/CNF electrode. Reproduced with permission. [141] Copyright 2017, Elsevier.

be capable of storing two different kinds of charge, including EDLCs provided by MCNFs and pseudocapacitance provided by SnO2. In EDLCs, the charge is stored electrostatically: positive electrodes are balanced by anions, whereas negative electrodes are balanced by cations at the interface of electrode and electrolyte. At or near the electrode surface, the proton or alkali metal cations adsorb on the surface of SnO2 and its oxidation state can change. SnO2 would then demonstrate pseudocapacitance unlike EDLCs [143]. The ability to produce high-performance supercapacitor electrode materials by such a simple process may lead to enhanced commercial opportunities for supercapacitors across a wide range of applications where high-power density is required.

In general, the physical/chemical properties of material strongly depend on the size and morphology of the specific material. Same with SnO_2 as an electrode material, decreasing the scale of SnO_2 to nanosize is a specific approach to improve the electrochemical performance because of the big surface area and providing a more electro-active site. Thus, researchers are keenly involved in emerging SnO_2 materials with several morphologies and dimensions for supercapacitors electrode. For example, He's group [144] designed a simple and facile preparation of SnO_2/C porous carbon composites that has uniform spherical morphology which is ascribed as the mosaic-designed microspheres by ethanol-thermal carbonization and steam activation method. The resultant electrode showed a high specific capacitance of 420 F/g with strong cyclic stability and a high energy density of 34.2 Wh kg^{-1}. These improvements might be belonged to the novel mosaic nanostructure where the spherical nature improved the electroactive surface, and the internal porous nature helped the electrolyte to entirely interact with SnO_2 nanoparticles.

In addition to this, SnO_2 is encapsulated in a tunable hollow double-shell novel structure (H-SnO_2/MesCHS) with a high surface area (747.7 m^2/g) and pore size (4.9 nm) prepared by hydrothermal and in-situ polymerization and silica template as sacrificial mesocarbon templates and used them for SCs electrode (Fig. 17) [145]. The prepared composites showed an excellent electrochemical response in Fig. 17(h–i) such as high specific capacitance of 470 F/g and long cyclic stability with ~88 capacity retention after 4000 cycles to their competitive electrodes. The achieved performance is attributed to the synergistic effects of MesCHS and SnO_2, where mesoporous double-shell hollow structure facilities more electrolyte penetration to react with SnO_2, and offers higher electrode/electrolyte interaction for ample active sites.

Le and co-workers [146] utilized an emerging wetness impregnation technique to incorporate SnO_2 nanoparticles in N doped mesoporous carbon framework followed by a thermal-reduction process and the surface area and pore size was affected by the amount of SnO_2 impregnation. The resultant optimized electrode with 15 wt% of

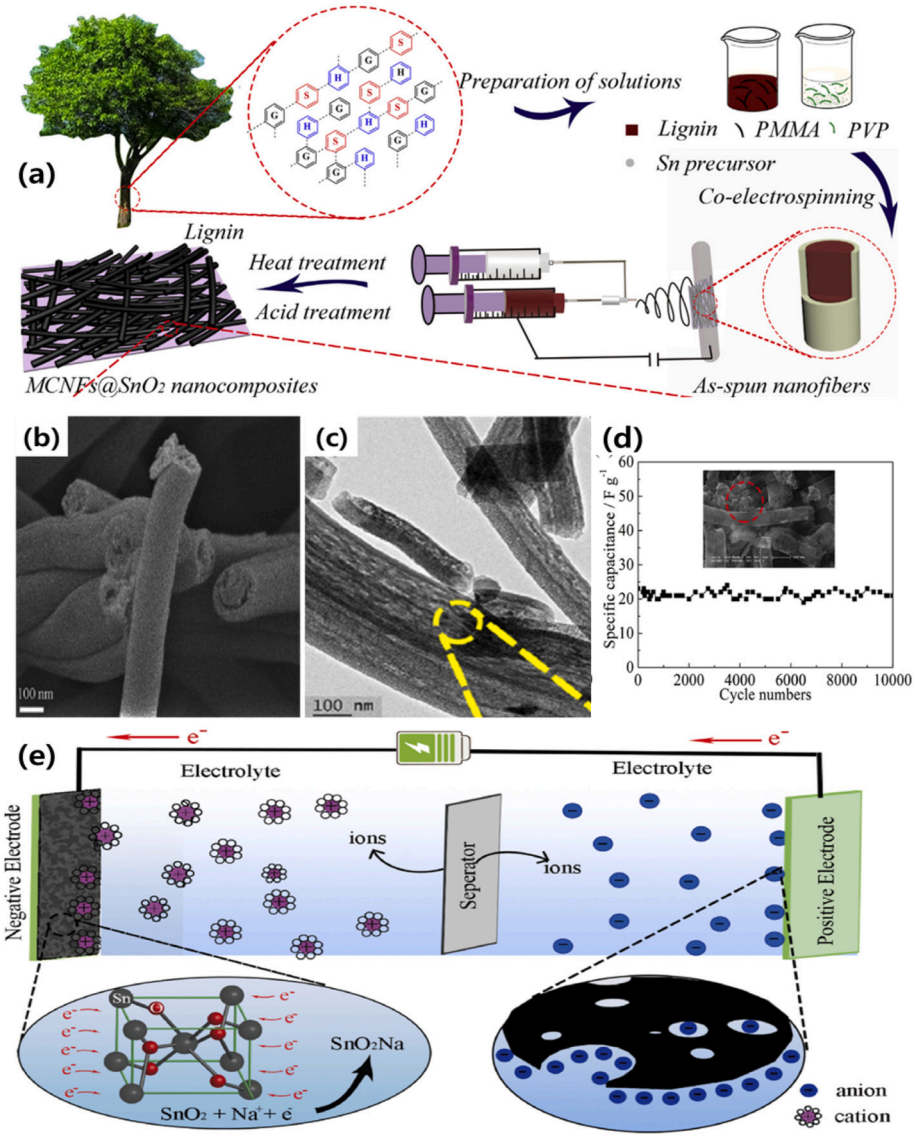

Fig. 16. (a) Schematic diagram of the preparation of MCNFs@SnO_2 via electrospinning, (b) SEM image of MCNFs@SnO_2, (c) TEM image of MCNFs@SnO_2, (d) electrochemical stability measurements of MCNFs@SnO_2 electrode, and (e) Graphical illustration of charge storage mechanism of the symmetric supercapacitor. Reproduced with permission. [143] Copyright 2017, Elsevier.

impregnated SnO_2 showed improved specific capacitance of 344 F/g at 50 mV/s and cycling stability of 5000 charge/discharge cycles with 92 % capacity retention.

The structure and surface area greatly influence the physic-chemical properties of SnO_2, which also plays an important factor in the choice of electrode constituents. So, it is greatly vital to make distinct morphological species which hold a large surface to volume ratio that helps to obtain more electro-reactive sites and superficial ion transport. Scalable and simple one-step synthesis way for the construction of Sn/SnO_2@C with high surface area (500 m^2/g) prepared by deep eutectic solvents assisted process [147]. Due to 3D interconnected buildings, the optimized electrode with high conductivity that was prepared at high-temperature graphitization showed high specific capacitance with about 100 % capacity retention over 5000 cycles.

Hong and co-workers [7] functionalized carbon cloth using acidification treatment and represented a flexible substrate growing SnO_2 nanoclusters by a solvothermal reaction followed by a calcination route. The functionalized carbon cloth wrapped with SnO_2 displayed a capacitance of 197.7 F/g or 1265.3 mF cm^2 at 1 A g 1 with over 95 % of capacitance retention over 5000 charge-discharge processes which are higher than the only graphene containing carbon cloth in two-electrode SC. In the prepared FCC@SnO_2 electrode, the functionalized carbon framework provided several growing spots for rising SnO_2, which offered conductive networks for fast ions transportation. Furthermore, the wrapped SnO_2 on the surfaces of carbon microfibers enables the charge storage via surface adsorption/desorption and contributes to their pseudocapacitance [148–154] Some pioneering examples of the addition of SnO_2 on the graphene substrate have been demonstrated with enhanced electrochemical performances.

2.1.3. SnO_x on conducting polymers

Pristine SnO_2 suffers from the limitations such as poor conductivity, agglomeration during continuous charge-discharge cycles, less stability, and difficulty in sustaining hydrous SnO_2 form. Such restrictions can be resolved by the hybridization of SnO_2 with other materials such as conducting polymers. For example, Polypyrrole (PPy) is a promising electrode material for supercapacitors due to its high electrical conductivity as well as good energy storage capacity. The group of Wang et al. [155] successfully synthesized a ternary nanocomposite graphene/SnO_2/PPy (GSP) as supercapacitor electrode material under a one-pot

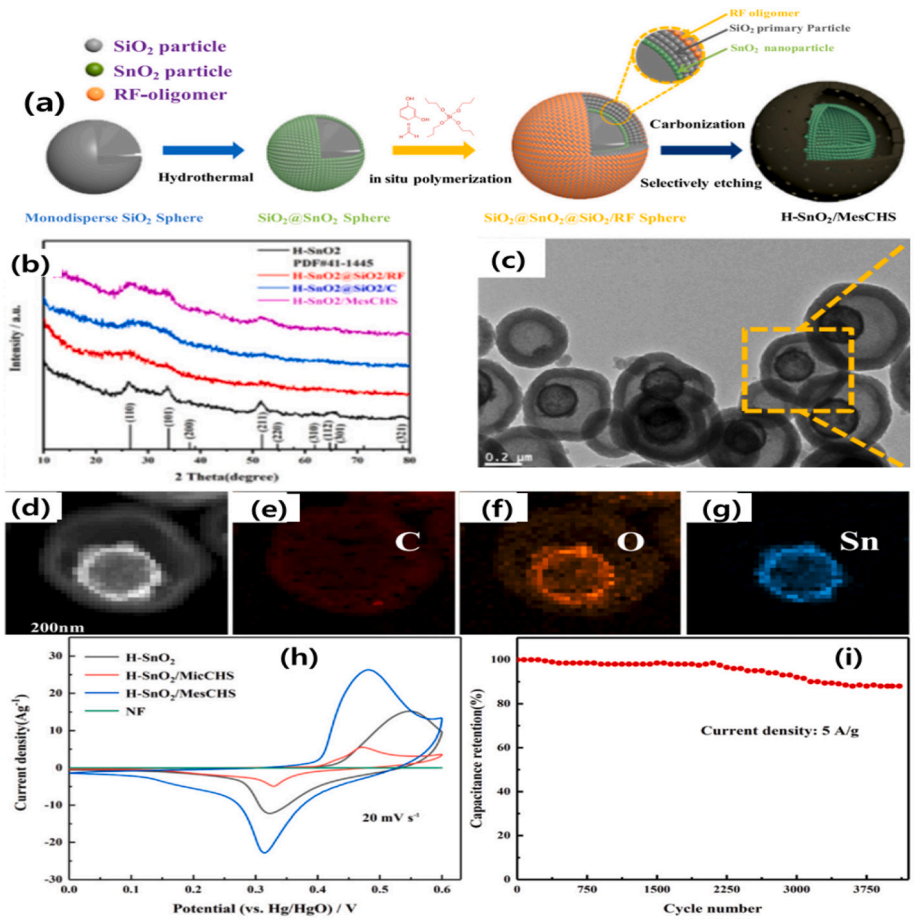

Fig. 17. (a) Schematic diagram of preparation of hollow double-shell H-SnO_2/MesCHS nanospheres, (b) XRD pattern of H-SnO_2/MesCHS composites, (c) TEM images of H-SnO_2/MesCHS nanospheres, (d) EDS elemental mapping for C, Sn, O, and (g) electrochemical measurements through (h) comparative CV curves of the H-SnO_2, H-SnO_2/MicCHS, H-SnO_2/MesCHS and NF at a scan rate of 20 mV/s^{-1}, and (d) Cyclic stability test for H-SnO_2/MesCHS at 5 A/g current. Reproduced with permission. [145] Copyright 2017, Elsevier.

synthesis process. The composite delivered a large specific capacitance of 616 F/g at 1 mV/s current density in a 1 M H_2SO_4 electrolyte. The electrochemical performance is attributed to the synergistic effect of all three components. The homogeneously dispersed graphene sheets act as a framework to sustain both the pseudocapacitive materials SnO_2 and PPy. The PPy film not only enhanced the surface area but also restricts the aggregation of SnO_2 during charge-discharge cycles. Also, Polyaniline (PANI) has attracted tremendous attention as an SC electrode due to its non-toxic nature and good electrical conductivity. Merely PANI displays a great capacitance, nevertheless, substantial capacitance declining observes due to various types of mechanical instability of PANI including puffiness, contraction and cracking upon charge-discharge practice. In this regard, the effect of morphology and crystal structure on the electrochemical performance of SCs was well explored by Hu et al. [156]. The SnO_2 nanoparticles embedded within netlike polyaniline not only provide good wettability by electrolyte but also facilitate rapid charge transfer and ionic diffusion. The material delivered a specific capacitance of 305.3 F/g at 5 mA cm^{-2} with 96 % of capacity retention after 500 cycles.

The synergistic contact between SnO_2 and PANI endorses the electrochemical performances of PANI. A binary nanocomposite of PANI/SnO_2 nanorod array was prepared using a combination of electropolymerization and seed-assisted hydrothermal process and exhibited a higher specific capacitance of 367.5 F/g compared to pure PANI (232.4 F/g) and retained almost 90 % capacity retention after 2000 cycles [157]. In another study, Wang and co-workers [158] synthesized SnO_2@PANI composite began from SnO crystals, after that an in-situ oxidation to SnO_2 using ultrasonication and the polymerization of aniline where SnO_2 homogeneously dispersed on the surface and inserted into the PANI texture. The variation of inorganic constituent and polymer framework greatly influenced the morphology and electrochemical performance of the prepared electrode. The resultant optimized electrode shows a higher capacitance value (335.5 F/g) and cyclic stability (10,000 cycles) due to the synergetic effect of SnO_2 with PANI which enlightens the capacitance and reduces the mechanical deprivation. The study showed opportunities for the combination of polymer with SnO_2 as electrode material for SCs [156,159,160].

2.1.4. *Doped SnO_x*

Foreign element (especially with transition metal) doping is a modest and effective way to modify the properties of materials and thus enhance the performance of the SnO_2 nanostructured and functional properties. The decoration of element dopants into active material yields an increased active surface, large surface area and extra diffusion transportation of e^-/ions diffusion. Also, the doping encourages the oxygen vacancies in the host lattice, resulting enhancement in electrical conductivity. Recently, various metal doping such as Ag, Zn, Co, Zr etc. has been tried to enhance specific capacitance and cycle stability. For example, Karthikeyan et al. [161] synthesized altered cobalt doped SnO_2 by the hydrothermal process at low temperature for the first time and exhibited a high capacitance value of 840 F/g compared to the pure SnO_2 (742.6 F/g) due to high crystallinity and porous structure, and the cobalt doping. Inspired by the importance of doping, Saravanakumar and co-workers [162] synthesized Zn doped SnO_2 NPs by sol-gel process using optimization of various surfactant effects and roles, and homogenous spherical Zn-SnO_2 NPs formed with the PEG-400 surfactant. This is due to the contribution of the vast amount of oxygen present in lengthy chains of PEG-400 adds the coordinative saturation of dangling bonds present on the out surface of the prepared materials. From the XRD results, there was a minor shift in the peak detected diffraction

peaks of Zn-SnO_2, which might be the outcome of the replacement of incorporation of Zn^{2+} into the lattice points of the tetragonal SnO_2 structure. The assisted PEG-400 Zn-SnO_2 showed a better specific capacitance value of 312.7 F/g with 90 % retention after the 500 cyclic processes. The same author in the same year has tried to explore the effect of Zn and Ag doping with SnO_2 NPs as electrode materials on the basis of high conducting dopant to low conducting dopant [163]. The uniform spherical Ag-SnO_2 electrode enabled high active sites due to Ag^{+2} dopant which exhibited a specific capacitance of 308 A/g at 0.5 A/g and a long GCD charge/discharge process for 5000 times at 2A/g with 67 % capacity retention.

Very similarly, Asaithambi et al. [85] synthesized SnO_2 spherical nanostructures with the doping effect of highly electrical conductive elements (Fe, Cu) and lower electrical conductive transition metal (Zn) dopant. The XRD pattern in Fig. 18(a) suggested that the peaks are somewhat shifted towards a lower 2theta value while matched to undoped SnO_2 and the peak intensities are also reduced caused by the possessions of the dopant of Fe, Cu, and Zn ions into the tetragonal SnO_2 lattice. The SEM analysis (Fig. 18(b–e)) of the samples shows that the undoped SnO_2 has spherical morphology, partaking grains in the size range of ~43 nm and decreases upon doping due to lower surface/grain boundary energy. Among them, Fe doped SnO_2 sample provided an enhanced specific capacitance (270 F/g at 0.5 A/g in Fig. 18(f)) and outstanding retention (98 % retention) after 2000 cycles (Fig. 18(g)). Similarly, Suthakaran et al. [164] introduced a hydrothermally synthesized surface assisted Zn-SnO_2 NPs using sodium hexametaphosphate (SHMP) as a capping agent and compare them with only SnO_2 and SHMP-SnO_2, where SHMP was used to hinder the SnO_2 NP from agglomeration. The electrochemical performance of the Zn doped SnO_2 electrode exhibited a greater capacitance compared to the undoped and SHMP assisted SnO_2 electrode. In addition to the different metal doping, the same author has introduced a novel Zr doped SnO_2 NPs using the same surface/capping agent and method in their aforesaid study [165]. In this, Zr was considered a suitable dopant for SnO_2 due to a similar ionic radius as the ionic radius of Zr ion (0.72 Å) is adjacent to Sn ion (0.69 Å) which could modulate the bandgap. Thus, Zr ions would simply substitute Sn ions in the crystal lattice and the obtained complex can alleviate the lattice configuration. The electrochemical results suggested that the doping of Zr in SnO_2 would substantially enhance the capacitive performance as compared to pure ones. Thus we can conclude that doping of metal in SnO_2 lattice act as an acceptor and the presence of oxygen vacancies work as a donor that progresses mass transport, consequently improving the SCs performance [165–167].

2.1.5. SnO_x on M_xO_y (M = Co, Ru, Mn, Fe, Mo) and others

Ruthenium is considered the most potential electrode material for SCs but, Ru-based SCs are not available commercially due to their less natural availability. However, due to its unique supercapacitive properties, it can be used in trace amounts with other metal oxides such as SnO_2, TiO_2, MoO, and Ta_2O_5 materials present in bulk. Their possible synergistic effect can boost the electrochemical performance of SC electrodes. For example, Shakir et al. reported Tin oxide-coated molybdenum oxide nanowires (SnO_2/MoO_3), synthesized through a hydrothermal and wet chemical process. MoO_3 nanowires have an average diameter of 100 nm while SnO_2 has a thin coating on MoO_3 nanowires with a uniform thickness of about 5–20 nm. The reported composite material delivered a specific capacitance of 295 F/g at 0.5 A g^{-1} in 1.0 M Na_2SO_4 electrolyte solution, which is better than the capacitance of its individual counterparts MoO_3 (69 F/g) and SnO_2 (96.6 F/g), with 97 % capacitance retention after 1000 cycles [151]. Alone SnO_2 and SnS_2 have generally been shown poor electrochemical performance due to volume expansion and poor capacity and electronic conductivity, but their heterostructure showed improved SCs performance. The low electrochemical performance of SnO_2 arises mainly from the discontinuities in the electrode material affected by the realization of agglomeration and cracks. In this regard, Prabukumar and co-workers [168]

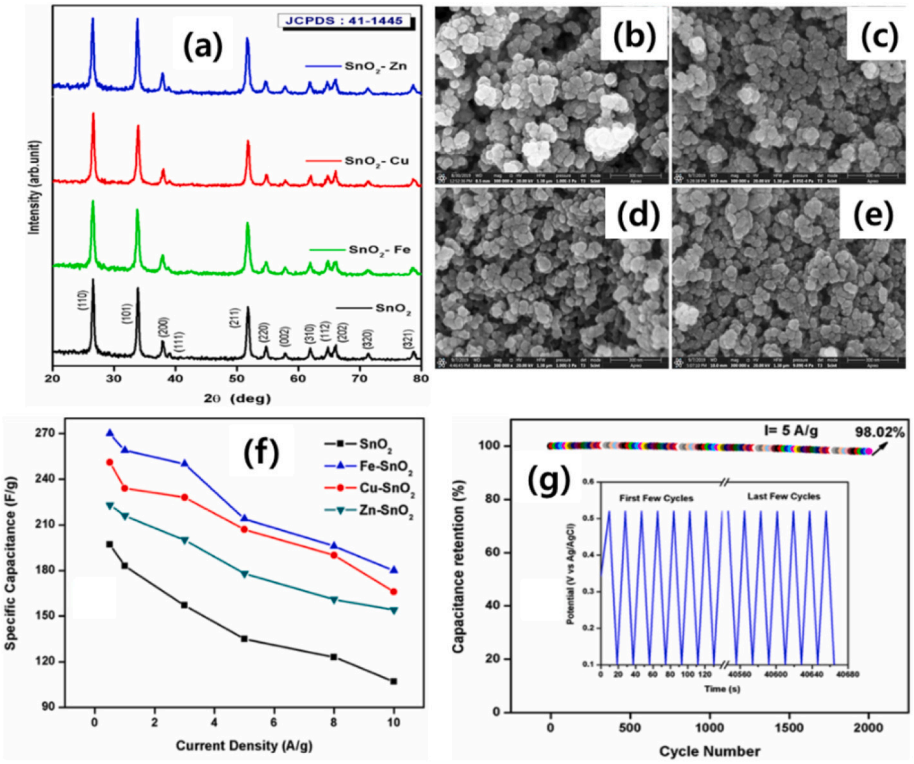

Fig. 18. (a) XRD pattern of undoped and Cu, Fe and Zn doped SnO_2 NP, (b) SEM images of (b) undoped SnO_2 NP, (c–e) Fe, Cu, and Zn doped SnO_2 NP, and electrochemical measurements through (f) comparative specific capacitance at different current density for the electrode, (g) cyclic stability test of optimized Fe-SnO_2 electrode at a current density of 0.5 A/g. Reproduced with permission. [85] Copyright 2017, Elsevier.

designed an electrode containing SnO_2 NPs decorated MoS2 nanosheets by ligand exchange process where the MoS2 nanosheets work as the support framework and conducting path between the SnO_2 NPs, exhibited an improved specific value to 61.6 F/g with 5 % capacity retention after 1000 cycles than that of bare SnO_2 NPs. A similar concept was adopted by Asen et al. [169] where SnS_2-SnO_2 nanocomposites were prepared by a simple and economical solvothermal process using two different precursors. The obtained electrode showed improved capacitance performance because of its compositional and structural advantages. It has been observed that in the neutral Na2SO4 electrolyte, the charging process is performed by adsorbing and desorbing Na + ions on the surface of the optimized SnO_2 nanoheterostructures as shown by the following process [169]:

$$(SnO_2)_{surface} + Na^+ + e^- \rightarrow (SnO_2{}^- - Na^+)_{surface}$$

SnS_2 can also undergo the following reaction as shown in equation:

$$(SnS_2)_{surface} + Na^+ + e^- \rightarrow (SnS_2{}^- + Na^+)_{surface}$$

Hence, this facilitates the effective storage of charges through adsorption and desorption processes.

The literature survey suggested that combine of SnO_2 with others shows a synergistic effect on SCs activity, particularly via improving electrical conductivity and shortening electron/proton pathways. Daneshvar et al. [170] designed a composite electrode using a MWCNT as a template for the preparation of porous SnO_2/Cu_xO by a facile electroless deposition process where morphology was controlled by pH and bath composition. The obtained SCs results showed higher electrochemical performance such as high capacitance (662 F/g) and long cyclic stability (retention of 94 % after 5000 cycles) that was high compared to several Sn-based electrodes. In this system, Sn acts as high wettability and electrical conductivity, and the middle layer between Cu and the MWCNTs offers a robust contact between them. Binary mixing of

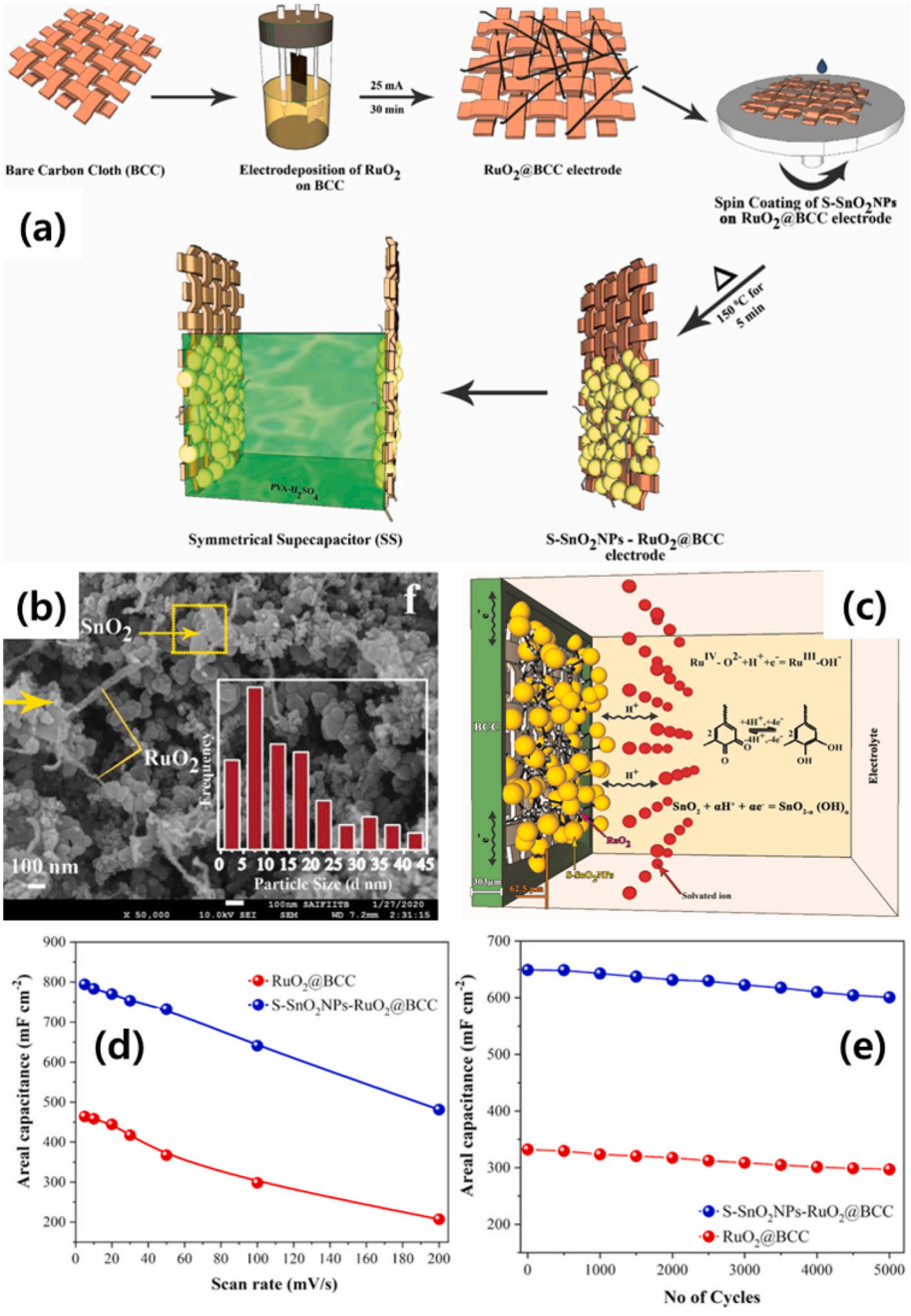

Fig. 19. (a) Schematic diagram of preparation process of S-SnO_2NPs–RuO_2@BCC electrode, (b) SEM surface images of S-SnO_2NPs–RuO_2@BCC composite and inset image of the particle size distribution of S-SnO_2NPs. (c) Graphic illustration of a probable charge transfer mechanism involved in the electrode, and electrochemical measurements through (d) comparative specific capacitance at different scan rates, (c) cyclic stability test for optimized electrode at a current density of 10 mA/cm^2. Reproduced with permission. [172] Copyright 2017, Elsevier.

RuO_x and SnO_x based on quite similar crystal parameters materials considered attention for SCs electrode due to the addition of SnO_2 in metal oxide expands the consumption amount of metal species and improves the electrochemical activity. For instance, Wu et al. [171] decorated RuO_2 onto SnO_2 xerogel to enhance its specific capacitance (15 Fg^{-1}) by three times than that of bare xerogel (5 Fg^{-1}) specific capacitance. The mass loading/coating thickness of electroactive material plays an important role in the electrochemical performance of SC; low mass loading reveals high capacitance but is not applicable for practical use while large mass loading retards the specific capacity owing to agglomeration, poor mechanical strength, low conductivity and diffusivity. Mevada et al. [172] synthesized a novel composite of SnO_2-RuOx electrode prepared by electrodeposition of RuO_2 followed by spin-coated as-synthesized SnO_2 NPs on carbon cloth which was used as a current collector as shown in Fig. 19. The prepared electrode with good compositional constancy and a large surface-to-volume ratio, confirming the better electrochemical performance including high areal capacitance of 794 mF/cm^2 and long cyclic stability of 5000 times with 87.5 % capacity retention than that without SnO_2 based electrodes. Hierarchical core-shell nanostructures have been demonstrated to be an effective way to enhance electrochemical performance. Core-shell heterostructures have several advantages over bulk materials, including providing a large interfacial area for charge transport and shortening the diffusion path for intercalation and de-intercalation of active species, as well as being able to achieve synergetic behaviour and multifunctionality [102,104,173]. Wang and co-workers [174] proposed a novel design of core-shell hierarchical nanostructure via combining SnO_2 nanowires and $Ni(OH)_2$ nanoflakes to synthesize 3D core-shell structures on flexible carbon cloth using a simple solution-based technique. Higher electrochemical performance of 1553 F g^{-1} (at 0.5 A g^{-1}) is achieved and it retained a capacitance of 934 F/g at a higher current density, indicating a very promising candidate for high energy supercapacitors.

Recently, the effect of doping of metal and non-metal ions in the electrochemical performance of SnO_2 nanostructures (Co, N-SnO_2) is studied by Xu et al. This results in band edge reconstruction of tin dioxide, thus showing 2.29 eV for SnO_2 to 0.68 eV for Co, N-SnO_2. A wearable bracelet-supercapacitor based on Co, N-SnO_2/ACF electrode delivered an outstanding energy density of 70.7 Wh kg^{-1} with a potential window of 2.0 V. This composite possessed a large specific capacitance of 361.2 F/g at 1 A g^{-1} with 103.3 % cycling stability after 10,000 charge-discharge cycles [175]. In an interesting approach to increase the electrochemical performance of SnO_2, which is generally found to be poor, Li et al. synthesized nano rod-like Fe_3O_4@SnO_2 nanocomposite. Using a one-step hydrothermal approach, the material delivered a specific capacitance of 7.013 mF cm^{-2} at 0.20 mA cm^{-2} [176]. The role of the porous SnO_2 layers in preventing the aggregation of γ-MnO_2 nanosheets is studied by Chan et al. After the addition of CNT, the tri-layered structure of CNT/SnO_2/MnO_2 showed larger specific capacitance than bare CNT-, and SnO_2-supported MnO_2 materials. The CNT/SnO_2/MnO_2 nanocomposite delivered a high specific capacitance of 427 F/g at a current density of 1 A g^{-1}. The improved electrochemical performance is attributed to the lower internal resistance of the hybrid composite electrode material [177].

Besides, several research studies even proposed adding SnO_2 with multiple materials. Wang et al. [178] prepared hierarchical Co_3O_4-SnO@SnO_2 nanostructures where uniform SnO_2 nanosheets grew on the surface of carbon cloth followed by a hydrothermal process and annealing process. In this system, the addition of Co_3O4 and PN junction hierarchically skeleton act a structure of nanospheres sheltered by nanoparticles that offer rapid conduction of electrons and ions between the electrolyte and active material. The prepared electrode presented a high specific capacitance of 1.056 F/cm^2 and admirable cyclic stability of 2000 charge/discharge times and retain 91.5 % capacity.

It is known that the surface of graphene oxide has negatively charged ions and Sn and Fe have positively charged ions that would easily be attached to the graphene oxide solution. Geerthana and co-workers [179] synthesized a Fe_2O_3/SnO_2/rGO nanocomposites with nano-Sn species on the surface of graphene oxide using a one-step hydrothermal route, reporting an electrode with a high specific capacitance of 821 F/g and outstanding cyclic stability of 10,000 times with ~99 % retention due to primarily ascribed to the surface assets of nanosized metal oxides and an outstanding conductive framework. This set of studies suggests that SnO_2 joint with inventive construction of metal oxide heterostructures efficiently increases the electrochemical performance of the SC electrode material and offers an innovative awareness for the organized progress of power density and energy density [177,180–192]. Table 2 showed an electrochemical performance comparison of tin-based electrode materials, synthesized through various techniques.

2.2. Tin-based sulfides ($SnS_{x=1\&2}$)

Recently, transition metal sulfides (TMSs) have attracted huge research attention in the field of energy storage. These are recognized by excellent physical properties like electrical conductivity, mechanical and thermal stability, and chemical properties like good redox behaviour [195,196]. Thus, found to be highly suitable in the form of electrode material for lithium-ion batteries and supercapacitors [83,197–199]. Considering the unique abilities of metal sulfides for SCs, several reports have been published on metal sulfides based on iron, cobalt, nickel, copper, molybdenum, and tin [15,195,196]. These sulfides are naturally abundant and possess tunable optical band gaps as well as layered structures, required for electrode materials in electrochemical energy storage. Metal sulfides are not only reported in the pure form but their hybrid form has also been explored. Their combination with conducting polymers or carbonaceous materials showed excellent supercapacitive performance. The synergistic characteristics of both materials contribute positively to conductivity, specific capacitance, and cyclic stability. The high conducting and porous nature of carbon materials provide a short ionic diffusion path for the electrolyte ions to penetrate, and the extreme redox nature of metal oxides promotes high specific capacitance and energy density [199–201]. The tin sulfide-based nanostructures, nanocomposites, and heterostructures have been synthesized by various methods such as hydrothermal method [200,201], chemical vapour deposition (CVD) [202], ball milling method [203], chemical precipitation [204], and vacuum evaporation [205]. Although the tin-based sulfides are quite potential material for SC electrodes, they have not been enormously explored from the commercial point of view, and therefore, very few results have been reported for Sn-based sulfide supercapacitors.

2.2.1. Pure Sn-based sulfides ($SnS_{x=1\&2}$)

TMCs or dichalcogenides (TMDCs) are enormously explored in the field of nano-electronics, optoelectronics, and flexible devices due to the tunable band gaps, high mechanical strength, and ability to possess various nanostructures [195,196]. Concerning the huge natural abundancy along with the property of large surface area and different morphologies, TMSs are found to be highly suitable for SC electrode materials [83,197]. Although the device performance relies on many parameters, optimization of electrode materials in the form of suitable nanostructures is of great significance for SCs. Tin disulfide (SnS_2) possesses a 2D layered crystal structure with weak van der Waal forces existing between the layers and has attracted significant attention as pseudocapacitor electrode materials. The layered CdI_2 structure with hexagonal lattice is an attractive property of SnS_2, enriched by a large surface area [206]. The key role of morphology in capacitance enhancement is well studied by Mishra et al. [207]. The unique carnation flower-like morphology provides a short and highly conducting channel for electrolyte ions to transport inside the electrode. The high output delivery (specific capacitance ~524.5 F/g at 0.08 A g^{-1}, power delivery ~12.3 W Kg^{-1}) assures the application of SnS_2 as an SC

Table 2
EC performance comparison of tin oxide based electrode materials for SCs.

Samples	Synthesis method	Morphology	Electrolyte	Specific capacitance	Cycling stability [%] (no. of cycles)	Ref.
SnO_2	Hydrothermal	Flower-shaped	1 M Na_2SO_4	187.7 F/g at 1 A/g	N/A (2000)	[10]
	SILAR method	Spherical nanograins	0.5 M Na_2SO_4	66 F/g at 10 mV/s	N/A	[20]
	Precipitation	Spherical shape	1 M H_2SO_4	523 F/g at 5 mV/s	97.7 (5000)	[86]
	Hydrothermal	Nanoclusters	1 M H_2SO_4	208.9 F/g at 0.1 A/g	119.3(10000)	[87]
	Hydrothermal	Quantum dots	PVA- H_2SO_4	315 F/g at 1 A/g	85 (3000)	[94]
	Potentiodynamic deposition	Nanostructured	1 M Na_2SO_4	285 F/g at 10 mV/s	88 (1000)	[96]
	Hydrothermal	Nanoparticles	0.1 M NaCl	24.58 F/g	N/A (1000)	[97]
	Hydrothermal	Micro-plates	3 M KOH	1080 F/g at 1 A/g	80.6 (1000)	[99]
	Solvothermal	Nanoparticles	0.1 M Na_2SO_4	50.3 F/g at 10 mV/s	97 (1000)	[100]
	Spray pyrolysis	Polyhedron-like grains	1 M KOH	119 F/g at 10 mV/s	N/A	[101]
	Hydrothermal	Hollow nanospheres	1 M KOH	332.7 F/g at 1 A/g	130 (2000)	[105]
	Hydrothermal	Nanoparticles	KOH	1.6 F/g at 5 mV/s	N/A	[106]
	Soft chemical	Quantum dots	0.5 M KOH	10 F/g at 20 mV/s	98 (1000)	[107]
	Electrochemical	Irregular spherical grains	0.1 M NaOH	43.07 F/g	N/A	[110]
	Hydrothermal	Spherical	1 M KOH	35.07 F/g at 0.25 A/g	N/A	[111]
SnO_x/graphene	Hydrothermal	Nanoplatelets	0.5 M Na_2SO_4	275 F/g at 5 mV/s	90 (2000)	[112]
	Pulse microwave-assisted deposition	Nanocrystals	1 M H_2SO_4	348 F/g at 50 mA/g	99 (1000)	[113]
	Supersonic spraying	Nanoparticles	PVA-LiCl	1008 mF/cm2 at 1.5 mA/cm^2	93 (10000)	[114]
	Hydrothermal	3D aerogel film	1 M H_2SO_4	4.314 F/cm2 at 1 mA/cm^2	60.47 (2000)	[115]
	Thermal reduction reaction	Composite	6 M KOH	378 F/g at 4 A/g	89 (5000)	[116]
	Hydrothermal	Nanocomposite	1 M H_2SO_4	545 F/g at 1 A/g	96 (5000)	[117]
	oxidation–reduction reaction	Nanocomposite		363.3 F/g at 5 mV/s	N/A	[118]
	Colloid electrostatic self-assembly	Nanoparticles	1 M Na_2SO_4	347.3 F/g at 5 mV/s	90 (3000)	[119]
	Bacteria-mediated	Nanoparticles	PVA- H_2SO_4	445 F/g at 2 A/g	84.1 (2500)	[121]
	Electrostatically self-assembled	Nanospheres	1 M H_2SO_4	337 F/g at 0.5 A/g	89 (5000)	[122]
	Metal sputtering	Nanoparticles	1 M Li_2SO_4	105 mF/cm^2 at 10 mV/s	95 (10000)	[123]
	Hydrothermal	Nanoparticles	1 M Na_2SO_4	180 F/g at 10 mV/s	N/A	[124]
	Hydrothermal	Nanoparticles	1 M H_2SO_4	488 F/g at 1 A/g	97.2 (5000)	[125]
	Hydrothermal	Hollow spheres	3.0 M KOH	947.4 F/g at 0.57 A/g	88.2 (1000)	[126]
	One-pot	Nanoparticles	1 M H_2SO_4	116 F/g at 10 mV/s	100 (5000)	[127]
	In-situ polymerization	Nanoparticles	1 M H_2SO_4	429 F/g at 1 A/g	133 (2000)	[128]
	Cathodically deposited	Tiny nanowires	0.5 M KCl	298 F/g at 10 mV/s	90 (1000)	[129]
SnO_x/CNT	Sonochemical	Nanoparticles	1 M Na_2SO_4	133.33 F/g at 0.5 mA/cm^2	N/A	[131]
	APPJ	Nanoparticles	2 M KCl	90 F/g at 2 mV/s	87 (1000)	[132]
	Ultrasound-assisted route	Nanoparticles	1 M Na_2SO_4	351 F/g at 0.5 mA/cm^2	64 (3000)	[133]
	Ultrasonication	Nanoparticles	KOH	224 F/g at 50 mV/s	81 (6000)	[134]
	APPJ	Nanoparticles	2 M KCl	188 F/g at 2 mV/s	N/A (1000)	[136]
	Sol-gel	Nanoparticles	1 M KOH	21 mF/cm2 at 10 mV/s	50 (5000)	[137]
SnO_x/CNFs	Vacuum-assisted	Nanorod	1 M KCl	0.148 F/g	N/A	[138]
	Solvent–thermal	Nanoparticles	1 M H_2SO_4	187 F/g at 20 mV/s	95 (1000)	[139]
	Electrospinning	Nanoparticles	6 M KOH	105 F/g	N/A	[140]
	One-step electrospinning	Nanofiber	6 M KOH	289 F/g at 10 mV/s	88 (5000)	[141]
	Electrospinning	dots	3 M KOH	225.4 F/g at 1 A/g	119 (2500)	[142]
	Co-electrospinning	Nanoparticles	6 M KOH	406 F/g at 0.5 A/g	95 (10000)	[143]
SnO_2@C	Ethanol-thermal carbonization	Microspheres	1 M KOH	420 F/g at 1 A/g	91 (2000)	[144]
H-SnO_2/MesCHS	In-situ polymerization	Hollow double shell	2 M KOH	470 F/g at 2 A/g	88.4 (4000)	[145]
SnO_2@N-CMK_3	Wetness impregnation	Nanoparticles	1 M Na2SO4	344 F/g at 5 mV/s	92.4 (5000)	[146]
Sn/SnO_2@C	Deep eutectic solvents assisted	Nanoparticles	2 M KOH	109.70 mAh/g at 1.42 mA/cm^2	100 (5000)	[147]
SnO_2/RF	Impregnation	Nanoparticles	1 M H_2SO_4	119.2 F/g	N/A	[148]
OMC/SnO_2	Wetness impregnation	Nanoparticles	0.5 M H_2SO_4	200 F/g at 200 mV/s	95 % (500)	[150]
SnO_2/MoO_3	Hydrothermal	Core shell nanowires	1 M Na2SO4	295 F/g	97 (1000)	[151]
sPS@SnO_2	Hydrothermal	Core shell	1 M KOH	44 F/g at 10 mV/s	N/A	[152]
ISCC-SnO_2	Colloidal processing	Hexagonal	1 M Na_2SO_4	42.7 mF/cm at 25 mV/s	N/A	[153]
SnO_2 mixed biochar	Co-precipitation	Nanorod	1 M H_2SO_4	465 F/g at 10 mV/s	76.6 (3500)	[154]
Graphene/SnO_2/PPy	One-pot	Nanoparticles	1 M H_2SO_4	616 F/g at 1 mV/s	98 (1000)	[155]
Polyaniline/SnO_2	Sol–gel	Netlike	1 M H_2SO_4	305.3 F/g at 5 mA/cm^2	95.5 (500)	[156]
PANI/SnO_2 NRA	Seed-assisted hydrothermal	Nanorod array	1 M H_2SO_4	367.5 F/g at 0.5 A/g	88.3 (2000)	[157]
SnO_2@PANI	In-situ polymerization	Nanoparticles	1 M H_2SO_4	335.5 F/g at 0.1 A/g	(10000)	[158]
PANI/SnO_2	In-situ polymerization	N/A	1 M H_2SO_4	1172 F/g at 1 A/g	88 (2000)	[159]
PANI/SnO_2	Precipitation	Agglomerated particle	1 M H_2SO_4	337 F/g at 2 mV/s	73 (2000)	[160]
Co-doped SnO_2	Hydrothermal	Nanoparticles	1 M H_2SO_4	840 F/g at 10 mV/s	N/A	[161]
Zn-SnO_2	Sol–gel	Nanoparticles	2 M KOH	312.7 F/g at 10 mV/s	92 (500)	[162]
Zn-SnO_2, Ag-SnO_2	Hydrothermal	Nanoparticles	N/A	308.2 F/g at 0.5 A/g	67 (5000)	[163]
Zn doped SnO_2	Hydrothermal	Spherical	6 M KOH	229 F/g at 5 mV/s	N/A	[164]
Zr doped SnO_2	Hydrothermal	Nanoparticles	6 M KOH	166 F/g at 5 mV/s	N/A	[165]

(*continued on next page*)

Table 2 (*continued*)

Samples	Synthesis method	Morphology	Electrolyte	Specific capacitance	Cycling stability [%] (no. of cycles)	Ref.
doped SnO_2@MoS_2	Hydrothermal	Micrograins	1 M H_2SO_4	242 F/g at 0.5 A/g	84 (5000)	[166]
Mn doped	Hydrothermal	Star type flakes	3 M KOH+ 0.1 M $K_4[Fe(CN)_6$	246.5 F/g at 5 mA/cm^2	94.16 (1000)	[167]
MoS_2–SnO_2	Ultrasonication bath	Nanoparticles	2 M KOH	61.6 F/g	90 (1000)	[168]
SnO_2/RuO_2	Incipient-wetness	N/A	1 M KOH	710 F/g	N/A	[171]
S-SnO_2NPs-RuO_2@BCC	Spin coating	Nanosphere	1 M H_2SO_4	794 mF/cm^2 at 5 mV/s	87.5 (5000)	[172]
Co, N-SnO_2	Hydrothermal	Nanoflower array	PVA- H_2SO_4	361.1 F/g at 1 A/g	103.3 (10000)	[175]
Fe_3O_4@SnO_2	Hydrothermal	Core–shell nanorod	1 M Na_2SO_4	2.7 mF/cm^2 at 1.0 mA/cm^2	82.8 (2000)	[176]
CNT/SnO_2/MnO_2	Wet chemical	Nanosheets	1 M Na_2SO_4	427 F/g at 1 A/g	98 (5000)	[177]
Co_3O_4-SnO@SnO_2	Hydrothermal	Nanospheres	1 M KOH	1.056 F/cm2 at 1.0 mA/cm^2	91.5 (2000)	[178]
a-Fe_2O_3/SnO_2/rGO	Hydrothermal	Nanoparticles	6 M KOH	517 F/g at 1 A/g	98.7 (10000)	[179]
Sb-doped SnO_2	Sol–gel	Nanocrystallites	1 M Na_2SO_4	33 F/g at 50 mV/s	N/A	[180]
SnO_2–Al_2O_3	Hydrothermal	Nanoparticles	3 M KCl	119 F/g	(1000)	[181]
SnO_2/MnO_2	Solution-based	Core shell	1 M Na_2SO_4	800 F/g at 1 A/g	98.8 (2000)	[182]
SnO_2/GNS	Single step process	Nanoparticles	0.1 M H_2SO_4	472 F/g at 50 mV/s	90 (1000)	[183]
MnO_2@SnO_2	Hydrothermal	Core shell	1 M Na_2SO_4	367.5 F/g at 2 mV/s	91.3 (2000)	[184]
3D Ni/SnO_2	Hydrothermal	Nanoflowers	1 M NaOH	410 mF/cm^2 at 1 mA/cm^2	93.6 (2500)	[185]
SnO_2·XH_2O	Hydrolysis precipitation	Spherical	0.5 M H_2SO_4	36.1 F/g at 5 mV/s	98 (2000)	[186]
SnO_2/Ni	Hydrothermal	Nanoparticles	6 M KOH	541 F/g at 10 A/g	98.1 (1000)	[187]
MnO_2–Fe_3O_4–SnO_2	Wet chemical	Spherical nanoflakes	PVA- Na_2SO_4	1.12 F/cm^2 at 5 mV/s	90 (5000)	[188]
TiO_2-SnO_2 doped RuO_2	Wet balling mill	Porous nanoparticles	0.5 M H_2SO_4	571 F/g	N/A	[189]
RuSnO	Sol–gel	Nanoparticles	1 M H_2SO_4	930 F/g	100 (1000)	[190]
SnO_2@RH-SiO_2	Microwave combustion	Nanospheres	0.5 M Na_2SO_4	448 F/g at 1 A/g	N/A	[191]
SnO_2/NiO	Sol–gel	Mesoporous	2 M KOH	464 F/g at 5 mV/s	87.24 (1000)	[192]
SnS_2-SnO_2	Solvothermal	Flower-like	0.5 M Na_2SO_4	70.2 F/g at 2 A/g	92 (3000)	[193]
CNT/SnO_2–CuxO	Electroless deposition	1D	6 M KOH	662 F/g	94 (5000)	[194]

electrode. However, the material depicts only a 66 % rate retention after 1000 cycles, attributed to the mechanical stress onto CF-SnS_2 due to the insertion and de-insertion of electrolyte ions during cycling. A study showing the effect of different morphologies on the electrochemical performance of SnS_2 is done by Parveen et al. (Fig. 20). The specific capacitance values of sheetlike SnS_2, flowerlike SnS_2, and ellipsoid-like SnS_2 were reported as 390.38 F/g, 117.11 F/g, and 431.82 F/g respectively at 1 A g^{-1} current density (Fig. 20(b–c)). The flowerlike SnS_2 delivered the highest performance, attributed to the large surface area and better pore size distribution [208].

Similarly, the significance of layered structure in the supercapacitive performance of SnS_2 is well studied by the group Kumar et al. [209]. Optimization over the precursor ratio of Sn/thiourea resulted in petal-shaped like 3-D SnS_2 layered structure as shown in Fig. 21(a). The material delivered outstanding performance with a specific capacitance of 1403 F/g at 1 mV/s with an 85.87 % rate retention after 5000 continuous charge-discharge cycles (Fig. 21(b–c)). The excellent output is attributed to the unique inherent petal-shaped structure, allowing rapid ion intercalation into the electrode material as mentioned in Fig. 21(d). As an asymmetric SC device, the material is capable to operate a commercial LED over a small charging time of 30 s [209].

Nowadays, ALD has been widely used for the fabrication of active electrodes in numerous energy-related fields such as solar photovoltaic and secondary batteries due to its precise control of the film thickness, high degree of conformity/uniformity over the complex 3D substrate, and the properties of ALD films, including composition/phase [210–213]. Recently, the polycrystalline hexagonal-SnS_2 layered thin film with extremely uniform and conformal was successfully grown by using the atomic layer deposition (ALD) technique by the group of Ansari et al. [214] (Fig. 22). Interestingly, the electrochemical performances of the two thin films with two different phases deposited at two different temperatures (160 °C and 180 °C) were examined and the capacitance value of SnS_x@NF grown at 160 °C is found to be higher than that of SnS_x@NF at 180 °C. Also, the film was deposited so uniform and conformal on the 3D complex NF as can be seen from Fig. 22(a–h), which is not possible from other deposition techniques.

The synthesized SnS_x@NF electrode delivered an areal capacitance of 805.5 mF/cm^2 at 0.5 mA/cm^2 current density with remarkable cyclic stability over 5000 charge-discharge cycles, as shown in Fig. 22(i–j) due to the layer-by-layer deposition that holds greatly physiochemical bonding with the substrate [214]. Not only the morphology but also the dimension of nanostructures greatly affects the electrode performance. Nanostructured electrodes with various dimensions play a key role in capacitance enhancement due to the structural dependent advantages. This helps accelerate the reaction mechanism during the diffusion process of electrolyte ions into the electrode [215]. For example, a 2D microstructure of SnS_2 nanorods brings the advantages of large surface area and short ionic diffusion pathways to the group of Sajjad et al. [216]. The synthesized material prepared by the hydrothermal process delivered an enhanced specific capacitance of 270 F/g at 10 mV/s with only 9 % loss in capacitance after 8000 continuous charge-discharge cycles (Fig. 23) [216].

Tin monosulfide (SnS) also comes under multifunctional materials and possesses a layered structure with different morphologies. This layered structure facilitates the intercalation and de-intercalation of electrolyte ions and thus helps in improving the energy density. Several reports have been published in recent years based on various dimension-oriented syntheses of SnS nanostructures [217,218]. For example, Chauhan et al. opted a solvothermal process and successfully synthesized one-dimensional SnS nanorods. The application of SnS as electrode material in SCs is attributed to the intrinsic layered structure, which owns a large surface area and more importantly reduces the diffusion path length for both the ions and electrons during charge-discharge processes. The surfactant-free nanorods delivered a specific capacitance of 70 F/g, an energy density of 1.49 Wh kg^{-1}, and a power density of 248.33 W/kg, which is comparably higher than SnS-carbon composite [219].

In general, the rapid reactions occurring at the electrode-electrolyte interfaces are a great factor contributing to the double-layer capacitance effect in capacitors employing active electrodes, such as SnS, as used in

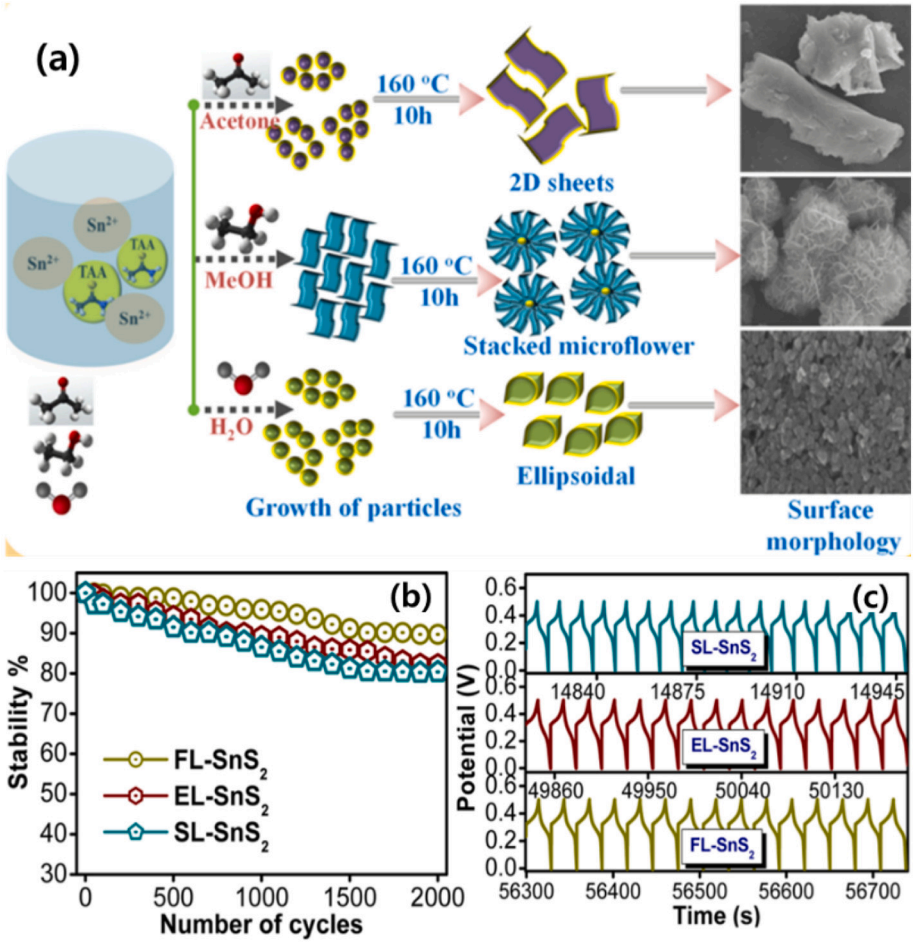

Fig. 20. (a) Schematic representation of the formation mechanism of SnS_2 nanoparticles with various morphologies, and (b–c) cyclic stability test versus CD cycles of EL-SnS_2, FL-SnS_2, and SL-SnS_2 electrodes. Reproduced with permission. [208] Copyright 2018, ACS.

this case. The following reactions may occur at the electrode-electrolyte interface of the SnS-nanorod electrode in the present system [219]:

$$\left(Sn^{II}S\right)_{surface} + Na^{+} \leftrightarrow Sn^{I}S - Na^{+} + e^{-}$$

or

$$SnS + 2Na^{+} + 2e^{-} \rightarrow Sn + Na_2S$$

The role of annealing temperature in determining the morphology, phase, and crystallinity of the SnS_x thin films was nicely explored by Reddy et al. The thin film synthesized by employing a solution-based spin-coating method showed the pure SnS phase when annealed at 500 °C. The resultant SnS thin film-based electrode delivered a specific capacitance of 42 F g^{-1} at a current density of 2 A g^{-1} [220]. In the electrode-electrolyte interface, redox reactions can occur in the following ways [220]:

$$SnS_2 + 2Na^{+} + 2e^{-} \leftrightarrow SnS + Na_2S$$

$$SnS + 2Na^{+} + 2e^{-} \leftrightarrow Sn + Na_2S$$

$$Sn + Na_2S + xNa^{+} \leftrightarrow Na_xSn + Na_2S$$

Barik et al. synthesized stannous sulfide (SnS) nanoparticles as SC electrode material through a simple hydrothermal process. The dimension of SnS nanoparticles was found to be 4–10 nm. The output-specific capacitance of the nanocomposite was reported as 201 F/g at 0.1 A g^{-1} current density [221]. The group of Rani et al. successfully deposited SnS onto Ni foam by using the hydrothermal technique. The binder-free electrode in an alkaline electrolyte medium delivered a specific capacitance of 686 F/g at 10 mV/s [222]. Although pure tin-based sulfides are not much explored as a pseudocapacitive electrode material for SCs, from the above-reviewed literature, it is obvious that they possess a potential for SC electrodes. They need further attention to overcome the limitations of less specific capacitance, energy density, and electrochemical stability.

2.2.2. *SnS_x (where x = 1,2) on carbonaceous materials*

Although the CdI_2 type layered structure of SnS_2 provides a large surface area for the accumulation of electrolyte ions, the poor structural stability, low electrical conductivity, and small specific capacitance delivery are the major limitations for the practical application of these materials in SCs. To overcome such problems, one of the noble approaches is to compound SnS_x types of materials with other potential materials. Carbon-based materials are quite prospective materials for commercialization. Their advantages include low cost, non-toxic nature, rich abundance, high chemical stability, large surface area, and good electric conductivity [42]. The major category includes activated carbon, carbon-nanotubes, carbon-nanofibers, and graphene. The performance of these materials has been widely explored in the literature which has been discussed in the prior section. Their various porous structure like micro, meso and macro greatly supports the overall electrochemical performance. Thus, many researchers tried to combine the SnS_x nanostructures with carbonaceous materials, to bring the synergistic contribution of both types. For example, graphene possesses a large surface area (~2600 m^2/g) and excellent electrical conductivity (~106 S cm^{-2}). Therefore, hybridized with SnS_2, and has been utilized

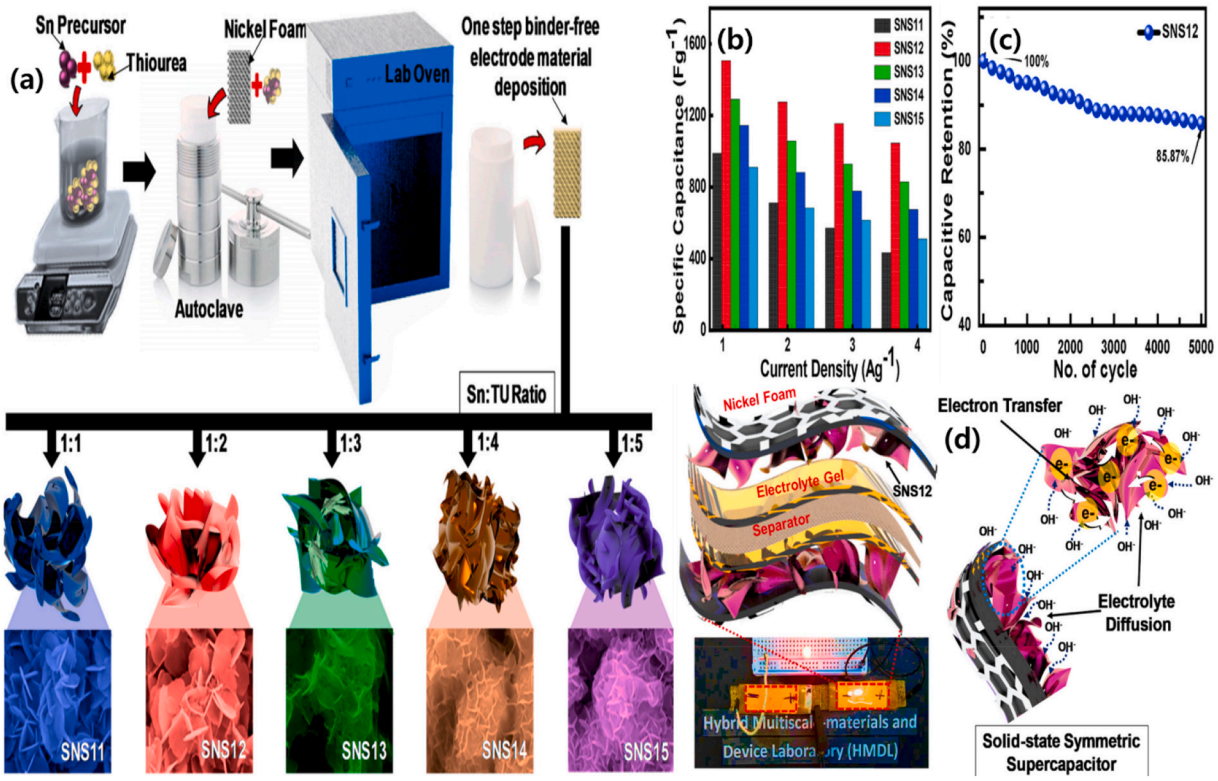

Fig. 21. (a) Schematic diagram and possible microstructure of preparation corresponding to the different ratios of Sn/TU, electrochemical performance measured by (b) comparative specific capacitance as a function of current density (c) cyclic stability test of the optimized SNS12 electrode, and (d) schematic illustration of charge-storage mechanism in this study. Reproduced with permission. [209] Copyright 2017, Elsevier.

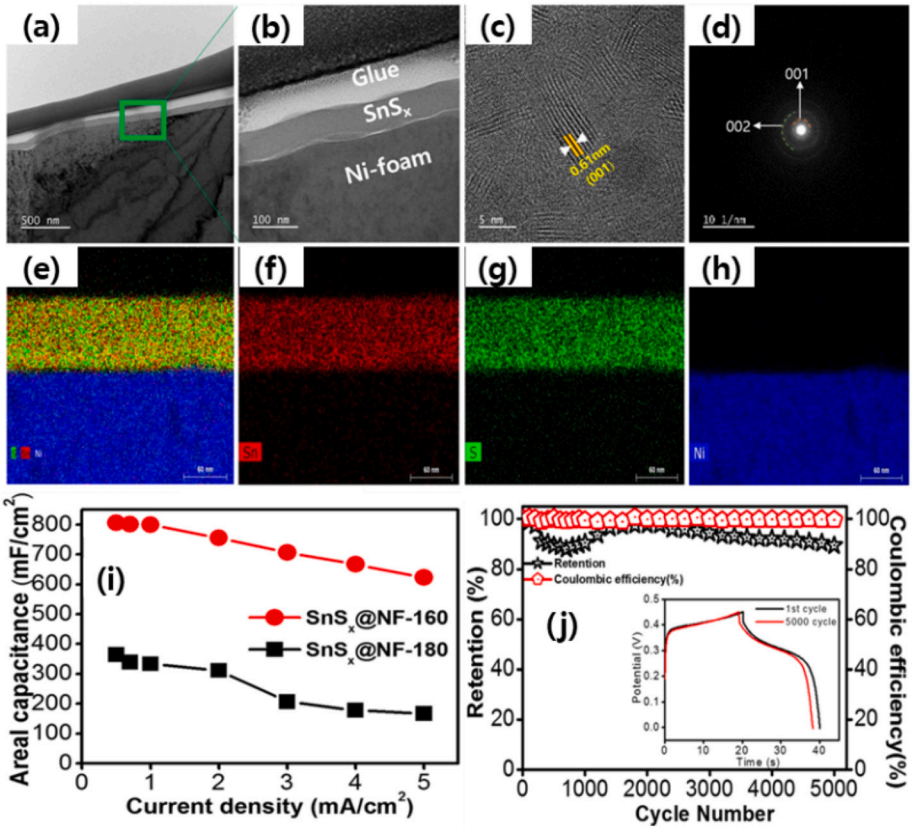

Fig. 22. (a–b) Cross-sectional TEM images, (c–d) the HRTEM images, and SAED arrays for the SnS_x@NF-160 electrode prepared by 500 ALD cycles, (e–h) the corresponding STEM elemental mapping confirming the uniform distribution of Sn, and S, on Ni foam, (i) Comparative Areal capacitances as a function of current density, and (j) Cyclic stability versus retention for ALD-SnS_x@NF-160 grown by 500 ALD cycles. The inset figure shows charge/discharge curves of the 1st and 5000th cycles. Reproduced with permission. [214] Copyright 2019, Nature.

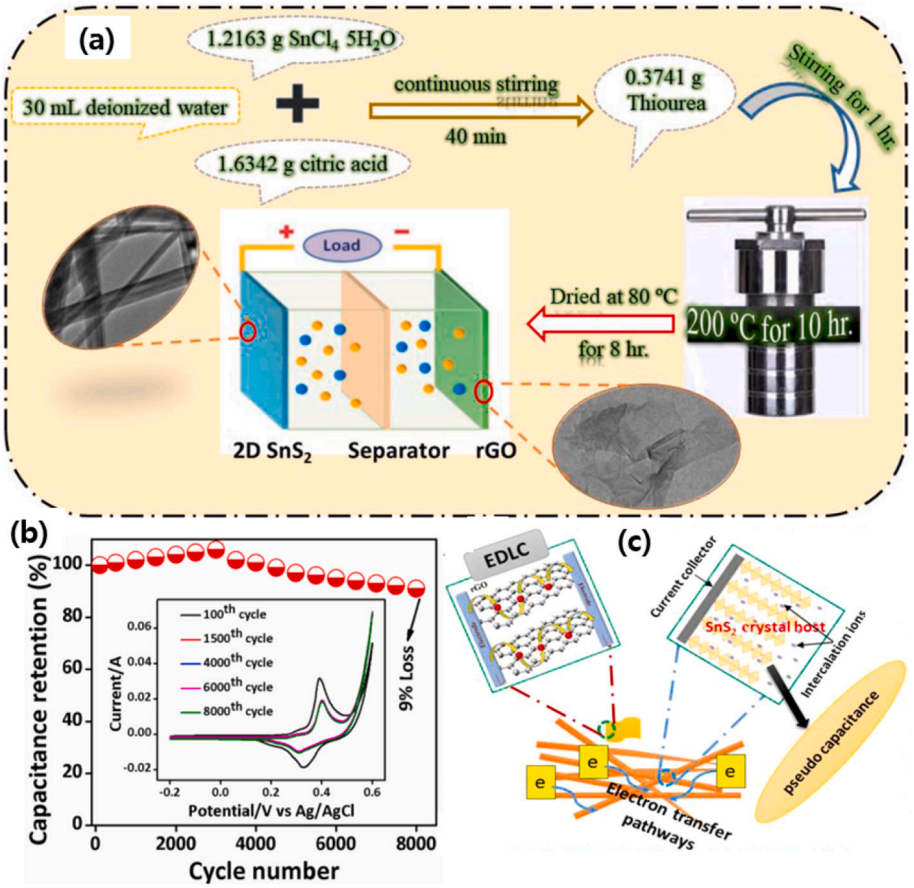

Fig. 23. (a) Schematic diagram of the preparation of SnS_2 nanorods by one pot-hydrothermal method, (b) cyclic stability test of the SnS_2//rGO HSC device after 4000 cycles, and (d) schematic illustration of charge-storage mechanism in this study. Reproduced with permission. [216] Copyright 2017, Elsevier.

as a composite electrode in electrochemical energy storage [83] Recently, Duangchuen and co-workers reported SnS_2/RGO nanocomposite for supercapacitor applications. Compared to SnS_2 nanoparticles, the SnS_2/RGO electrode material delivered better results (specific capacitance of 273.54 F/g at 0.3 A g^{-1} current density, capacitance retention of 84.25 % after 1000 cycles. The conducting RGO network type structure promotes electronic conductivity and prevents the agglomeration of the structure during continuous charge-discharge cycles [223]. There are two redox reaction peaks on the CV curves of SnS2 NPs and all SnS2/RGO NCP electrodes around the oxidation peak (0.35–0.38 V) and the reduction peak (0.25–0.26 V), specifying that pseudocapacitors possess storage charge functionality due to reversible redox reaction between SnS2 on the electrode surface and electrolyte ions (K+) [223].

$$SnS_2 + K^+ + e^- \leftrightarrow SnS + SK$$

As shown by the above mechanism, Sn oxidation states are changed between Sn4+ and Sn2+ ions in SnS2 NPs and all SnS2/RGO NCP electrodes. Additionally, NPs and NCPs made of SnS2/RGO can store charge through adsorption/desorption of electrolytes (K+) on their surfaces that can be understood by the following process [223]:

$$(SnS_2)_{surf} + K^+ + e^- \leftrightarrow (SnS_2^- + SK)_{surf}$$

A hybrid nanosheet-like structure of SnS_2/rGO composite is successfully synthesized by Shi et al. with various properties as shown in Fig. 24. The author reported the role of rGO as an aggregation controller and an active site with multiple porosities. The well-dispersed SnS_2 nanodots onto rGO showed a high specific capacitance of 871.7 C g^{-1} with 95.1 % capacitance retention. As an asymmetric SC device, the SnS_2/rGO//AC delivered an energy density of 29.06 Wh kg^{-1} at 747.32 W Kg^{-1} power density [224]. Similarly, the group of Chauhan et al. explored SnS_2/RGO as supercapacitor electrode material. The 2D hexagonal nanosheets of SnS_2 with reduced graphene oxide showed high specific capacitance as well as good energy and power density (~16.67 Wh kg^{-1} at 488 W Kg^{-1}). Also, the material possessed a 95 % capacitance retention after 1000 charge-discharge cycles. The synergistic contribution of both materials is attributed to the remarkable electrochemical performance [200].

The effect of various concentrations of graphene on the electrochemical performance of SnS/graphene nanocomposite is well studied by Ravuri et al. utilizing the wet chemical method, the synthesized material delivered a specific capacitance of 984 F/g at 5 mV/s in 6 M aqueous KOH electrolyte. The excellent electronic conductivity of graphene greatly improves the electrochemical behaviour by facilitating the pseudocapacitance effect [225]. Li et al. fabricated nanocomposites based on Carbon-coated SnS as electrode materials for supercapacitor through the ball milling method. The nanocomposite consists of SnS particles with sizes of about 20–30 nm and was found to be homogeneously distributed throughout the hierarchical porous structure and delivered a specific capacitance of 28.47 F/g [203]. Due to the poor electronic conductivity, low structural stability, and irreversible faradaic reactions, SnS_x types have not been widely explored in the literature, but the addition of carbon-based materials significantly improves electrochemical performance. Hence, the future research direction must focus on the hybridization of carbonaceous materials with the new morphologies and crystal structure of SnS_x types of materials.

2.2.3. SnS_x on M (M = Li, Na, K, Mo) and others

The application of SnS_x type crystal structure for SCs is mainly due to the layered structure. These are quite analog to graphite, which is a

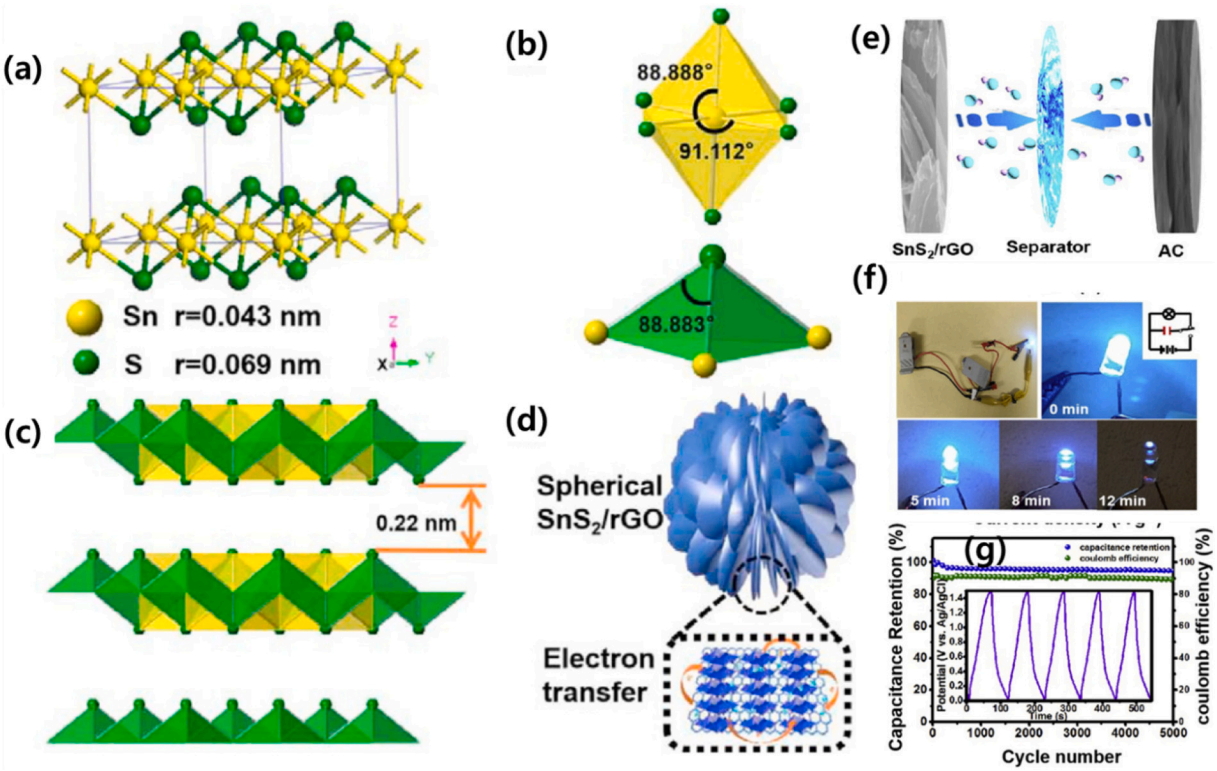

Fig. 24. (a) Crystal lattice structure diagram of SnS_2. (b) SSn3 tetrahedral and SnS6 octahedral. (c) SnS_2 super cell viewed towards (010) direction. (d) Electron transfer of spherical SnS_2/rGO, (e) assembly diagram of the SnS_2/rGO//AC ASC device, (f) Photos of the ASC device lighting up a blue LED light, and (g) The cycling test of the ASC device and (the inset of i) the GCD curves in the last 5 cycles. Reproduced with permission. [224] Copyright 2020, Elsevier. (For interpretation of the references to colour in this figure legend, the reader is referred to the web version of this article.)

highly suitable intercalation host for other metal ions. They can be exfoliated to single or few-layered 2D structures, providing the benefits of large specific surface area as well as excellent ionic conductivity. Such morphologies enhance the capacitance due to the pseudocapacitance effect that arises from the diffusion of metal ions like Na^+, Li^+, and K^+ into the layers [196,226]. For example, Setayeshmehr et al. compared the electrochemical performance of pure SnS_2 and alkali metal-doped (Li, Na, K, and Cs) SnS_2 nanostructures using simple one-pot synthesis as shown in Fig. 25. The SnS_2 layered structure with Na dopant showed the best performance. It is attributed to the higher conductivity and expansion of interlayer space along with the increased number of electroactive sites. The Na-doped SnS_2 delivered a high capacitance of 269 F/g at 1 A g^{-1} current density [227].

The introduction of doping metal/non-metal ions modifies the nanostructure and band structure of SnS_2, which offers novel potential for upgrading the electrochemical performance of SnS_2. Chu et al. [228] synthesized various metals (Ni, Co, Mn) doped SnS_2-graphene aerogel (M-SnS_2-GA) via a solvothermal process using metal chlorides and thioacetamide as precursors as shown in Fig. 26. Digital pictures in Fig. 26 (b–e) demonstrate the prepared in cylindrically shapes with the 1 cm SnS_2-GA has a yellow colour, resulting from SnS_2 and the rest of the samples exhibited deeper colour owing to the doping with metal. An optimized Mn-SnS_2-GA electrode showed the best supercapacitance performance in terms of specific capacitance and outstanding cycling

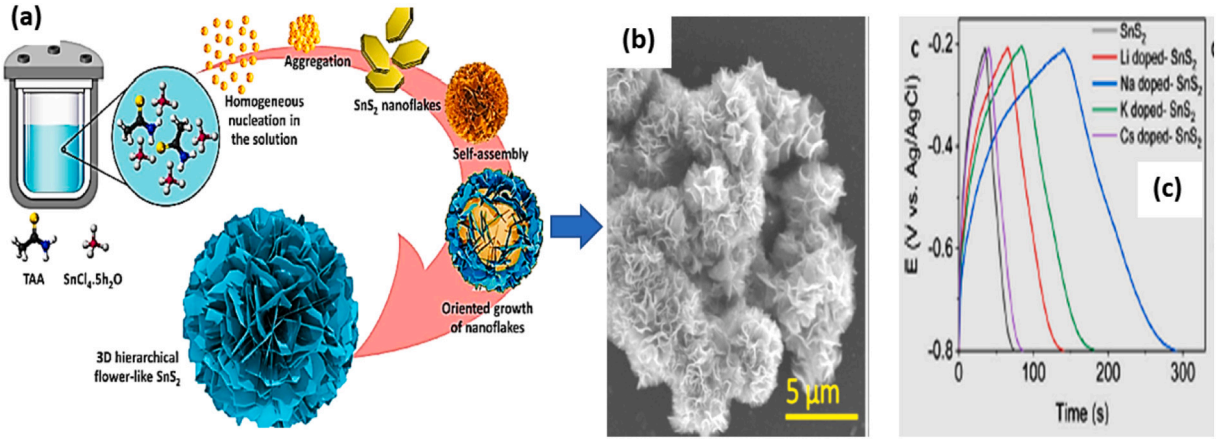

Fig. 25. (a, b, and c) Schematic image of the formation mechanism of 3D flower-like SnS_2 nanostructures prepared by solvothermal method, FESEM image of SnS_2 nanoflowers prepared after a reaction time of 24 h, the charge-discharge profile of SnS_2 doped with various alkali metals. Reproduced with permission. [227] Copyright 2021, Elsevier.

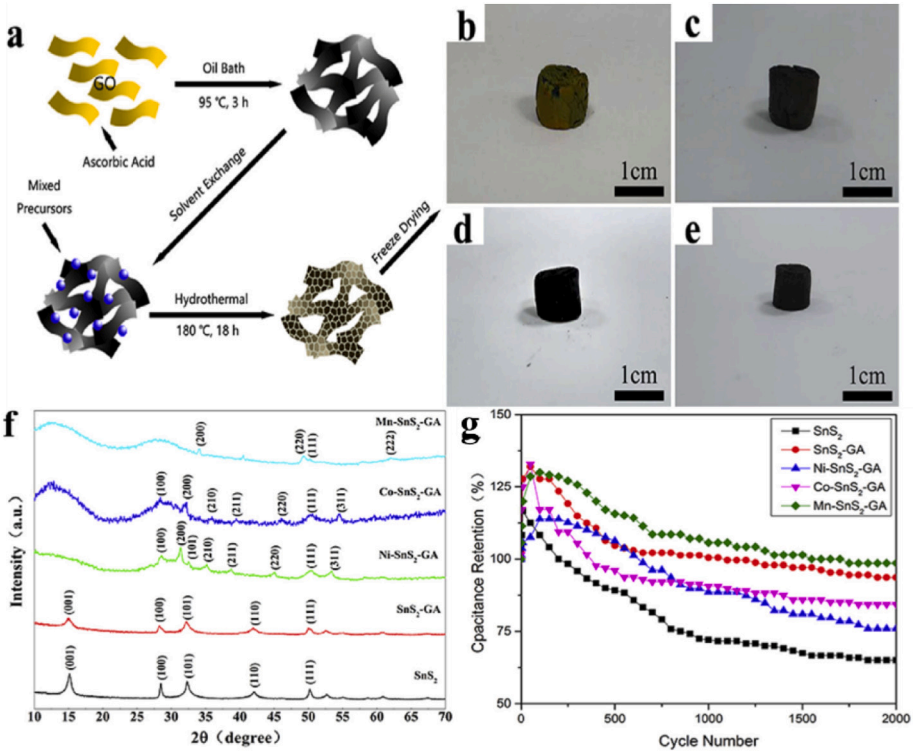

Fig. 26. (a) Schematic diagram of the preparation of metal-doped SnS_2-GA, the digital photographs of (b) SnS_2-GA, (c) Ni-SnS_2-GA, (d) Co-SnS_2-GA, and (e) Mn-SnS_2-GA (f) the XRD patterns of the prepared samples, and (g) cyclic stability tests of the representative samples. Reproduced with permission. [228] Copyright 2020, Elsevier. (For interpretation of the references to colour in this figure, the reader is referred to the web version of this article.)

stability (523.51 F/g at the scan rate of 5 mV/s, 98.57 % retention after 2000 cycles at 10 A/g) among other electrodes.

In another work, the group of Ma et al. [199] fabricated Molybdenum doped SnS_2 hierarchical mesoporous architectures through hydrothermal technique. The addition of Molybdenum as a dopant in the SnS_2 crystal structure caused the structural and lattice dislocation, resulting in the few-layered and expanded architecture. Compared to bare SnS_2 (specific capacitance 89.4 F/g at 1 A g^{-1}), the Mo-SnS_2 delivered a better specific capacitance value of 213.2 F/g at 1 A g^{-1} current density. The improved performance is credited to the mesoporous structure with a large surface area and few-layered features [199]. Among other metal chalcogenides, the SnS_2 possesses poor electrochemical properties. To increase the supercapacitive behaviour, the example of the addition of copper as a conductive transition metal to SnS_2 is given by the group of Hussain et al. [229] Utilizing the hydrothermal approach, the group synthesized ternary Cu_2SnS_3 (CTS) metal chalcogenides as supercapacitor electrode material. The micro-flower-based morphology of CTS delivered a specific capacitance of 183 F/g at 1 A g^{-1} in the three-electrode cell test system. Also, the CTS composite-based electrode retained an 88.5 % capacitance after 2000 cycles. The synergistic effect of the conductivity of copper and the layered structure of SnS_2 resulted in improved performance.

Although SnS_2 possesses a layered structure, the 2D SnS_2 nanosheets are present in a stacked manner, which provides small interlayer spacing. Thus, greatly reducing the electrochemical performance. To address such an issue one of the strategies is the formation of heterojunction materials within a single system. This facilitates the rapid charge transfer process. For instance, Wang et al. employed the heterojunction approach by combining 2D SnS_2 and 2D MoS_2 crystal structures and formed SnS_2/MoS_2 heterojunction as SC electrode material. The novel configuration showed improved performance than bare SnS_2 material, as the material delivered a high specific capacitance of 466.6 F/g at 1 A g^{-1} current density. An asymmetric SC device based on this configuration exhibited an energy density of 115 Wh kg^{-1} at 2230 W Kg^{-1} of power density. The structure is also capable of preventing agglomeration and stacking during the cycling process [230]. To utilize the combined effect of SnS_2 and Ni_3S_2 as electrode material in supercapacitors, group of Pant et al. opted for a hydrothermal approach to construct a hybrid structure of SnS_2–Ni_3S_2 onto nickel foam. The 3D flakelike structure possessed a width of around 170 nm, the specific capacity of 272 mAh/g at a 4 mA/cm^2 current density with 91 % capacitance retention after 5000 cycles. The large surface area and good porosity are attributed to the enhanced electrochemical performance [201]. Similarly, Wang et al. prepared a 3D flower-like heterostructured configuration of SnS_2/MoS_2 by applying a non-toxic hydrothermal method [231]. Compared to the reported work [230], the 3D SnS_2/MoS_2 delivered a capacitance of 105.4 F/g at a high current density of 2.35 A g^{-1}. The nanosheet-like structure of MoS_2 and nanoplate-like morphology of MoS_2 helped in the rapid electronic transport and hence improved the electrochemical performance [201]. Enaganti et al. [232] fabricated a MoS_2/SnS_2 as a 2D/0D Structure onto flexible cellulose paper for the SC electrode. The material MoS_2/SnS_2 delivered a high specific capacitance of 422.2 F/g at 0.5 A g^{-1} than the bare SnS_2 electrode (~277.1 F/g). It is because SnS_2 quantum dots generate new electroactive sites for the occurrence of more redox reactions in 3 M aqueous KOH electrolytes [232]. In the heterojunction structure formation like other metal sulfides, cobalt sulfides also show potential application in SCs. These are promising due to the availability of various phases and good material linking properties in the formation of heterostructures [233,234]. For example, Kumar et al. explored the heterostructure formation of SnS_2@Co_3S_4 with the help of the SILAR method as shown in Fig. 27. The 2D layered heterostructure exhibited a high specific capacitance value of 1580 F/g with 94.8 % capacitance retention after 3000 cycles [234].

The tin sulfides-based materials are extensively explored as anode materials for lithium-ion batteries. However, the incorporation of metal ions into tin sulfides has resulted in new SC research. This approach is unique and holds promising usage in SCs. In this series, Wang et al.

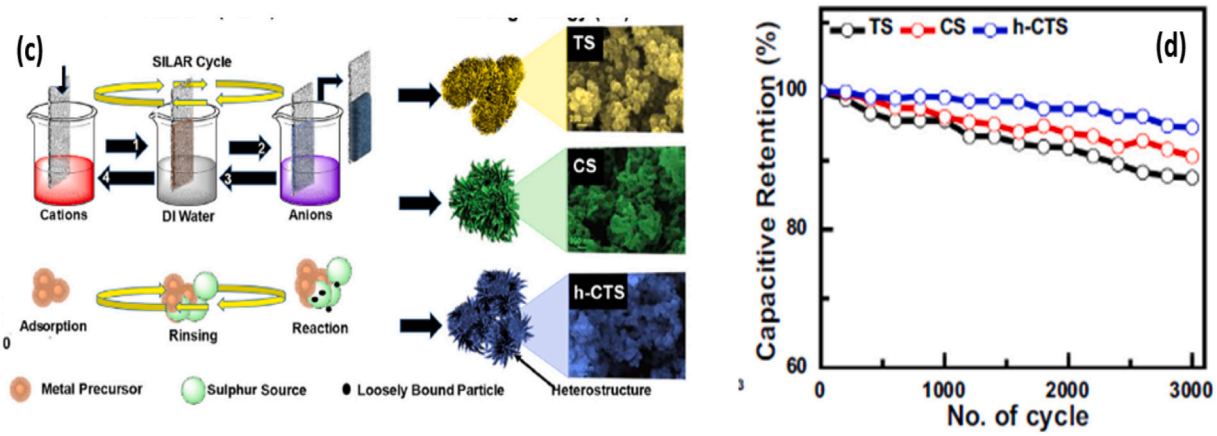

Fig. 27. (c and d) Pictorial representation for the synthesis process of bi-layered SnS_2@Co_3S_4 heterostructure based electrode material, cycling performance plot for 3000 continuous charge-discharge cycles. Reproduced with permission. [234] Copyright 2020, Elsevier.

[235] synthesized Cu_2SnS_3 as electrode material with the help of the solvothermal process. The role of morphology in the capacitive performance is signified here, as the Cu_2SnS_3 microspheres exhibited better performance compared to Cu_2SnS_3 nanoparticles. The output delivery is as, a specific capacitance of 406 C g^{-1} at 1 A g^{-1}, energy density of 85.6 Wh kg^{-1} at a power density of 720 W Kg^{-1}. The large specific surface area along with average pore size distribution is credited to the enhanced performance [235]. In an interesting approach, Lokhande et al. synthesized Cu_2SnS_4 thin-film electrodes using the SILAR technique for SC application. The EC performance is evaluated in different electrolytes and found to be highest in 1 M aqueous NaOH electrolyte. The material showed a specific capacitance of 704 F/g and a high energy density of 27.77 Wh kg^{-1} at a power density of 7.14 KW Kg^{-1}. The orthorhombic structure with conducting and binder-free thin films enabled improved performance [236]. In the above-reviewed section, SnO_2 is found to be a promising candidate for SC electrodes due to its high chemical stability and good redox activity [123–126]. Also, tin disulfide (SnS_2) is a quite important electrode material due to the CdI_2 type layered hexagonal structure. Hence, the combination of these two materials in the form of heterostructure can be a promising route that can synergistically combine the advantages of both materials. For example, recently Asen and co-workers successfully synthesized SnS_2-SnO_2 nano-heterostructures with the help of a solvothermal technique. Utilizing the two different precursors, the thioacetamide (TAA) based SnS_2-SnO_2 material delivered a high specific capacitance of 70.2 F/g at 2 A g^{-1} current density than thiourea based electrode (specific capacitance of 31.5 F/g at 2 A g^{-1}). With the well-defined porous structure with the combined properties of SnS_2 and SnO_2, the material showed better electrochemical performance than bare SnS_2 and SnO_2 [193]. All the metal oxides are not ideally suitable as SC electrode material. For instance, copper oxides are the most abundant oxides in nature but are poor active electrodes due to the low electrochemical redox activity and small operating voltage window. Other metal oxides like CoO and NiO are far superior to CuO in their native form [237]. However, the activity of such metal oxides can be enhanced by hybridizing them with other potential materials like graphene oxide. In this direction, a good example is given by the group of Hatui et al. Utilizing the eco-friendly hydrothermal technique, the group synthesized SnS_2@Cu_2O/rGO nanoflowers as cathode for SCs. The material delivered an outstanding electrochemical performance with a specific capacitance of 1806 F/g at 0.6 A g^{-1} in a three-electrode system. As a device, the material is capable of lighting a blue LED light for a few seconds. The performance enhancement is credited to the reduced graphene oxide, which acted as a base for the occurrence of pseudocapacitance reactions, and SnS_2 as a generator of more electroactive sites for faradaic processes to occur. The composite material provides short pathways, hence, facilitates the rapid motion of electrolyte ions, resulting in a fast charge-discharge process [238]. The potential range of an electrode material plays a crucial role in energy and power density enhancement. Although SCs are well known for high power delivery, low energy density is the major limitation that needs to be overcome. The tin sulfide-based electrodes also suffer from a low potential range (~0.5 V). Therefore, they have poor rate capability and inferior energy and power densities. The addition of polymers into tin sulfides can improve the potential range as, they not only provide conductive support, and stability but also help in the growth of nano-sized tin sulfides. For example, Wang and co-workers have successfully grown 2D SnS_2@PANI@GF as a flexible SC electrode for the first time. The composite material showed high mechanical stability as SnS_2 nanoflakes act as a protective coating for PANI and thus reduced the risk of structural and electrochemical degradation. The potential tolerance has raised to 0.95 V and delivered a remarkable specific capacitance of 365 F/g at a 10 mV/s scan rate. The synergetic effect of both SnS_2 and PANI contributes positively to the overall performance [239]. The energy density of SCs can also be increased by following the asymmetric device configuration strategy. The optimization and choice of electrode material in the form of anode and cathode are very crucial here. The tin sulfide based electrodes can also be utilized in this configuration as these are highly chemically stable, non-toxic and offers a large specific surface area [177].

A similar approach is followed by Patil and co-workers. The group has successfully synthesized a solid-state asymmetric SC device with MnO_2 acting as a positive electrode and SnS as negative electrode material with PVA-$LiClO_4$ as a solid gel electrolyte. The device exhibited a high specific capacitance of 120 F/g, an energy density of 29.8 Wh kg^{-1} at a power density of 1.25 kW Kg^{-1} with 95.3 % capacitance retention after 5000 cycles [240]. On the other hand, the SnS based electrode also tested. According to the CV profile, the charge storage is a result of both redox reactions as well as EDLC-type reactions at potential positions of −0.6 and −1.0 V. It is evident from the CV curves that the electrode exhibits asymmetrical kinetic irreversibility on the reduction and oxidation sides. Each electrode exhibits a clear increase in the area under the CV curve with an increase in scanning rate. During charging, OH^- ions are intercalated into the KOH electrolyte, while during discharging, the ions are deintercalated. Based on the following reaction, the charge is transferred between O-SnS electrode materials [240]:

$$SnS + OH^- \rightarrow SnSOH + e^-$$

It is well recognized theoretically as well as experimentally that nanoarchitectures enriched by porous geometry and well define morphology contributes to the high electrochemical performance of SC electrodes. A challenging task to construct 3D porous SnS nanostructures from 2D SnS nano form is done by Liu et al. as shown in Fig. 28(a). The

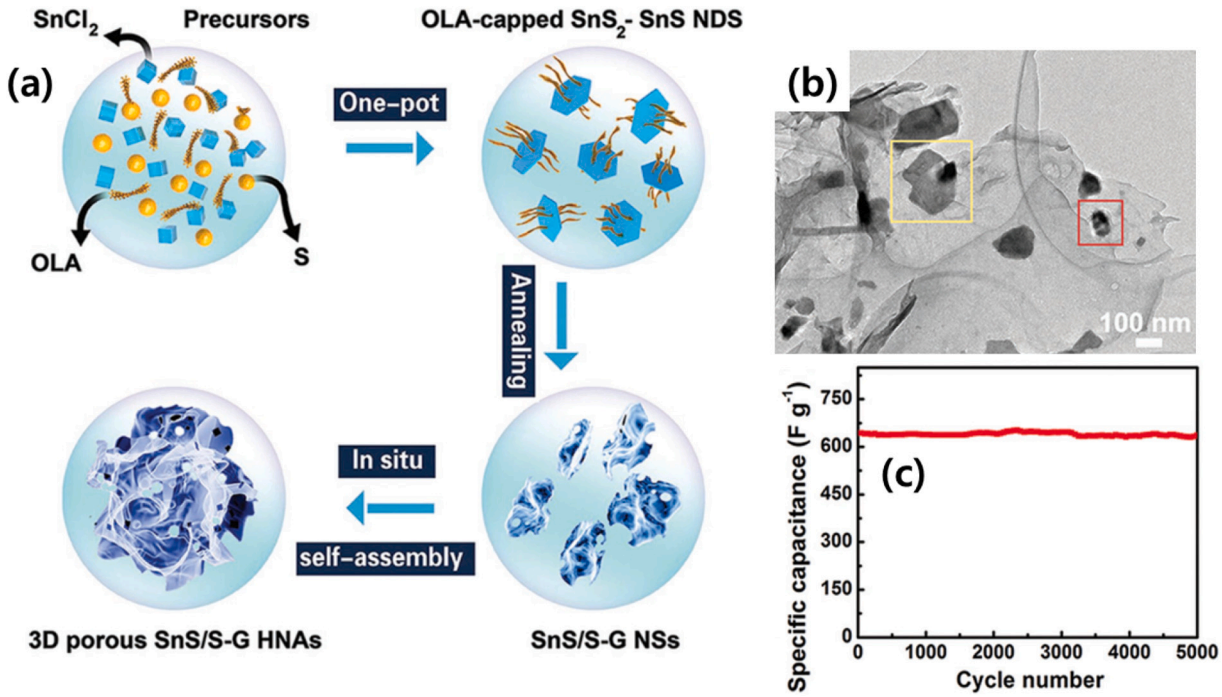

Fig. 28. (a) Schematic diagram of the preparation of 3D porous SnS/S-G HNAs, (b) related low -magnification TEM images, and (c) cyclic stability test for the same electrodes. Reproduced with permission. [241] Copyright 2020, Elsevier.

Table 3
Comparison of tin sulfide-based active electrode materials for supercapacitor.

Samples	Synthesis method	Morphology	Electrolyte	Specific capacitance	Cycling stability [%] (no. of cycles)	Ref.
SnS_x	Solvothermal	Carnation flower	I M KCl	524.5 F/g at 0.08 A/g	66 (1000)	[207]
	Solvothermal	Flowerlike	2 M KOH	431 F/g at 1 A/g	90 (2000)	[208]
	Solvothermal	3D petal-like	1 M KOH	1403 F/g at 1 mV/s	85.8 (5000)	[209]
	ALD	Nanogranular	2 M KOH	805.5 mF/cm^2 at 0.5 mA/cm^2	90 (5000)	[214]
	Hydrothermal	Nanorods	1 M NaOH	270 F/g at 10 mV/s	91 (8000)	[216]
	Solvothermal	Nanorods	2 M Na_2SO_4	70 F/g at 0.5 mA/cm^2	60 (500)	[219]
	Solution-based spin-coating	Hexagonal flakes	0.2 M NaOH	42 F/g at 2 A/g	90 (1000)	[220]
	Hydrothermal	Nanoparticles	1 M KOH	201 F/g at 0.1 A/g	88 (1000)	[221]
	Hydrothermal	Nanoparticles	N/A	145 F/g at 5 A/g	N/A	[222]
	Hydrothermal	Flakelike	3.5 M KOH	213.2 F/g at 1 A/g	89 (1000)	[199]
SnS_2-SnO_2	Solvothermal	Nanosheets	0.5 M Na_2SO_4	149 F/g at 2 A/g	92 (3000)	[193]
SnS_2/RGO	Hydrothermal	Nanoplatelet	2 M Na_2SO_4	500 F/g at 0.5 A/g	95 (1000)	[200]
SnS_2–Ni_3S_2@NiF	Hydrothermal	Flake-like	2 M KOH	272 mAh/g at 4 mA/cm^2	91 (3000)	[201]
Carbon-coated SnS	High-energy ball milling	Nanocluster	0.1 M KOH	30.12 F/g at 10 mV/s	N/A	[203]
SnS/carbon	Chemical precipitation	Net-like	0.1 M KOH	36.16 F/g	N/A	[204]
SnS_2/RGO	Hydrothermal	Nanoparticles	2 M KOH	273.5 F/g at 0.3 A/g	84.2 (1000)	[223]
SnS_2/rGO	Hydrothermal	Sphere	3 M KOH	871.7C/g at 1 A/g	94.9 (1000)	[224]
SnS/G	Wet chemical	Nanoparticles	6 M KOH	984 F/g at 5 mV/s	N/A	[225]
SnS_2/g-C_3N_4	Hydrothermal	Flower-like	3 M KOH	552 F/g at 0.5 A/g	95.8 (15000)	[226]
Na doped- SnS_2	Solvothermal	3D flower-like	0.5 M Na_2SO_4	269 F/g at 1 A/g	91 (4500)	[227]
M-SnS_2-GA	Solvothermal	Nanosheets	6 M KOH	532.51 F/g at 5 mV/s	98.57 (2000)	[228]
Cu_2SnS_3	Hydrothermal	Flower-Like	1 M KOH	183 F/g at 1 A/g	88.5 (2000)	[229]
2D/2D SnS_2/MoS_2	Hydrothermal	Nanosheets	0.5 M KOH	466.6 at 1 A/g	88.2 (500)	[230]
SnS_2/MoS_2	Hydrothermal	3D flower-like	1 M KCl	105.7 F/g at 2.35 A/g	90.4 (1000)	[231]
2D/0DMoS_2/SnS_2	Hydrothermal	Flower-like	3 M KOH	422.2 F/g at 0.5 A/g	65 (1000)	[232]
$Ni_{1.77}Co_{1.23}S_4$	Hydrothermal	Capsule-like	2 M KOH	224.5 mAh/g at 0.25 A/g	87 (1000)	[233]
SnS_2@Co_3S_4	SILAR	Cauliflowers	2 M KOH	1580 F/g at 1 mV/s	94.8 (3000)	[234]
Cu_2SnS_3	Solvothermal	Nanosheet	3 M KOH	406C/g at 1 A/g	(2000)	[235]
Cu_4SnS_4	Chemical technique	Spherical	1 M NaOH	704 F/g at 0.5 A/g	72 (2000)	[236]
SnS_2@Cu_2O/rGO	Hydrothermal	Nanoflowers	1 M KOH	1290 F/g at 1 A/g	90 (1000)	[238]
SnS_2@ PANi@GF	Electrochemically deposited	Nanoflake	1 M HCl	365 F/g at 10 mV/s	73 (5000)	[239]
O-SnS	Chemically deposited	Nanoflowers	1 M Na_2SO_4	1203 F/g at 5 mV/s	95.3 (5000)	[240]
SnS_2-g-C_3N_4	Solvothermal	Flower-Like	0.2 M Na_2SO_4	210.3 at 1 A/g	84 (1500)	[242]
Copper tin sulfides	Hydrothermal	Nanoflowers	N/A	856 F/g at 2 mV/s	N/A	[243]
SnS_2/G	Ball-milling	Nanosheets	1 M KOH	565 F/g at 1 A/g	90 (3000)	[244]
SnS_2@CF-2	Hydrothermal	Nanoplate	1 M KOH	283.6 F/g at 1 A/g	71.3 (10000)	[245]
SnS/S-G HNAs	Wet chemical	Sheet-like	6 M KOH	642 F/g	99.1 (5000)	[246]

group reported the successful synthesis of 3D porous SnS/S-doped graphene hybrid nanostructure and employed it in flexible solid-state SC (Fig. 28(b)). The 3D porous structure allowed a pseudocapacitance effect and resulted in a high specific capacitance of 642 F/g with outstanding cycling stability up to 5000 cycles as displayed in Fig. 28(c) [241].

From the above-reviewed literature, the Sn-based sulfides hold key as promising SC electrode material (Table 3) due to a) high chemical stability and therefore eludes the corrosion effect, b) the large specific surface area provided by the layered structure, c) non-toxic and environmentally friendly nature, d) the n-type semiconducting nature with a bandgap of 2.2 eV [228,230,242–245]. However, the Sn-sulfides suffer from low redox activity, less conductivity, and poor reversibility. To improve the electrochemical performance of Sn-based sulfides numerous efforts have been reported in the literature that is reviewed above in depth. Although the efforts are innovative, promising, cost-effective, and highly desirable for SC development, for the commercialization of SCs based on Sn-based sulfides, it is quite important to explore them at a large scale by utilizing new and advanced techniques. Also, based on previous reports the investigation of tin sulfide-based nanostructures as a supercapacitor electrode is not so much expanded and the electrochemical behaviour of SnS_x for pseudocapacitors still needs to be further investigated.

3. Future perspectives and conclusions

3.1. Future perspectives

With the rapid technological advancements in SCs based applications from miniature portable electronics to hybrid electric vehicles, it is quite challenging to explore revolutionary electrode materials. The potential electrode materials are characterized by chemical stability, non-toxicity, low cost, large specific surface area, and excellent conductivity. In this domain, the Sn-based materials have attracted the interest of researchers and technologists to develop next-generation SC devices. Herein, we have comprehensively reviewed tin-based oxides, sulfides, and their composite form as electrode materials for SCs. The literature based on electrochemical performance along with various synthesis techniques, morphologies, nanoarchitectures is provided to facilitate the understanding of the material. No doubt, the tin-based electrode materials are cheap and possess a large theoretical capacity (≈780 mAh g^{-1}) as energy storage material. The material has been significantly explored for lithium and sodium-ion batteries however, for supercapacitors it is far behind commercialization and is limited to the laboratory only. Likewise, other metals such as nickel, cobalt, magnesium, iron, etc., tin-based materials have not been enormously explored as SC electrodes and therefore limited literature is available on it. The major limitations in the widespread application along with possible solutions are outlined as (a) pure tin faces poor electrochemical stability and shows limited cycling performance. Introducing conducting phases like the incorporation of carbon-based materials, other metals, or metal oxides, and conducting polymers are a few approaches proven to improve the cyclic stability and rate capability. (b) Tin-based oxides possess a large theoretical capacity (≈780 mAh g^{-1}), are chemically stable compared to other metal oxides, and have a long lifetime. But the poor conductivity of the material results in small electroactive mass loading efficiency and therefore less electrolyte wettability. Such hindrance in electrochemical performance can be overcome by introducing high-class conducting components such as good-quality porous carbon nanomaterials, conducting polymers, inorganic precursors etc., enriched by attractive physical and chemical features for efficient conductivity. (c) Tin-based sulfides are naturally abundant and possess tunable optical band gaps as well as layered structures, highly desirable for outstanding electrochemical behaviour as SC electrodes. But the 2D layered structures of SnS_x materials are present in a stacked manner, which provides small interlayer spacing. Thus, greatly reducing the electrochemical performance. To address this issue formation of heterojunction materials within a single system could be a good strategy. Tailoring the hetero-structured morphology with various dimensions could facilitate the rapid charge transfer process, due to the short ionic diffusion pathways for the electrolyte ions to penetrate. This increases the electrode wettability and therefore improves the performance. There are, however, several shortcomings with the performance of bare or hybrid electrodes in real-world applications. According to theoretical predictions, hybrid electrodes will not reach their energy density and power density. There are several problems associated with hybrid electrodes, including high contact resistance between the individual components, limited access to active areas, and swelling or shrinking of electrode materials. As a solution to these problems, high specific surface area electrodes with rational pore distributions are recommended. A selective selection should be made based on the crystallinity, crystal structure, morphology, and porosity of each individual. Concerning the wide industrial applications of nanostructured Sn-based electrode materials, cost considerations, their manufacturing process, and the feasibility of large-scale production are also required. Besides material issues related to electrode fabrication, electrode engineering is an important factor that has yet to be well studied in the literature. For electrochemical supercapacitors to achieve high energy and power densities, electrode materials with well-designed 3D architectures are essential. For Sn-based materials, the morphology and chemical state of tin should be meticulously examined. For example, a more sensitive technique such as electron energy loss spectroscopy and in-situ XPS should be used. In addition to establishing material characterization, simulation and modeling can be used to predict and explore Sn-based materials' electrochemical properties based on their composition. For the design of electrode materials, simulations of different models for various dimensional materials are also useful. EDLC theory is the basis for these modified models. Models allow changing one factor at a time, revealing internal distributions of electric fields, interfacial phenomena, and mass transport phenomena. The advancement in the synthesis technologies via a novel green approach can hold the key to bringing the above-mentioned transformations. Last but not the least, tin-containing electrode compounds demonstrate useful properties including semiconducting nature, layered structure, environmentally benign, and economical. Additional progress is required for the application of Sn-based SCs in several innovative gadgets with many features including self-healing, auto charging, long-term cycle life, etc.

Currently, smart wearable systems are being developed for next-generation stretchable electronic devices that have a high performance and an elastic mechanical response [247]. Developing supercapacitors that are independent and stretchable is a key challenge in the design process for the next generation of smart batteries, especially when the electrodes have to withstand repeated deformations far beyond that of rigid smart batteries [248]. A 3D porous Sn-based electrode can address charge transport limitations in commercial SCs in a manner that is more efficient than existing 2D electrodes and planar SCs geometries. Using 3D printing techniques has many benefits, including the ability to design with flexibility, which improves the energy density and power density while enabling the development of wearable devices with SC devices. In order to improve electrochemical performance, complex 3D structures, which are hierarchically constructed, should be printed with a high degree of resolution, accuracy, surface finish, architecture modeling, and structural flexibility in 3D-printed parts. Further findings in the field of exclusive shape/structure and configuration of Sn-based electrode materials would clue to the prospective consumption of these materials. Thus, there exists a huge research gap to explore Sn-based electrode materials in the form of oxides, sulfides and hybrid forms for upgrading the electrochemical performances of these materials for supercapacitors.

3.2. Conclusions

Supercapacitors are of huge importance for applications that require speedy charge/discharge, wide-ranging working temperature windows, extended cyclic stability, high efficiency, and reliability. They possess the potential to replace traditional batteries and capacitors in several applications ranging from automotive to renewable energy. Electrode materials are considered an important feature in the enhancement of the electrochemical performance of SCs. Sn-based electrodes involving their oxides and sulfides are quite promising in the field of supercapacitors. Their unique abilities are high conductivity, thermal and chemical stability, nontoxic nature, and huge natural abundance. To gain the vastly controlled morphology of Sn-based electrode materials, numerous approaches based on wet-chemical and vapour phases have been explored so far. Since there is a direct relationship between nanoarchitectures and electrochemical performance, these materials are explored with 1D, 2D, 3D, and hierarchical structures. The Sn-based materials are not so much explored for supercapacitors because of their deprived electrical conductivity and poor electrochemical stability that need to be overcome. Introducing conducting phases like the incorporation of carbon-based materials, other metal, or metal oxides, and conducting polymers are a few approaches proven to improve the electrochemical performance. More expansion in the current Sn-based electrode compounds is essential for the application of supercapacitors in many progressive applications. The report investigates research based on current improvements done in the preparation of tin-based materials and their hybrids, with the support of different synthesis techniques. The best examples for providing the performance evaluation have been explored. The above-summarized studies show that some other Sn-based electrodes also demonstrate reasonably appealing candidates for SCs, nevertheless few critical concerns and challenges need to be addressed for further discoveries to recognize their superior applications for energy storage in the future.

Declaration of competing interest

The authors declare that they have no known competing financial interests or personal relationships that could have appeared to influence the work reported in this paper.

Data availability

Data will be made available on request.

Acknowledgements

This research was supported by National R&D Program through the National Research Foundation of Korea (NRF) funded by the Ministry of Science and ICT, Republic of Korea (2021M3H4A3A02099209). And, this work was also supported by the 2020 Yeungnam University Research Grant.

References

[1] M. Li, J. Lu, X. Ji, Y. Li, Y. Shao, Z. Chen, C. Zhong, K. Amine, Design strategies for nonaqueous multivalent-ion and monovalent-ion battery anodes, Nat. Rev. Mater. 5 (2020) 276–294, https://doi.org/10.1038/s41578-019-0166-4.
[2] N. Parveen, S.A. Ansari, M.Z. Ansari, M.O. Ansari, Manganese oxide as an effective electrode material for energy storage: a review, Environ. Chem. Lett. (2021), https://doi.org/10.1007/s10311-021-01316-6.
[3] W. Raza, F. Ali, N. Raza, Y. Luo, K.H. Kim, J. Yang, S. Kumar, A. Mehmood, E. E. Kwon, Recent advancements in supercapacitor technology, Nano Energy 52 (2018) 441–473, https://doi.org/10.1016/j.nanoen.2018.08.013.
[4] S. Liu, L. Wei, H. Wang, Review on reliability of supercapacitors in energy storage applications, Appl. Energy 278 (2020), 115436, https://doi.org/10.1016/j.apenergy.2020.115436.
[5] X. Li, B. Wei, Supercapacitors based on nanostructured carbon, Nano Energy 2 (2013) 159–173, https://doi.org/10.1016/j.nanoen.2012.09.008.
[6] R. Ramya, R. Sivasubramanian, M.V. Sangaranarayanan, Conducting polymers-based electrochemical supercapacitors - Progress and prospects, Electrochim. Acta 101 (2013) 109–129, https://doi.org/10.1016/j.electacta.2012.09.116.
[7] X. Hong, S. Li, R. Wang, J. Fu, Hierarchical SnO2 nanoclusters wrapped functionalized carbonized cotton cloth for symmetrical supercapacitor, J. Alloys Compd. 775 (2019) 15–21, https://doi.org/10.1016/j.jallcom.2018.10.099.
[8] R. Sahoo, D.T. Pham, T.H. Lee, T.H.T. Luu, J. Seok, Y.H. Lee, Redox-driven route for widening voltage window in asymmetric supercapacitor, ACS Nano 12 (2018) 8494–8505, https://doi.org/10.1021/acsnano.8b04040.
[9] S. Kong, K. Cheng, T. Ouyang, Y. Gao, K. Ye, G. Wang, D. Cao, Facile electrodepositing processed of RuO2-graphene nanosheets-CNT composites as a binder-free electrode for electrochemical supercapacitors, Electrochim. Acta 246 (2017) 433–442, https://doi.org/10.1016/j.electacta.2017.06.019.
[10] Y. Liu, Y. Jiao, Z. Zhang, F. Qu, A. Umar, X. Wu, Hierarchical SnO2 nanostructures made of intermingled ultrathin nanosheets for environmental remediation, smart gas sensor, and supercapacitor applications, ACS Appl. Mater. Interfaces 6 (2014) 2174–2184, https://doi.org/10.1021/am405301v.
[11] D. Deng, M.G. Kim, J.Y. Lee, J. Cho, Green energy storage materials: nanostructured TiO2 and Sn-based anodes for lithium-ion batteries, energy and environmentalScience 2 (2009) 818–837, https://doi.org/10.1039/b823474d.
[12] Q. Zhao, L. Ma, Q. Zhang, C. Wang, X. Xu, SnO2-based nanomaterials: synthesis and application in lithium-ion batteries and supercapacitors, J. Nanomater. 2015 (2015), https://doi.org/10.1155/2015/850147.
[13] M. Zhang, T. Wang, G. Cao, Promises and challenges of tin-based compounds as anode materials for lithium-ion batteries, Int. Mater. Rev. 60 (2015) 330–352, https://doi.org/10.1179/1743280415Y.0000000004.
[14] L. Liu, F. Xie, J. Lyu, T. Zhao, T. Li, B.G. Choi, Tin-based anode materials with well-designed architectures for next-generation lithium-ion batteries, J. Power Sources 321 (2016) 11–35, https://doi.org/10.1016/j.jpowsour.2016.04.105.
[15] M. Zhao, Q. Zhao, J. Qiu, H. Xue, H. Pang, Tin-based nanomaterials for electrochemical energy storage, RSC Adv. 6 (2016) 95449–95468, https://doi.org/10.1039/c6ra19877e.
[16] H. Ying, W.Q. Han, Metallic sn-based anode materials: application in high-performance lithium-ion and sodium-ion batteries, Adv. Sci. 4 (2017), https://doi.org/10.1002/advs.201700298.
[17] B. Huang, Z. Pan, X. Su, L. An, Tin-based materials as versatile anodes for alkali (earth)-ion batteries, J. Power Sources 395 (2018) 41–59, https://doi.org/10.1016/j.jpowsour.2018.05.063.
[18] P. Shinde, C.S. Rout, Advances in synthesis, properties and emerging applications of tin sulfides and its heterostructures, Materials Chemistry Frontiers. 5 (2021) 516–556, https://doi.org/10.1039/d0qm00470g.
[19] S. Zhao, S. Li, T. Guo, S. Zhang, J. Wang, Y. Wu, Y. Chen, Advances in sn-based catalysts for electrochemical CO2 reduction, Nano-Micro Lett. 11 (2019) 1–19, https://doi.org/10.1007/s40820-019-0293-x.
[20] S.N. Pusawale, P.R. Deshmukh, C.D. Lokhande, Chemical synthesis of nanocrystalline SnO 2 thin films for supercapacitor application, Appl. Surf. Sci. 257 (2011) 9498–9502, https://doi.org/10.1016/j.apsusc.2011.06.043.
[21] R.K. Selvan, I. Perelshtein, N. Perkas, A. Gedanken, Synthesis of hexagonal-shaped SnO2 nanocrystals and SnO2@C nanocomposites for electrochemical redox supercapacitors, J. Phys. Chem. C 112 (2008) 1825–1830, https://doi.org/10.1021/jp076995q.
[22] A.C. Forse, C. Merlet, J.M. Griffin, C.P. Grey, New perspectives on the charging mechanisms of supercapacitors, J. Am. Chem. Soc. 138 (2016) 5731–5744, https://doi.org/10.1021/jacs.6b02115.
[23] Y. Liu, Y. Jiao, Z. Zhang, F. Qu, A. Umar, X. Wu, Hierarchical SnO2 nanostructures made of intermingled ultrathin nanosheets for environmental remediation, smart gas sensor, and supercapacitor applications, ACS Appl. Mater. Interfaces 6 (2014) 2174–2184, https://doi.org/10.1021/am405301v.
[24] J. Suárez-Guevara, V. Ruiz, P. Gomez-Romero, Hybrid energy storage: high voltage aqueous supercapacitors based on activated carbon-phosphotungstate hybrid materials, J. Mater. Chem. A 2 (2014) 1014–1021, https://doi.org/10.1039/c3ta14455k.
[25] S.K. Tiwari, J. Mishra, G. Hatui, G.C. Nayak, in: Conducting Polymer Hybrids, 2017, pp. 117–142, https://doi.org/10.1007/978-3-319-46458-9.
[26] L. Zhang, X.S. Zhao, Carbon-based materials as supercapacitor electrodes, Chem. Soc. Rev. 38 (2009) 2520–2531, https://doi.org/10.1039/b813846j.
[27] M. Endo, T. Takeda, Y.J. Kim, K. Koshiba, K. Ishii, High power electric double layer capacitor (EDLC's); from operating principle to pore size control in advanced activated carbons, carbonScience 1 (2001) 117–128.
[28] X. Chen, R. Paul, L. Dai, Carbon-based supercapacitors for efficient energy storage, Natl. Sci. Rev. 4 (2017) 453–489, https://doi.org/10.1093/nsr/nwx009.
[29] H. Ji, X. Zhao, Z. Qiao, J. Jung, Y. Zhu, Y. Lu, L.L. Zhang, A.H. MacDonald, R. S. Ruoff, Capacitance of carbon-based electrical double-layer capacitors, Nat. Commun. 5 (2014), https://doi.org/10.1038/ncomms4317.
[30] N. Parveen, S.A. Ansari, M.Z. Ansari, M.O. Ansari, Manganese oxide as an effective electrode material for energy storage: a review, Environ. Chem. Lett. 20 (2022) 283–309, https://doi.org/10.1007/s10311-021-01316-6.
[31] J. Xie, P. Yang, Y. Wang, T. Qi, Y. Lei, C.M. Li, Puzzles and confusions in supercapacitor and battery: theory and solutions, J. Power Sources 401 (2018) 213–223, https://doi.org/10.1016/j.jpowsour.2018.08.090.
[32] H. Gao, F. Xiao, C.B. Ching, H. Duan, High-performance asymmetric supercapacitor based on graphene hydrogel and nanostructured MnO 2, ACS Appl. Mater. Interfaces 4 (2012) 2801–2810, https://doi.org/10.1021/am300455d.

[33] X. Hu, W. Zhang, X. Liu, Y. Mei, Y. Huang, Nanostructured mo-based electrode materials for electrochemical energy storage, Chem. Soc. Rev. 44 (2015) 2376–2404, https://doi.org/10.1039/c4cs00350k.
[34] J. Yan, Z. Fan, T. Wei, W. Qian, M. Zhang, F. Wei, Fast and reversible surface redox reaction of graphene-MnO2 composites as supercapacitor electrodes, Carbon N. Y. 48 (2010) 3825–3833, https://doi.org/10.1016/j.carbon.2010.06.047.
[35] J.-M. Tarascon, M. Armand, Issues and challenges facing rechargeable lithium batteries, Nature 414 (2001) 359–367, https://doi.org/10.1038/35104644.
[36] V. Aravindan, J. Gnanaraj, Y.S. Lee, S. Madhavi, Insertion-type electrodes for nonaqueous li-ion capacitors, Chem. Rev. 114 (2014) 11619–11635, https://doi.org/10.1021/cr5000915.
[37] F. Zhang, T. Zhang, X. Yang, L. Zhang, K. Leng, Y. Huang, Y. Chen, A high-performance supercapacitor-battery hybrid energy storage device based on graphene-enhanced electrode materials with ultrahigh energy density, energy and environmental, Science 6 (2013) 1623–1632, https://doi.org/10.1039/c3ee40509e.
[38] A.G. Pandolfo, A.F. Hollenkamp, Carbon properties and their role in supercapacitors, J. Power Sources 157 (2006) 11–27, https://doi.org/10.1016/j.jpowsour.2006.02.065.
[39] H. Pan, J. Li, Y.P. Feng, Carbon nanotubes for supercapacitor, Nanoscale Res. Lett. 5 (2010) 654–668, https://doi.org/10.1007/s11671-009-9508-2.
[40] F. Li, S. Bashir, J.L. Liu, Nanostructured materials for next-generation energy storage and conversion: fuel cells, nanostructured materials for next-generation energy storage and conversion, Fuel Cells (2018) 1–556, https://doi.org/10.1007/978-3-662-56364-9.
[41] M. Rose, Y. Korenblit, E. Kockrick, L. Borchardt, M. Oschatz, S. Kaskel, G. Yushin, Hierarchical micro- and mesoporous carbide-derived carbon as a high-performance electrode material in supercapacitors, Small 7 (2011) 1108–1117, https://doi.org/10.1002/smll.201001898.
[42] Z. Yang, J. Tian, Z. Yin, C. Cui, W. Qian, F. Wei, Carbon nanotube- and graphene-based nanomaterials and applications in high-voltage supercapacitor: a review, Carbon N. Y. 141 (2019) 467–480, https://doi.org/10.1016/j.carbon.2018.10.010.
[43] R. Banavath, S.S. Nemala, S.-H. Kim, S. Bohm, M.Z. Ansari, D. Mohapatra, P. Bhargava, Industrially scalable exfoliated graphene nanoplatelets by high-pressure airless spray technique for high-performance supercapacitors, FlatChem. 33 (2022), 100373, https://doi.org/10.1016/j.flatc.2022.100373.
[44] V.V.N. Obreja, On the performance of supercapacitors with electrodes based on carbon nanotubes and carbon activated material-a review, Physica E 40 (2008) 2596–2605, https://doi.org/10.1016/j.physe.2007.09.044.
[45] D.S. Kim, D.J. Chung, H.-I. Park, M.Z. Ansari, T. Song, H. Kim, Direct nitradated graphite felt as an electrode material for the vanadium redox flow battery, Bull. Kor. Chem. Soc. 39 (2018) 281–286, https://doi.org/10.1002/bkcs.11380.
[46] D.Y. Yeom, W. Jeon, N.D.K. Tu, S.Y. Yeo, S.S. Lee, B.J. Sung, H. Chang, J.A. Lim, H. Kim, High-concentration boron doping of graphene nanoplatelets by simple thermal annealing and their supercapacitive properties, Sci. Rep. 5 (2015) 1–10, https://doi.org/10.1038/srep09817.
[47] J. Li, G. Zhang, C. Fu, L. Deng, R. Sun, C.P. Wong, Facile preparation of nitrogen/sulfur co-doped and hierarchical porous graphene hydrogel for high-performance electrochemical capacitor, J. Power Sources 345 (2017) 146–155, https://doi.org/10.1016/j.jpowsour.2017.02.011.
[48] Z. Yang, J. Ma, B. Bai, A. Qiu, D. Losic, D. Shi, M. Chen, Free-standing PEDOT/polyaniline conductive polymer hydrogel for flexible solid-state supercapacitors, Electrochim. Acta 322 (2019), 134769, https://doi.org/10.1016/j.electacta.2019.134769.
[49] K. Zhou, Y. He, Q. Xu, Q. Zhang, A. Zhou, Z. Lu, L.K. Yang, Y. Jiang, D. Ge, X. Y. Liu, H. Bai, A hydrogel of ultrathin pure polyaniline nanofibers: oxidant-templating preparation and supercapacitor application, ACS Nano 12 (2018) 5888–5894, https://doi.org/10.1021/acsnano.8b02055.
[50] C. An, Y. Zhang, H. Guo, Y. Wang, Metal oxide-based supercapacitors: progress and prospectives, nanoscaleAdvances 1 (2019) 4644–4658, https://doi.org/10.1039/c9na00543a.
[51] L. Fu, Q. Qu, R. Holze, V.V. Kondratiev, Y. Wu, Composites of metal oxides and intrinsically conducting polymers as supercapacitor electrode materials: the best of both worlds? J. Mater. Chem. A 7 (2019) 14937–14970, https://doi.org/10.1039/c8ta10587a.
[52] M.Z. Ansari, K.-M. Seo, S.-H. Kim, S.A. Ansari, Critical aspects of various techniques for synthesizing metal oxides and fabricating their composite-based supercapacitor electrodes: a review, Nanomaterials. 12 (2022) 1873, https://doi.org/10.3390/nano12111873.
[53] L. Huang, D. Chen, Y. Ding, S. Feng, Z.L. Wang, M. Liu, Nickel-cobalt hydroxide nanosheets coated on NiCo2O4 nanowires grown on carbon fiber paper for high-performance pseudocapacitors, Nano Lett. 13 (2013) 3135–3139, https://doi.org/10.1021/nl401086t.
[54] S. Ramesh, D. Vikraman, K. Karuppasamy, H.M. Yadav, A. Sivasamy, H.S. Kim, J. H. Kim, H.S. Kim, Controlled synthesis of SnO2@NiCo2O4/nitrogen doped multiwalled carbon nanotube hybrids as an active electrode material for supercapacitors, J. Alloys Compd. 794 (2019) 186–194, https://doi.org/10.1016/j.jallcom.2019.04.258.
[55] M.Z. Ansari, D.K. Nandi, P. Janicek, S.A. Ansari, R. Ramesh, T. Cheon, B. Shong, S.H. Kim, Low-temperature atomic layer deposition of highly conformal tin nitride thin films for energy storage devices, ACS Appl. Mater. Interfaces 11 (2019) 43608–43621, https://doi.org/10.1021/acsami.9b15790.
[56] L. Eliad, G. Salitra, A. Soffer, D. Aurbach, Ion sieving effects in the electrical double layer of porous carbon electrodes: estimating effective ion size in electrolytic solutions, J. Phys. Chem. B 105 (2001) 6880–6887, https://doi.org/10.1021/jp010086y.
[57] X. Zhang, X. Wang, L. Jiang, H. Wu, C. Wu, J. Su, Effect of aqueous electrolytes on the electrochemical behaviors of supercapacitors based on hierarchically porous carbons, J. Power Sources 216 (2012) 290–296, https://doi.org/10.1016/j.jpowsour.2012.05.090.
[58] K. Keum, G. Lee, H. Lee, J. Yun, H. Park, S.Y. Hong, C. Song, J.W. Kim, J.S. Ha, Wire-shaped supercapacitors with organic electrolytes fabricated via layer-by-layer assembly, ACS Appl. Mater. Interfaces 10 (2018) 26248–26257, https://doi.org/10.1021/acsami.8b07113.
[59] Q. Zhang, J. Rong, D. Ma, B. Wei, The governing self-discharge processes in activated carbon fabric-based supercapacitors with different organic electrolytes, energy and environmental, Science 4 (2011) 2152–2159, https://doi.org/10.1039/c0ee00773k.
[60] C. Arbizzani, M. Biso, D. Cericola, M. Lazzari, F. Soavi, M. Mastragostino, Safe, high-energy supercapacitors based on solvent-free ionic liquid electrolytes, J. Power Sources 185 (2008) 1575–1579, https://doi.org/10.1016/j.jpowsour.2008.09.016.
[61] H. Zhong, F. Xu, Z. Li, R. Fu, D. Wu, High-energy supercapacitors based on hierarchical porous carbon with an ultrahigh ion-accessible surface area in ionic liquid electrolytes, Nanoscale 5 (2013) 4678–4682, https://doi.org/10.1039/c3nr00738c.
[62] D. Karabelli, J.C. Leprêtre, F. Alloin, J.Y. Sanchez, Poly(vinylidene fluoride)-based macroporous separators for supercapacitors, Electrochim. Acta 57 (2011) 98–103, https://doi.org/10.1016/j.electacta.2011.03.033.
[63] B. Qin, Y. Han, Y. Ren, D. Sui, Y. Zhou, M. Zhang, Z. Sun, Y. Ma, Y. Chen, A ceramic-based separator for high-temperature supercapacitors, energyTechnology 6 (2018) 306–311, https://doi.org/10.1002/ente.201700438.
[64] C.Y. Bon, L. Mohammed, S. Kim, M. Manasi, P. Isheunesu, K.S. Lee, J.M. Ko, Flexible poly(vinyl alcohol)-ceramic composite separators for supercapacitor applications, J. Ind. Eng. Chem. 68 (2018) 173–179, https://doi.org/10.1016/j.jiec.2018.07.043.
[65] Z. Wang, P. Tammela, M. Strømme, L. Nyholm, Cellulose-based supercapacitors: material and performance considerations, Adv. Energy Mater. 7 (2017), https://doi.org/10.1002/aenm.201700130.
[66] B. Szubzda, A. Szmaja, M. Ozimek, S. Mazurkiewicz, Polymer membranes as separators for supercapacitors, Appl. Phys. A Mater. Sci. Process. 117 (2014) 1801–1809, https://doi.org/10.1007/s00339-014-8674-y.
[67] Y.M. Shulga, S.A. Baskakov, V.A. Smirnov, N.Y. Shulga, K.G. Belay, G.L. Gutsev, Graphene oxide films as separators of polyaniline-based supercapacitors, J. Power Sources 245 (2014) 33–36, https://doi.org/10.1016/j.jpowsour.2013.06.094.
[68] L. Liu, H. Zhao, Y. Wang, Y. Fang, J. Xie, Y. Lei, Evaluating the role of nanostructured current collectors in energy storage capability of supercapacitor electrodes with thick electroactive materials layers, Adv. Funct. Mater. 28 (2018) 1–9, https://doi.org/10.1002/adfm.201705107.
[69] C. Portet, P.L. Taberna, P. Simon, C. Laberty-Robert, Modification of Al current collector surface by sol-gel deposit for carbon-carbon supercapacitor applications, Electrochim. Acta 49 (2004) 905–912, https://doi.org/10.1016/j.electacta.2003.09.043.
[70] T.C. Bryce, S.A. Stephen, E.P. Luther, Nanoporous metal foams, Angew. Chem. Int. Ed. 49 (2010) 4544–4565, https://doi.org/10.1002/anie.200902994.
[71] L. Liu, H. Zhao, Y. Lei, Review on nanoarchitectured current collectors for pseudocapacitors, SmallMethods 3 (2019) 1–25, https://doi.org/10.1002/smtd.201800341.
[72] Y. Huang, Y. Li, Q. Gong, G. Zhao, P. Zheng, J. Bai, J. Gan, M. Zhao, Y. Shao, D. Wang, L. Liu, G. Zou, D. Zhuang, J. Liang, H. Zhu, C. Nan, Hierarchically mesostructured aluminum current collector for enhancing the performance of supercapacitors, ACS Appl. Mater. Interfaces 10 (2018) 16572–16580, https://doi.org/10.1021/acsami.8b03647.
[73] K.V.G. Raghavendra, R. Vinoth, K. Zeb, C.V.V. Muralee Gopi, S. Sambasivam, M. R. Kummara, I.M. Obaidat, H.J. Kim, An intuitive review of supercapacitors with recent progress and novel device applications, J. Energy Storage 31 (2020), 101652, https://doi.org/10.1016/j.est.2020.101652.
[74] Yurii Maletin, Natalia Stryzhakova, Sergii Zelinskyi, Sergey Chernukhin, Dmytro Tretyakov, Hugo Mosqueda, Natalia Davydenko, Dmytro Drobnyi, New approach to ultracapacitor technology: what it can offer to electrified vehicles, J. Energy Power Eng. 9 (2015) 585–591, https://doi.org/10.17265/1934-8975/2015.06.010.
[75] N. Ghaviha, J. Campillo, M. Bohlin, E. Dahlquist, Review of application of energy storage devices in railway transportation, Energy Procedia 105 (2017) 4561–4568, https://doi.org/10.1016/j.egypro.2017.03.980.
[76] K.J. Sreekanth, R. Al Foraih, A. Al-Mulla, B. Abdulrahman, Feasibility analysis of energy storage technologies in power systems for arid region, J. Energy Resour. Technol. Trans. ASME 141 (2019), https://doi.org/10.1115/1.4040931.
[77] World of Renewables, World of Renewables. Maxwell Technologies Reports Strong Demand for BOOSTCAP® Ultracapacitor-Based Energy Storage Solutions for Wind Turbines, 2021.
[78] H. Liu, X. Liu, S. Wang, H.K. Liu, L. Li, Transition metal based battery-type electrodes in hybrid supercapacitors: a review, Energy Storage Mater. 28 (2020) 122–145, https://doi.org/10.1016/j.ensm.2020.03.003.
[79] J.M. Liang, L.J. Zhang, D.G. XiLi, J. Kang, Research progress on tin-based anode materials for sodium ion batteries, Rare Metals 39 (2020) 1005–1018, https://doi.org/10.1007/s12598-020-01453-x.
[80] H. Mou, W. Xiao, C. Miao, R. Li, L. Yu, Tin and tin compound materials as anodes in lithium-ion and sodium-ion batteries: a review, Front. Chem. 8 (2020) 1–14, https://doi.org/10.3389/fchem.2020.00141.

[81] G.K. Dalapati, H. Sharma, A. Guchhait, N. Chakrabarty, P. Bamola, Q. Liu, G. Saianand, A.M. Sai Krishna, S. Mukhopadhyay, A. Dey, T.K.S. Wong, S. Zhuk, S. Ghosh, S. Chakrabortty, C. Mahata, S. Biring, A. Kumar, C.S. Ribeiro, S. Ramakrishna, A.K. Chakraborty, S. Krishnamurthy, P. Sonar, M. Sharma, Tin oxide for optoelectronic, photovoltaic and energy storage devices: a review, J. Mater. Chem. A 9 (2021) 16621–16684, https://doi.org/10.1039/d1ta01291f.
[82] K. Van Daele, B. De Mot, M. Pupo, N. Daems, D. Pant, R. Kortlever, T. Breugelmans, Sn-based electrocatalyst stability: a crucial piece to the puzzle for the electrochemical CO2Reduction toward formic acid, ACS Energy Lett. 6 (2021) 4317–4327, https://doi.org/10.1021/acsenergylett.1c02049.
[83] M. Setayeshmehr, M. Haghighi, K. Mirabbaszadeh, A review of tin disulfide (SnS 2) composite electrode materials for supercapacitors, Energy Storage (2021) 1–19, https://doi.org/10.1002/est2.295.
[84] F. Xin, M.S. Whittingham, Challenges and development of tin-based anode with high volumetric capacity for li-ion batteries, Electrochem. Energy Rev. 3 (2020) 643–655, https://doi.org/10.1007/s41918-020-00082-3.
[85] S. Asaithambi, P. Sakthivel, M. Karuppaiah, G.U. Sankar, K. Balamurugan, R. Yuvakkumar, M. Thambidurai, G. Ravi, Investigation of electrochemical properties of various transition metals doped SnO2 spherical nanostructures for supercapacitor applications, J. Energy Storage 31 (2020), 101530, https://doi.org/10.1016/j.est.2020.101530.
[86] C. Mevada, P.S. Chandran, M. Mukhopadhyay, Room-temperature synthesis of tin oxide nanoparticles using gallic acid monohydrate for symmetrical supercapacitor application, J. Energy Storage 28 (2020), 101197, https://doi.org/10.1016/j.est.2020.101197.
[87] L. Wang, H. Ji, F. Zhu, Z. Chen, Y. Yang, X. Jiang, J. Pinto, G. Yang, Large-scale preparation of shape controlled SnO and improved capacitance for supercapacitors: from nanoclusters to square microplates, Nanoscale 5 (2013) 7613–7621, https://doi.org/10.1039/c3nr00951c.
[88] T. Lu, Y. Zhang, H. Li, L. Pan, Y. Li, Z. Sun, Electrochemical behaviors of graphene-ZnO and graphene-SnO2 composite films for supercapacitors, Electrochim. Acta 55 (2010) 4170–4173, https://doi.org/10.1016/j.electacta.2010.02.095.
[89] M. Jayalakshmi, K. Balasubramanian, Hydrothermal synthesis of CuO-SnO2 and CuO-SnO2-Fe2O3 mixed oxides and their electrochemical characterization in neutral electrolyte, Int. J. Electrochem. Sci. 4 (2009) 571–581.
[90] C.C. Hu, C.C. Wang, K.H. Chang, A comparison study of the capacitive behavior for sol-gel-derived and co-annealed ruthenium-tin oxide composites, Electrochim. Acta 52 (2007) 2691–2700, https://doi.org/10.1016/j.electacta.2006.09.026.
[91] J.H. Chang, M.F. Lin, Y.L. Kuo, C.R. Yang, J.Z. Chen, Flexible rGO-SnO2 supercapacitors converted from pastes containing SnCl2 liquid precursor using atmospheric-pressure plasma jet, Ceram. Int. 47 (2021) 1651–1659, https://doi.org/10.1016/j.ceramint.2020.08.281.
[92] Y. Haldorai, Y.S. Huh, Y.K. Han, Surfactant-assisted hydrothermal synthesis of flower-like tin oxide/graphene composites for high-performance supercapacitors, New J. Chem. 39 (2015) 8505–8512, https://doi.org/10.1039/c5nj01442e.
[93] A.J. Samuel, A.S. Deepi, G. Srikesh, A.S. Nesaraj, One pot synthesis and characterisation of two dimensional tin doped strontium oxide nanostructuted electrode materials for electrochemical supercapacitor applications, Mater. Technol. 00 (2020) 1–11, https://doi.org/10.1080/10667857.2020.1819087.
[94] J. Geng, C. Ma, D. Zhang, X. Ning, Facile and fast synthesis of SnO2 quantum dots for high performance solid-state asymmetric supercapacitor, J. Alloys Compd. 825 (2020), 153850, https://doi.org/10.1016/j.jallcom.2020.153850.
[95] J. Duay, E. Gillette, J. Hu, S.B. Lee, Controlled electrochemical deposition and transformation of hetero-nanoarchitectured electrodes for energy storage, Phys. Chem. Chem. Phys. 15 (2013) 7976–7993, https://doi.org/10.1039/c3cp50724f.
[96] K. Rajendra Prasad, N. Miura, Electrochemical synthesis and characterization of nanostructured tin oxide for electrochemical redox supercapacitors, Electrochem. Commun. 6 (2004) 849–852, https://doi.org/10.1016/j.elecom.2004.06.009.
[97] M.Mohan Rao, M. Jayalaksmi, B.Ramachandra Reddy, S.S. Madhavendra, M. Lakshmi Kantam, Recognizing nano SnO as an electrode material for electrochemical double layer capacitors, Chemistry Letters. 34 (2005) 712–713, https://doi.org/10.1246/cl.2005.712.
[98] Z. Zhuang, F. Huang, Z. Lin, H. Zhang, Aggregation-induced fast crystal growth of SnO2 nanocrystals, J. Am. Chem. Soc. 134 (2012) 16228–16234, https://doi.org/10.1021/ja305305r.
[99] H. Chen, X. Wang, L. Guan, L. Chen, J. Tao, Surface engineering of layered SnO micro-plates for impressive high supercapacitor performance, Mater. Chem. Phys. 238 (2019), 121889, https://doi.org/10.1016/j.matchemphys.2019.121889.
[100] D. Wei, Z. Xu, J. Liang, X. Li, Y. Qian, Rational design of SnO2 aggregation nanostructure with uniform pores and its supercapacitor application, J. Mater. Sci. Mater. Electron. 26 (2015) 6143–6147, https://doi.org/10.1007/s10854-015-3194-x.
[101] A.A. Yadav, SnO2 thin film electrodes deposited by spray pyrolysis for electrochemical supercapacitor applications, J. Mater. Sci. Mater. Electron. 27 (2016) 1866–1872, https://doi.org/10.1007/s10854-015-3965-4.
[102] C. Zhu, H. Wang, C. Guan, Recent progress on hollow array architectures and their applications in electrochemical energy storage, Nanoscale Horiz. 5 (2020) 1188–1199, https://doi.org/10.1039/d0nh00332h.
[103] X. Xu, C. Guan, L. Xu, Y.H. Tan, D. Zhang, Y. Wang, H. Zhang, D.J. Blackwood, J. Wang, M. Li, J. Ding, Three dimensionally free-formable graphene foam with designed structures for energy and environmental applications, ACS Nano 14 (2020) 937–947, https://doi.org/10.1021/acsnano.9b08191.
[104] C. Guan, X. Wang, Q. Zhang, Z. Fan, H. Zhang, H.J. Fan, Highly stable and reversible lithium storage in SnO2 nanowires surface coated with a uniform hollow shell by atomic layer deposition, Nano Lett. 14 (2014) 4852–4858, https://doi.org/10.1021/nl502192p.
[105] Y. Kang, Z. Li, K. Xu, X. He, S. Wei, Y. Cao, Hollow SnO2 nanospheres with single-shelled structure and the application for supercapacitors, J. Alloys Compd. 779 (2019) 728–734, https://doi.org/10.1016/j.jallcom.2018.11.234.
[106] D. Dodoo-Arhin, R.A. Nuamah, P.K. Jain, D.O. Obada, A. Yaya, Nanostructured stannic oxide: synthesis and characterisation for potential energy storage applications, Results in Physics. 9 (2018) 1391–1402, https://doi.org/10.1016/j.rinp.2018.04.057.
[107] V. Bonu, B. Gupta, S. Chandra, A. Das, S. Dhara, A.K. Tyagi, Electrochemical supercapacitor performance of SnO2 quantum dots, Electrochim. Acta 203 (2016) 230–237, https://doi.org/10.1016/j.electacta.2016.03.153.
[108] Z. Yang, J. Ma, B. Bai, A. Qiu, D. Losic, D. Shi, M. Chen, Free-standing PEDOT/polyaniline conductive polymer hydrogel for flexible solid-state supercapacitors, Electrochim. Acta 322 (2019), 134769, https://doi.org/10.1016/j.electacta.2019.134769.
[109] S. Wang, S.P. Jiang, X. Wang, Microwave-assisted one-pot synthesis of metal/metal oxide nanoparticles on graphene and their electrochemical applications, Electrochim. Acta 56 (2011) 3338–3344, https://doi.org/10.1016/j.electacta.2011.01.016.
[110] R.S. Mane, J. Chang, D. Ham, B.N. Pawar, T. Ganesh, B.W. Cho, J.K. Lee, S. H. Han, Dye-sensitized solar cell and electrochemical supercapacitor applications of electrochemically deposited hydrophilic and nanocrystalline tin oxide film electrodes, Curr. Appl. Phys. 9 (2009) 87–91, https://doi.org/10.1016/j.cap.2007.11.013.
[111] S.K. Godlaveeti, A.R. Somala, S.S. Sana, M. Ouladsmane, A.A. Ghfar, R. R. Nagireddy, Evaluation of pH effect of tin oxide (SnO2) nanoparticles on photocatalytic degradation, dielectric and supercapacitor applications, J. Clust. Sci. 7 (2021), https://doi.org/10.1007/s10876-021-02092-7.
[112] Z. Li, T. Chang, G. Yun, J. Guo, B. Yang, 2D tin dioxide nanoplatelets decorated graphene with enhanced performance supercapacitor, J. Alloys Compd. 586 (2014) 353–359, https://doi.org/10.1016/j.jallcom.2013.10.037.
[113] C. te Hsieh, W.Y. Lee, C.E. Lee, H. Teng, Electrochemical capacitors fabricated with tin oxide/graphene oxide nanocomposites, J. Phys. Chem. C 118 (2014) 15146–15153, https://doi.org/10.1021/jp502958w.
[114] T. Kim, E.P. Samuel, C. Park, A. Aldalbahi, F. Alotaibi, S.S. Yoon, Y. il Kim, Wearable fabric supercapacitors using supersonically sprayed reduced graphene and tin oxide, Journal of Alloys and Compounds. 856 (2021) 157902, https://doi.org/10.1016/j.jallcom.2020.157902.
[115] S. Tan, J. Li, L. Zhou, P. Chen, D. Xu, Z. Xu, Fabrication of a flexible film electrode based on cellulose nanofibers aerogel dispersed with functionalized graphene decorated with SnO2 for supercapacitors, J. Mater. Sci. 53 (2018) 11648–11658, https://doi.org/10.1007/s10853-018-2413-2.
[116] S. Ramesh, H.M. Yadav, Y.J. Lee, G.W. Hong, A. Kathalingam, A. Sivasamy, H. S. Kim, H.S. Kim, J.H. Kim, Porous materials of nitrogen doped graphene oxide@SnO2 electrode for capable supercapacitor application, Sci. Rep. 9 (2019) 2–11, https://doi.org/10.1038/s41598-019-48951-2.
[117] J. Jayachandiran, J. Yesuraj, M. Arivanandhan, B. Muthuraaman, R. Jayavel, D. Nedumaran, Bifunctional investigation of ultra-small SnO2nanoparticle decorated rGO for ozone sensing and supercapacitor applications, RSC Adv. 11 (2020) 856–866, https://doi.org/10.1039/d0ra10137k.
[118] S.P. Lim, N.M. Huang, H.N. Lim, Solvothermal synthesis of SnO2/graphene nanocomposites for supercapacitor application, Ceram. Int. 39 (2013) 6647–6655, https://doi.org/10.1016/j.ceramint.2013.01.102.
[119] Y. Wang, Y. Liu, J. Zhang, Colloid electrostatic self-assembly synthesis of SnO2/graphene nanocomposite for supercapacitors, J. Nanopart. Res. 17 (2015) 1–10, https://doi.org/10.1007/s11051-015-3228-6.
[120] V. Velmurugan, U. Srinivasarao, R. Ramachandran, M. Saranya, A.N. Grace, Synthesis of tin oxide/graphene (SnO2/G) nanocomposite and its electrochemical properties for supercapacitor applications, Mater. Res. Bull. 84 (2016) 145–151, https://doi.org/10.1016/j.materresbull.2016.07.015.
[121] K.K. Liu, Q. Jiang, C. Kacica, H.G. Derami, P. Biswas, S. Singamaneni, Flexible solid-state supercapacitor based on tin oxide/reduced graphene oxide/bacterial nanocellulose, RSC Adv. 8 (2018) 31296–31302, https://doi.org/10.1039/c8ra05270k.
[122] P.J. Sephra, P. Baraneedharan, M. Sivakumar, T.D. Thangadurai, K. Nehru, Size controlled synthesis of SnO2 and its electrostatic self- assembly over reduced graphene oxide for photocatalyst and supercapacitor application, Mater. Res. Bull. 106 (2018) 103–112, https://doi.org/10.1016/j.materresbull.2018.05.038.
[123] S. Byun, B. Shin, J. Yu, Metal sputtered graphene based hybrid films comprising tin oxide/reduced graphene oxide/Ni as electrodes for high-voltage electrochemical capacitors, Carbon N Y 129 (2018) 1–7, https://doi.org/10.1016/j.carbon.2017.11.098.
[124] S.R. Eedulakanti, A.K. Gampala, K. Venkateswara Rao, Ch. Shilpa Chakra, V. Gedela, R. Boddula, Ultrasonication assisted thermal exfoliation of graphene-tin oxide nanocomposite material for supercapacitor, Materials Science for Energy Technologies. 2 (2019) 372–376, https://doi.org/10.1016/j.mset.2019.03.007.
[125] Y. Xu, L. Wang, Y. Zhou, J. Guo, S. Zhang, Y. Lu, Synthesis of heterostructure SnO2/graphitic carbon nitride composite for high-performance electrochemical supercapacitor, J. Electroanal. Chem. 852 (2019), 113507, https://doi.org/10.1016/j.jelechem.2019.113507.
[126] L. Lin, S. Chen, T. Deng, W. Zeng, Oxygen-deficient stannic oxide/graphene for ultrahigh-performance supercapacitors and gas sensors, Nanomaterials 11 (2021) 1–13, https://doi.org/10.3390/nano11020372.
[127] W. Wang, W. Lei, T. Yao, X. Xia, W. Huang, Q. Hao, X. Wang, One-pot synthesis of graphene/SnO2/PEDOT ternary electrode material for supercapacitors,

Electrochim. Acta 108 (2013) 118–126, https://doi.org/10.1016/j.electacta.2013.07.012.
[128] G. Chen, Q.F. Lü, H.B. Zhao, SnO2-decorated Graphene/Polyaniline nanocomposite for a high-performance supercapacitor electrode, J. Mater. Sci. Technol. 31 (2015) 1101–1107, https://doi.org/10.1016/j.jmst.2015.09.013.
[129] M. Wu, L. Zhang, D. Wang, C. Xiao, S. Zhang, Cathodic deposition and characterization of tin oxide coatings on graphite for electrochemical supercapacitors, J. Power Sources 175 (2008) 669–674, https://doi.org/10.1016/j.jpowsour.2007.09.062.
[130] Y. Zhang, M. Liu, S. Sun, L. Yang, The preparation and characterization of SnO2/rGO nanocomposites electrode materials for supercapacitor, Adv. Compos. Lett. 29 (2020) 1–7, https://doi.org/10.1177/2633366X20909839.
[131] V. Vinoth, J.J. Wu, A.M. Asiri, T. Lana-Villarreal, P. Bonete, S. Anandan, SnO2-decorated multiwalled carbon nanotubes and Vulcan carbon through a sonochemical approach for supercapacitor applications, Ultrason. Sonochem. 29 (2016) 205–212, https://doi.org/10.1016/j.ultsonch.2015.09.013.
[132] C. Xu, Y. Chiu, P. Yeh, J. Chen, SnO 2/CNT nanocomposite supercapacitors fabricated using scanning atmospheric-pressure plasma jets SnO 2/CNT nanocomposite supercapacitors fabricated using scanning atmospheric-pressure plasma jets, (n.d.).
[133] M. Krishnaveni, J.J. Wu, S. Anandan, M. Ashokkumar, Facile synthesis of SnO2nanoparticle intercalated unzipped multi-walled carbon nanotubesviaan ultrasound-assisted route for symmetric supercapacitor devices, sustainable, Energy Fuels 4 (2020) 5120–5131, https://doi.org/10.1039/d0se00702a.
[134] R.B. Rakhi, H.N. Alshareef, Enhancement of the energy storage properties of supercapacitors using graphene nanosheets dispersed with metal oxide-loaded carbon nanotubes, J. Power Sources 196 (2011) 8858–8865, https://doi.org/10.1016/j.jpowsour.2011.06.038.
[135] S. Ramesh, D. Vikraman, K. Karuppasamy, H.M. Yadav, A. Sivasamy, H.S. Kim, J. H. Kim, H.S. Kim, Controlled synthesis of SnO2@NiCo2O4/nitrogen doped multiwalled carbon nanotube hybrids as an active electrode material for supercapacitors, J. Alloys Compd. 794 (2019) 186–194, https://doi.org/10.1016/j.jallcom.2019.04.258.
[136] C.H. Xu, J.Z. Chen, Atmospheric-pressure plasma jet processed SnO2/CNT nanocomposite for supercapacitor application, Ceram. Int. 42 (2016) 14287–14291, https://doi.org/10.1016/j.ceramint.2016.06.023.
[137] H. Abdollahi, M. Samkan, M.A. Mohajerzadeh, Z. Sanaee, S. Mohajerzadeh, Fabrication and investigation of high performance CNT-incorporated tin-oxide supercapacitor, J. Mater. Sci. Mater. Electron. 29 (2018) 7468–7479, https://doi.org/10.1007/s10854-018-8738-4.
[138] Ob. Kwon, B.K. Deka, J. Kim, H.W. Park, Electrochemical performance evaluation of tin oxide nanorod-embedded woven carbon fiber composite supercapacitor, International Journal of Energy Research. 42 (2018) 490–498, https://doi.org/10.1002/er.3827.
[139] J. Mu, B. Chen, Z. Guo, M. Zhang, Z. Zhang, C. Shao, Y. Liu, Tin oxide (SnO2) nanoparticles/electrospun carbon nanofibers (CNFs) heterostructures: controlled fabrication and high capacitive behavior, J. Colloid Interface Sci. 356 (2011) 706–712, https://doi.org/10.1016/j.jcis.2011.01.032.
[140] Z. Liu, D. Fu, F. Liu, G. Han, C. Liu, Y. Chang, Y. Xiao, M. Li, S. Li, Mesoporous carbon nanofibers with large cage-like pores activated by tin dioxide and their use in supercapacitor and catalyst support, Carbon N Y 70 (2014) 295–307, https://doi.org/10.1016/j.carbon.2014.01.011.
[141] E. Samuel, B. Joshi, H.S. Jo, M.T. Swihart, J.M. Yun, K.H. Kim, S.S. Yoon, Y. il Kim, Flexible and freestanding core-shell SnOx/carbon nanofiber mats for high-performance supercapacitors, Journal of Alloys and Compounds. 728 (2017) 1362–1371, https://doi.org/10.1016/j.jallcom.2017.09.103.
[142] Y. Luan, G. Nie, X. Zhao, N. Qiao, X. Liu, H. Wang, X. Zhang, Y. Chen, Y.Z. Long, The integration of SnO2 dots and porous carbon nanofibers for flexible supercapacitors, Electrochim. Acta 308 (2019) 121–130, https://doi.org/10.1016/j.electacta.2019.03.204.
[143] M. Cao, W. Cheng, X. Ni, Y. Hu, G. Han, Lignin-based multi-channels carbon nanofibers @ SnO2 nanocomposites for high-performance supercapacitors, Electrochim. Acta 345 (2020), https://doi.org/10.1016/j.electacta.2020.136172.
[144] C. He, Y. Xiao, H. Dong, Y. Liu, M. Zheng, K. Xiao, X. Liu, H. Zhang, B. Lei, Mosaic-structured SnO2@C porous microspheres for high-performance supercapacitor electrode materials, Electrochim. Acta 142 (2014) 157–166, https://doi.org/10.1016/j.electacta.2014.07.077.
[145] G. Yang, Z. Zhang, Z. Zhang, L. Zhang, Y. Xue, J. Yang, C. Peng, Rational construction of well-defined hollow double shell SnO2/mesoporous carbon spheres heterostructure for supercapacitors, J. Alloys Compd. 873 (2021), 159810, https://doi.org/10.1016/j.jallcom.2021.159810.
[146] H.T.T. Le, D.T. Ngo, V.A.D. Dang, T.T.B. Hoang, C.J. Park, Decoration of mesoporous carbon electrodes with tin oxide to boost their supercapacitive performance, New J. Chem. 44 (2020) 12654–12663, https://doi.org/10.1039/d0nj02585b.
[147] G.M. Thorat, H.S. Jadhav, W.J. Chung, J.G. Seo, Collective use of deep eutectic solvent for one-pot synthesis of ternary Sn/SnO2@C electrode for supercapacitor, J. Alloys Compd. 732 (2018) 694–704, https://doi.org/10.1016/j.jallcom.2017.10.176.
[148] S.W. Hwang, S.H. Hyun, Synthesis and characterization of tin oxide/carbon aerogel composite electrodes for electrochemical supercapacitors, J. Power Sources 172 (2007) 451–459, https://doi.org/10.1016/j.jpowsour.2007.07.061.
[149] R.K. Selvan, I. Perelshtein, N. Perkas, A. Gedanken, Synthesis of hexagonal-shaped SnO2 nanocrystals and SnO 2@C nanocomposites for electrochemical redox supercapacitors, J. Phys. Chem. C 112 (2008) 1825–1830, https://doi.org/10.1021/jp076995q.
[150] P. Liu, B. Tang, J. Zhao, J. Feng, J. Xu, Ordered mesoporous carbon/SnO2 composites as the electrode material for supercapacitors, J. Wuhan Univ. Technol. Mater. Sci. Ed. 26 (2011) 407–411, https://doi.org/10.1007/s11595-011-0239-8.
[151] I. Shakir, M. Shahid, M. Nadeem, D.J. Kang, Tin oxide coating on molybdenum oxide nanowires for high performance supercapacitor devices, Electrochim. Acta 72 (2012) 134–137, https://doi.org/10.1016/j.electacta.2012.04.002.
[152] S. Ren, Y. Yang, M. Xu, H. Cai, C. Hao, X. Wang, Hollow SnO2 microspheres and their carbon-coated composites for supercapacitors, Colloids Surf. A Physicochem. Eng. Asp. 444 (2014) 26–32, https://doi.org/10.1016/j.colsurfa.2013.12.028.
[153] R. Kumar, R.K. Nekouei, V. Sahajwalla, In-situ carbon-coated tin oxide (ISCC-SnO2) for micro-supercapacitor applications, Carbon Letters 30 (2020) 699–707, https://doi.org/10.1007/s42823-020-00142-0.
[154] I. Kaushal, S. Maken, A.K. Sharma, SnO2 mixed banana peel derived biochar composite for supercapacitor application, korean chemical engineering, Research. 56 (2018) 694–704, https://doi.org/10.9713/kcer.2018.56.5.694.
[155] W. Wang, Q. Hao, W. Lei, X. Xia, X. Wang, Graphene/SnO 2/polypyrrole ternary nanocomposites as supercapacitor electrode materials, RSC Adv. 2 (2012) 10268–10274, https://doi.org/10.1039/c2ra21292g.
[156] Z.A. Hu, Y.L. Xie, Y.X. Wang, L.P. Mo, Y.Y. Yang, Z.Y. Zhang, Polyaniline/SnO2 nanocomposite for supercapacitor applications, Mater. Chem. Phys. 114 (2009) 990–995, https://doi.org/10.1016/j.matchemphys.2008.11.005.
[157] Y. Xie, F. Zhu, Electrochemical capacitance performance of polyaniline/tin oxide nanorod array for supercapacitor, J. Solid State Electrochem. 21 (2017) 1675–1685, https://doi.org/10.1007/s10008-017-3525-3.
[158] L. Wang, L. Chen, B. Yan, C. Wang, F. Zhu, X. Jiang, Y. Chao, G. Yang, In situ preparation of SnO2@polyaniline nanocomposites and their synergetic structure for high-performance supercapacitors, J. Mater. Chem. A 2 (2014) 8334–8341, https://doi.org/10.1039/c3ta15266a.
[159] T.T. Liu, Y.H. Zhu, E.H. Liu, Z.Y. Luo, T.T. Hu, Z.P. Li, R. Ding, Fe3+/Fe2+ redox electrolyte for high-performance polyaniline/SnO2 supercapacitors, Trans. Nonferrous Metals Soc. China (Engl. Ed.) 25 (2015) 2661–2665, https://doi.org/10.1016/S1003-6326(15)63889-4.
[160] B.P. Prasanna, D.N. Avadhani, V. Raj, K.Y. Kumar, M.S. Raghu, Fabrication of PANI/SnO2 hybrid nanocomposites via interfacial polymerization for high performance supercapacitors applications, Surf. Eng. Appl. Electrochem. 55 (2019) 463–471, https://doi.org/10.3103/S1068375519040100.
[161] K. Karthikeyan, S. Amaresh, D. Kalpana, R. Kalai Selvan, Y.S. Lee, Electrochemical supercapacitor studies of hierarchical structured co 2-substituted SnO2 nanoparticles by a hydrothermal method, J. Phys. Chem. Solids 73 (2012) 363–367, https://doi.org/10.1016/j.jpcs.2011.09.026.
[162] B. Saravanakumar, G. Ravi, V. Ganesh, F. Ameen, A. Al-Sabri, R. Yuvakkumar, Surfactant assisted zinc doped tin oxide nanoparticles for supercapacitor applications, J. Sol-Gel Sci. Technol. 86 (2018) 521–535, https://doi.org/10.1007/s10971-018-4685-z.
[163] B. Saravanakumar, S.P. Ramachandran, G. Ravi, V. Ganesh, S. Ravichandran, P. Muthu Mareeswaran, R. Yuvakkumar, Enhanced pseudocapacitive performance of SnO2, Zn-SnO2, and Ag-SnO2 nanoparticles, Ionics (Kiel) 24 (2018) 4081–4092, https://doi.org/10.1007/s11581-018-2727-8.
[164] S. Suthakaran, S. Dhanapandian, N. Krishnakumar, N. Ponpandian, Hydrothermal synthesis of surfactant assisted zn doped SnO2 nanoparticles with enhanced photocatalytic performance and energy storage performance, J. Phys. Chem. Solids 141 (2020), 109407, https://doi.org/10.1016/j.jpcs.2020.109407.
[165] S. Suthakaran, S. Dhanapandian, N. Krishnakumar, N. Ponpandian, P. Dhamodharan, M. Anandan, Surfactant-assisted hydrothermal synthesis of zr doped SnO2 nanoparticles with photocatalytic and supercapacitor applications, Mater. Sci. Semicond. Process. 111 (2020), 104982, https://doi.org/10.1016/j.mssp.2020.104982.
[166] S. Asaithambi, P. Sakthivel, M. Karuppaiah, K. Balamurugan, R. Yuvakkumar, M. Thambidurai, G. Ravi, Synthesis and characterization of various transition metals doped SnO2@MoS2 composites for supercapacitor and photocatalytic applications, J. Alloys Compd. 853 (2021), 157060, https://doi.org/10.1016/j.jallcom.2020.157060.
[167] A. Murugan, V. Siva, A. Shameem, S.A. Bahadur, S. Sasikumar, N. Nallamuthu, Structural and charge density distribution studies on tin oxide nanoparticles for supercapacitor application, J. Energy Storage 28 (2020), 101194, https://doi.org/10.1016/j.est.2020.101194.
[168] C. Prabukumar, M.Mohamed Jaffer Sadiq, D.Krishna Bhat, K.Udaya Bhat, SnO2 nanoparticles functionalized MoS2 nanosheets as the electrode material for supercapacitor applications, Materials Research Express. 6 (2019), https://doi.org/10.1088/2053-1591/ab2200.
[169] P. Asen, M. Haghighi, S. Shahrokhian, N. Taghavinia, One step synthesis of SnS2-SnO2 nano-heterostructured as an electrode material for supercapacitor applications, J. Alloys Compd. 782 (2019) 38–50, https://doi.org/10.1016/j.jallcom.2018.12.176.
[170] F. Daneshvar, A. Aziz, A.M. Abdelkader, T. Zhang, H.-J. Sue, M.E. Welland, Porous SnO 2 –Cu x O nanocomposite thin film on carbon nanotubes as electrodes for high performance supercapacitors, Nanotechnology 30 (2019), 015401, https://doi.org/10.1088/1361-6528/aae5c6.
[171] N.L. Wu, S.L. Kuo, M.H. Lee, Preparation and optimization of RuO2-impregnated SnO2 xerogel supercapacitor, J. Power Sources 104 (2002) 62–65, https://doi.org/10.1016/S0378-7753(01)00873-4.
[172] C. Mevada, M. Mukhopadhyay, High mass loading tin oxide-ruthenium oxide-based nanocomposite electrode for supercapacitor application, J. Energy Storage 31 (2020), 101587, https://doi.org/10.1016/j.est.2020.101587.

[173] C. Guan, X. Li, H. Yu, L. Mao, L.H. Wong, Q. Yan, J. Wang, A novel hollowed CoO-in-CoSnO3 nanostructure with enhanced lithium storage capabilities, Nanoscale 6 (2014) 13824–13830, https://doi.org/10.1039/c4nr04505j.
[174] Q. Ke, C. Guan, M. Zheng, Y. Hu, K.H. Ho, J. Wang, 3D hierarchical SnO2@Ni(OH)2 core-shell nanowire arrays on carbon cloth for energy storage application, J. Mater. Chem. A 3 (2015) 9538–9542, https://doi.org/10.1039/c5ta01133g.
[175] J. Xu, Y. Xie, Dual-defects induced band edge reconstruction of tin dioxide via cobalt and nitrogen co-doping for wearable supercapacitor application, J. Power Sources 493 (2021), 229685, https://doi.org/10.1016/j.jpowsour.2021.229685.
[176] L. Ruizhi, X. Ren, F. Zhang, C. Du, J. Liu, Synthesis of Fe3O4@SnO2 core–shell nanorod film and its application as a thin-film supercapacitor electrode, Chem. Commun. 48 (2012) 5010–5012, https://doi.org/10.1039/c2cc31786a.
[177] Y.H. Chan, C.Y. Tsai, Y.J. Shih, M.S. Wu, Nanostructured tin oxide layer as a porous template for the growth of manganese oxide nanobouquets and a conductive support network for supercapacitors, Electrochim. Acta 364 (2020), 137329, https://doi.org/10.1016/j.electacta.2020.137329.
[178] Z. Wang, Y. Long, D. Cao, D. Han, F. Gu, A high-performance flexible supercapacitor based on hierarchical Co3O4-SnO@SnO2 nanostructures, Electrochim. Acta 307 (2019) 341–350, https://doi.org/10.1016/j.electacta.2019.03.230.
[179] M. Geerthana, S. Prabhu, S. Harish, M. Navaneethan, R. Ramesh, M. Selvaraj, Design and preparation of ternary α-Fe2O3/SnO2/rGO nanocomposite as an electrode material for supercapacitor, J. Mater. Sci. Mater. Electron. (2021), https://doi.org/10.1007/s10854-021-06128-6.
[180] N.L. Wu, Nanocrystalline oxide supercapacitors, Mater. Chem. Phys. 75 (2002) 6–11, https://doi.org/10.1016/S0254-0584(02)00022-6.
[181] M. Jayalakshmi, N. Venugopal, K.P. Raja, M.M. Rao, Nano SnO2-Al2O3 mixed oxide and SnO2-Al2O3-carbon composite oxides as new and novel electrodes for supercapacitor applications, J. Power Sources 158 (2006) 1538–1543, https://doi.org/10.1016/j.jpowsour.2005.10.091.
[182] J. Yan, E. Khoo, A. Sumboja, P.S. Lee, Facile coating of manganese oxide on tin oxide nanowires with high-performance capacitive behavior, ACS Nano 4 (2010) 4247–4255, https://doi.org/10.1021/nn100592d.
[183] S. Patil, V. Patil, S. Sathaye, K. Patil, Facile room temperature methods for growing ultra thin films of graphene nanosheets, nanoparticulate tin oxide and preliminary assessment of graphene-tin oxide stacked layered composite structure for supercapacitor application, RSC Adv. 4 (2014) 4094–4104, https://doi.org/10.1039/c3ra46576d.
[184] Y.M. Dai, S.C. Tang, J.Q. Peng, H.Y. Chen, Z.X. Ba, Y.J. Ma, X.K. Meng, MnO2@SnO2 core-shell heterostructured nanorods for supercapacitors, Mater. Lett. 130 (2014) 107–110, https://doi.org/10.1016/j.matlet.2014.05.090.
[185] X. Meng, M. Zhou, X. Li, J. Yao, F. Liu, H. He, P. Xiao, Y. Zhang, Synthesis of SnO2 nanoflowers and electrochemical properties of Ni/SnO2 nanoflowers in supercapacitor, Electrochim. Acta 109 (2013) 20–26, https://doi.org/10.1016/j.electacta.2013.07.052.
[186] S. Wang, J. Zhao, S. Gao, Y. Gao, X. Liu, Y. Wu, J. Xu, Hydrolysis precipitation synthesis of SnO2·XH2O as electrode materials for supercapacitors, Xiyou Jinshu Cailiao Yu Gongcheng 45 (2016) 62–65, https://doi.org/10.1016/s1875-5372(16)30047-9.
[187] S. Hao, Y. Sun, Y. Liu, Y. Zhang, G. Hu, Facile synthesis of porous SnO2film grown on ni foam applied for high-performance supercapacitors, J. Alloys Compd. 689 (2016) 587–592, https://doi.org/10.1016/j.jallcom.2016.07.278.
[188] J. Zhu, S. Tang, S. Vongehr, H. Xie, X. Meng, Optimized spherical manganese oxide-ferroferric oxide-tin oxide ternary composites as advanced electrode materials for supercapacitors, Nanotechnology 26 (2015), https://doi.org/10.1088/0957-4484/26/37/374001.
[189] X. Li, F. Zheng, Y. Luo, Y. Wu, F. Lu, Preparation and electrochemical performance of TiO2-SnO2 doped RuO2 composite electrode for supercapacitors, Electrochim. Acta 237 (2017) 177–184, https://doi.org/10.1016/j.electacta.2017.03.191.
[190] S.L. Kuo, N.L. Wu, Composite supercapacitor containing tin oxide and electroplated ruthenium oxide, Electrochem. Solid-State Lett. 6 (2003) 85–87, https://doi.org/10.1149/1.1563872.
[191] R. Vijayan, G.S. Kumar, G. Karunakaran, N. Surumbarkuzhali, S. Prabhu, R. Ramesh, Microwave combustion synthesis of tin oxide-decorated silica nanostructure using rice husk template for supercapacitor applications, J. Mater. Sci. Mater. Electron. 31 (2020) 5738–5745, https://doi.org/10.1007/s10854-020-03142-y.
[192] B. Varshney, M.J. Siddiqui, A.H. Anwer, M.Z. Khan, F. Ahmed, A. Aljaafari, H. H. Hammud, A. Azam, Synthesis of mesoporous SnO2/NiO nanocomposite using modified sol–gel method and its electrochemical performance as electrode material for supercapacitors, Sci. Rep. 10 (2020) 1–13, https://doi.org/10.1038/s41598-020-67990-8.
[193] P. Asen, M. Haghighi, S. Shahrokhian, N. Taghavinia, One step synthesis of SnS2-SnO2 nano-heterostructured as an electrode material for supercapacitor applications, J. Alloys Compd. 782 (2019) 38–50, https://doi.org/10.1016/j.jallcom.2018.12.176.
[194] F. Daneshvar, A. Aziz, A.M. Abdelkader, T. Zhang, H.-J. Sue, M.E. Welland, Porous SnO 2 –Cu x O nanocomposite thin film on carbon nanotubes as electrodes for high performance supercapacitors, Nanotechnology 30 (2019), 015401, https://doi.org/10.1088/1361-6528/aae5c6.
[195] J.H. Han, S. Lee, J. Cheon, Synthesis and structural transformations of colloidal 2D layered metal chalcogenide nanocrystals, Chem. Soc. Rev. 42 (2013) 2581–2591, https://doi.org/10.1039/c2cs35386e.
[196] X. Rui, H. Tan, Q. Yan, Nanostructured metal sulfides for energy storage, Nanoscale 6 (2014) 9889–9924, https://doi.org/10.1039/c4nr03057e.
[197] M.Z. Ansari, S.A. Ansari, N. Parveen, M.H. Cho, T. Song, Lithium ion storage ability, supercapacitor electrode performance, and photocatalytic performance of tungsten disulfide nanosheets, New J. Chem. 42 (2018) 5859–5867, https://doi.org/10.1039/c8nj00018b.
[198] D.K. Nandi, S. Yeo, M.Z. Ansari, S. Sinha, T. Cheon, J. Kwon, H. Kim, J. Heo, T. Song, S.H. Kim, Thickness-dependent electrochemical response of plasma enhanced atomic layer deposited WS2 anodes in na-ion battery, Electrochim. Acta 322 (2019), 134766, https://doi.org/10.1016/j.electacta.2019.134766.
[199] L. Ma, L. Xu, X. Zhou, X. Xu, L. Zhang, Molybdenum-doped few-layered SnS2 architectures with enhanced electrochemical supercapacitive performance, RSC Adv. 5 (2015) 105862–105868, https://doi.org/10.1039/c5ra18634j.
[200] H. Chauhan, M.K. Singh, P. Kumar, S.A. Hashmi, S. Deka, Development of SnS2/RGO nanosheet composite for cost-effective aqueous hybrid supercapacitors, Nanotechnology 28 (2017), https://doi.org/10.1088/1361-6528/28/2/025401.
[201] B. Pant, G.P. Ojha, M. Park, One-pot synthesis, characterization, and electrochemical studies of tin-nickel sulfide hybrid structures on nickel foam for supercapacitor applications, J. Energy Storage 32 (2020), 101954, https://doi.org/10.1016/j.est.2020.101954.
[202] L.S. Price, I.P. Parkin, A.M.E. Hardy, R.J.H. Clark, T.G. Hibbert, K.C. Molloy, Atmospheric pressure chemical vapor deposition of tin sulfides (SnS, Sn2S3, and SnS2) on glass, Chem. Mater. 11 (1999) 1792–1799, https://doi.org/10.1021/cm990005z.
[203] Y. Li, H. Xie, J. Wang, Preparation and electrochemical performances of carbon-coated nanoscale SnS for supercapacitors, J. Solid State Electrochem. 15 (2011) 1115–1119, https://doi.org/10.1007/s10008-010-1150-5.
[204] Y. Li, H. Xie, J. Tu, Nanostructured SnS/carbon composite for supercapacitor, Mater. Lett. 63 (2009) 1785–1787, https://doi.org/10.1016/j.matlet.2009.05.036.
[205] M.S. Balogun, W. Qiu, J. Jian, Y. Huang, Y. Luo, H. Yang, C. Liang, X. Lu, Y. Tong, Vanadium nitride nanowire supported SnS2 nanosheets with high reversible capacity as anode material for lithium ion batteries, ACS Appl. Mater. Interfaces 7 (2015) 23205–23215, https://doi.org/10.1021/acsami.5b07044.
[206] Y. Huang, E. Sutter, J.T. Sadowski, M. Cotlet, O.L.A. Monti, D.A. Racke, M. R. Neupane, D. Wickramaratne, R.K. Lake, B.A. Parkinson, P. Sutter, Tin disulfide-an emerging layered metal dichalcogenide semiconductor: materials properties and device characteristics, ACS Nano 8 (2014) 10743–10755, https://doi.org/10.1021/nn504481r.
[207] R.K. Mishra, G.W. Baek, K. Kim, H.I. Kwon, S.H. Jin, One-step solvothermal synthesis of carnation flower-like SnS 2 as superior electrodes for supercapacitor applications, Appl. Surf. Sci. 425 (2017) 923–931, https://doi.org/10.1016/j.apsusc.2017.07.045.
[208] N. Parveen, S.A. Ansari, H.R. Alamri, M.O. Ansari, Z. Khan, M.H. Cho, Facile synthesis of SnS2 nanostructures with different morphologies for high-performance supercapacitor applications, ACS Omega. 3 (2018) 1581–1588, https://doi.org/10.1021/acsomega.7b01939.
[209] N. Kumar, D. Mishra, S.Y. Kim, Y. Yoo, S.H. Jin, Evolution of hierarchically formed petal-like 3 dimensional layer structures for SnS2 via ratio control of Sn/thiourea and their electrochemical charge storage behavior, Ceram. Int. (2021), https://doi.org/10.1016/j.ceramint.2021.04.100.
[210] Y.G. Bak, J.W. Park, Y.J. Park, M.Z. Ansari, S. NamGung, B.Y. Cho, S.-H. Kim, H. Y. Lee, In-zn-sn-O thin film based transistor with high-k HfO2 dielectric, Thin Solid Films 753 (2022), 139290, https://doi.org/10.1016/j.tsf.2022.139290.
[211] M.Z. Ansari, P. Janicek, D.K. Nandi, K. Palka, S. Slang, D.H. Kim, T. Cheon, S. H. Kim, Influence of post-annealing on structural, optical and electrical properties of tin nitride thin films prepared by atomic layer deposition, Appl. Surf. Sci. 538 (2021), https://doi.org/10.1016/j.apsusc.2020.147920.
[212] M.Z. Ansari, P. Janicek, D.K. Nandi, S. Slang, M. Bouska, H. Oh, B. Shong, S. H. Kim, Low-temperature growth of crystalline Tin(II) monosulfide thin films by atomic layer deposition using a liquid divalent tin precursor, Appl. Surf. Sci. 565 (2021), https://doi.org/10.1016/j.apsusc.2021.150152.
[213] D.K. Nandi, S. Yeo, M.Z. Ansari, S. Sinha, T. Cheon, J. Kwon, H. Kim, J. Heo, T. Song, S.H. Kim, Thickness-dependent electrochemical response of plasma enhanced atomic layer deposited WS2 anodes in na-ion battery, Electrochim. Acta 322 (2019), https://doi.org/10.1016/j.electacta.2019.134766.
[214] M.Z. Ansari, N. Parveen, D.K. Nandi, R. Ramesh, S.A. Ansari, T. Cheon, S.H. Kim, Enhanced activity of highly conformal and layered tin sulfide (SnSx) prepared by atomic layer deposition (ALD) on 3D metal scaffold towards high performance supercapacitor electrode, Sci. Rep. 9 (2019), https://doi.org/10.1038/s41598-019-46679-7.
[215] P.K. Panda, A. Grigoriev, Y.K. Mishra, R. Ahuja, Progress in supercapacitors: roles of two dimensional nanotubular materials, Nanoscale Adv. 2 (2020) 70–108, https://doi.org/10.1039/c9na00307j.
[216] M. Sajjad, Y. Khan, W. Lu, One-pot synthesis of 2D SnS2 nanorods with high energy density and long term stability for high-performance hybrid supercapacitor, J. Energy Storage 35 (2021), 102336, https://doi.org/10.1016/j.est.2021.102336.
[217] Y. Zhang, J. Lu, S. Shen, H. Xu, Q. Wang, Ultralarge single crystal SnS rectangular nanosheets, Chem. Commun. 47 (2011) 5226–5228, https://doi.org/10.1039/c0cc05528j.
[218] J. Ning, K. Men, G. Xiao, L. Wang, Q. Dai, B. Zou, B. Liu, G. Zou, Facile synthesis of iv–vi SnS nanocrystals with shape and size control: nanoparticles, nanoflowers and amorphous nanosheets, Nanoscale 2 (2010) 1699–1703, https://doi.org/10.1039/c0nr00052c.
[219] H. Chauhan, M.K. Singh, S.A. Hashmi, S. Deka, Synthesis of surfactant-free SnS nanorods by a solvothermal route with better electrochemical properties towards

supercapacitor applications, RSC Adv. 5 (2015) 17228–17235, https://doi.org/10.1039/c4ra15563g.
[220] B.P. Reddy, M.C. Sekhar, S.V.P. Vattikuti, Y. Suh, S.H. Park, Solution-based spin-coated tin sulfide thin films for photovoltaic and supercapacitor applications, Mater. Res. Bull. 103 (2018) 13–18, https://doi.org/10.1016/j.materresbull.2018.03.016.
[221] R. Barik, N. Devi, V.K. Perla, S.K. Ghosh, K. Mallick, Stannous sulfide nanoparticles for supercapacitor application, Appl. Surf. Sci. 472 (2019) 112–117, https://doi.org/10.1016/j.apsusc.2018.03.172.
[222] B.Jansi Rani, S.P. Keerthana, G. Ravi, R. Yuvakkumar, D. Velauthapillai, M. Thambidurai, C. Dang, In situ hydrothermal growth of SnS/Ni foam for electrochemical energy storage and conversion, Mater. Lett. 273 (2020), https://doi.org/10.1016/j.matlet.2020.127958.
[223] T. Duangchuen, A. Karaphun, L. Wannasen, I. Kotutha, E. Swatsitang, Effect of SnS2 concentrations on electrochemical properties of SnS2/RGO nanocomposites synthesized by a one-pot hydrothermal method, Appl. Surf. Sci. 487 (2019) 634–646, https://doi.org/10.1016/j.apsusc.2019.05.116.
[224] Y. Shi, L. Sun, Y. Zhang, H. Si, C. Sun, J. Gu, Y. Gong, X. Li, Y. Zhang, SnS2 nanodots decorated on RGO sheets with enhanced pseudocapacitive performance for asymmetric supercapacitors, J. Alloys Compd. 853 (2021), 156903, https://doi.org/10.1016/j.jallcom.2020.156903.
[225] S. Ravuri, C.A. Pandey, R. Ramchandran, S.K. Jeon, A.N. Grace, Wet chemical synthesis of SnS/graphene nanocomposites for high performance supercapacitor electrodes, Int. J. Nanosci. 17 (2018) 1–8, https://doi.org/10.1142/S0219581X17600225.
[226] Y. Xu, Y. Zhou, J. Guo, S. Zhang, Y. Lu, Preparation of SnS2/g-C3N4 composite as the electrode material for supercapacitor, J. Alloys Compd. 806 (2019) 343–349, https://doi.org/10.1016/j.jallcom.2019.07.130.
[227] M. Setayeshmehr, M. Haghighi, K. Mirabbaszadeh, Binder-free 3D flower-like alkali doped- SnS2 electrodes for high-performance supercapacitors, Electrochim. Acta 376 (2021), 137987, https://doi.org/10.1016/j.electacta.2021.137987.
[228] H. Chu, F. Zhang, L. Pei, Z. Cui, J. Shen, M. Ye, Ni, co and mn doped SnS2-graphene aerogels for supercapacitors, J. Alloys Compd. 767 (2018) 583–591, https://doi.org/10.1016/j.jallcom.2018.07.126.
[229] K. Sk, J.S.Yu. Hussain, Surfactant-free one-pot hydrothermal growth of micro-flower-like copper tin sulfide electrode material for pseudocapacitor applications, J. Electrochem. Soc. 165 (2018) E592–E597, https://doi.org/10.1149/2.1061811jes.
[230] B. Wang, R. Hu, J. Zhang, Z. Huang, H. Qiao, L. Gong, X. Qi, 2D/2D SnS2/MoS2 layered heterojunction for enhanced supercapacitor performance, J. Am. Ceram. Soc. 103 (2020) 1088–1096, https://doi.org/10.1111/jace.16778.
[231] L. Wang, Y. Ma, M. Yang, Y. Qi, One-pot synthesis of 3D flower-like heterostructured SnS2/MoS2 for enhanced supercapacitor behavior, RSC Adv. 5 (2015) 89069–89075, https://doi.org/10.1039/c5ra16300e.
[232] P.K. Enaganti, V. Selamneni, P. Sahatiya, S. Goel, MoS2/cellulose paper coupled with SnS2quantum dots as 2D/0D electrode for high-performance flexible supercapacitor, New J. Chem. 45 (2021) 8516–8526, https://doi.org/10.1039/d1nj00364j.
[233] Y. Tang, S. Chen, S. Mu, T. Chen, Y. Qiao, S. Yu, F. Gao, Synthesis of capsule-like porous hollow nanonickel cobalt sulfides via cation exchange based on the kirkendall effect for high-performance supercapacitors, ACS Appl. Mater. Interfaces 8 (2016) 9721–9732, https://doi.org/10.1021/acsami.6b01268.
[234] N. Kumar, D. Mishra, S.Y. Kim, S.H. Jin, Two dimensional, bi-layered SnS2@Co3S4 heterostructure formation via SILAR method: toward high performance supercapacitors with superior electrodes, Mater. Lett. 262 (2020), 127173, https://doi.org/10.1016/j.matlet.2019.127173.
[235] C. Wang, H. Tian, J. Jiang, T. Zhou, Q. Zeng, X. He, P. Huang, Y. Yao, Facile synthesis of different morphologies of Cu2SnS3 for high-performance supercapacitors, ACS Appl. Mater. Interfaces 9 (2017) 26038–26044, https://doi.org/10.1021/acsami.7b07190.
[236] A.C. Lokhande, A. Patil, A. Shelke, P.T. Babar, M.G. Gang, V.C. Lokhande, D. S. Dhawale, C.D. Lokhande, J.H. Kim, Binder-free novel Cu4SnS4 electrode for high-performance supercapacitors, Electrochim. Acta 284 (2018) 80–88, https://doi.org/10.1016/j.electacta.2018.07.170.
[237] _KBSIS~1, (n.d.).
[238] G. Hatui, G. Chandra Nayak, G. Udayabhanu, Y.K. Mishra, D.D. Pathak, Template-free single pot synthesis of SnS2@Cu2O/reduced graphene oxide (rGO) nanoflowers for high performance supercapacitors, New J. Chem. 41 (2017) 2702–2716, https://doi.org/10.1039/c6nj02965e.
[239] H. Wang, D. Chao, J. Liu, J. Lin, Z.X. Shen, Nanoengineering of 2D tin sulfide nanoflake arrays incorporated on polyaniline nanofibers with boosted capacitive behavior, 2D Materials 5 (2018), https://doi.org/10.1088/2053-1583/aabd12.
[240] A.M. Patil, V.C. Lokhande, U.M. Patil, P.A. Shinde, C.D. Lokhande, High performance all-solid-state asymmetric supercapacitor device based on 3D nanospheres of β-MnO 2 and nanoflowers of O-SnS, ACS Sustain. Chem. Eng. 6 (2018) 787–802, https://doi.org/10.1021/acssuschemeng.7b03136.
[241] C. Liu, S. Zhao, Y. Lu, Y. Chang, D. Xu, Q. Wang, Z. Dai, J. Bao, M. Han, 3D porous nanoarchitectures derived from SnS/S-doped graphene hybrid nanosheets for flexible all-solid-state supercapacitors, Small 13 (2017) 1–9, https://doi.org/10.1002/smll.201603494.
[242] S.A. Ansari, M.H. Cho, Growth of three-dimensional flower-like SnS2 on g-C3N4 sheets as an efficient visible-light photocatalyst, photoelectrode, and electrochemical supercapacitance material, Sustain. Energy Fuels 1 (2017) 510–519, https://doi.org/10.1039/c6se00049e.
[243] Z. Bi, L. Huang, C. Shang, X. Wang, G. Zhou, Stable copper tin sulfide nanoflower modified carbon quantum dots for improved supercapacitors, Journal of Chemistry. 2019 (2019), https://doi.org/10.1155/2019/6109758.
[244] Sunil, P. Lonkar, V.v. Pillai, S.P. Patole, S.M. Alhassan, Scalable in situ synthesis of 2D–2D-type graphene-wrapped SnS 2 nanohybrids for enhanced supercapacitor and electrocatalytic applications, ACS Applied Energy Materials. 3 (2020) 4995–5005, https://doi.org/10.1021/acsaem.0c00519.
[245] D. Wang, X. Yan, C. Zhou, J. Wang, X. Yuan, H. Jiang, Y. Zhu, X. Cheng, R. Li, A free-standing electrode based on 2D SnS2 nanoplates@3D carbon foam for high performance supercapacitors, Int. J. Energy Res. 44 (2020) 8542–8554, https://doi.org/10.1002/er.5540.
[246] C. Liu, S. Zhao, Y. Lu, Y. Chang, D. Xu, Q. Wang, Z. Dai, J. Bao, M. Han, 3D porous nanoarchitectures derived from SnS/S-doped graphene hybrid nanosheets for flexible all-solid-state supercapacitors, Small 13 (2017) 1–9, https://doi.org/10.1002/smll.201603494.
[247] X. Xu, Y.H. Tan, J. Ding, C. Guan, 3D printing of next-generation electrochemical energy storage devices: from multiscale to multimaterial, Energy Environ. Mater. (2021), https://doi.org/10.1002/eem2.12175.
[248] J. Yang, Q. Cao, X. Tang, J. Du, T. Yu, X. Xu, D. Cai, C. Guan, W. Huang, 3D-printed highly stretchable conducting polymer electrodes for flexible supercapacitors, J. Mater. Chem. A 9 (2021) 19649–19658, https://doi.org/10.1039/d1ta02617h.